A Biophysical Analysis of the Occlusal Wear of Dental Materials

Ronald L. Sakaguchi

Sponsoring establishment:

Thames Polytechnic
School of Mathematics, Statistics, and Computing
London, England

Collaborating establishment:

University of Minnesota
School of Dentistry, Biomaterials Program
Minneapolis, Minnesota, USA

Thesis submitted to the Council for National Academic Awards in partial fulfillment of the requirements for the degree of Doctor of Philosophy

September, 1988

To Professors Mark Cross and William H. Douglas

Abstract

A Biophysical Analysis of the Occlusal Wear of Dental Materials

Ronald L. Sakaguchi

An artificial oral environment was used to clinically simulate the dental wear process and surface friction between opposing maxillary and mandibular elements. Measurement of surface friction between occlusal surfaces of natural premolar teeth demonstrated large variation. High viscosity lubricants and surfactant containing lubricants were capable of reducing the surface friction. The enamel appeared otherwise insensitive to natural and artificial salivary fluids. Orientation of opposing enamel prisms was critical for reduction of interocclusal friction. A critical choice of prosthetic dental materials evaluated for wear included amalgam, porcelain, and composite opposed by a natural third molar palatal cusp. The wear of amalgam was slight (volume loss 0.0307 ± .0036 mm^3 and depth .072 ± .0017 mm at 300K masticatory cycles) and wear of the opposing enamel was not measurable. SEM demonstrated smearing between the amalgam and the enamel cusp, thus supporting an adhesive wear mechanism. The wear of porcelain (volume .165 ± .037 mm^3, depth .127 ± .02 mm at 300K masticatory cycles) demonstrated a ploughing effect on the surface supporting an abrasive wear mechanism. The composite wear was intermediate (volume .046 ± .007 mm^3, depth .059 ± .01 mm). Posterior composites are thought to wear by an abrasive as well as fatigue mechanism. The artificial mouth demonstrated a high correlation (0.98) with clinical studies. Wear of enamel opposed by enamel demonstrated a high degree of variability. The physiologic occlusal orientation between enamel pairs appeared important. A finite element model of a natural and crowned premolar tooth was developed consisting of 586 triangular elements and 343 nodes using ANSYS and IFECS finite element analysis software. Validation of the model was achieved via a physical model of a natural premolar tooth with strain gages. A new full coverage restoration design employing layering of composite restorative materials was proposed and tested. The model predicted a problem of fatigue crack propagation through the restoration which was confirmed in preliminary clinical trials. This provided further evidence for the fatigue mechanism of wear in composite restorations. On the basis of the wear studies conducted, recommendations for restorative treatment design were presented.

Preface

This dissertation represents several years of research conducted in the Biomaterials laboratory at the University of Minnesota School of Dentistry, Minneapolis, Minnesota, under the direction of Professor Dr. William H. Douglas and at the School of Mathematics, Statistics, and Computing at Thames Polytechnic, London, England under the direction of Professor Mark Cross. This work has enjoyed the collaboration of many outstanding people to whom are extended immense appreciation.

A tremendous amount of gratitude, respect, and admiration is expressed to Bill and Mark for their teaching, guidance, support, and encouragement as teachers, mentors, colleagues, and friends. They emphasized the importance of uniting the theoretical and real worlds.

Many thanks also to my colleagues and friends of the Biomaterials team: to Dr. Ralph DeLong for his many critical suggestions, discussions, and review of the manuscript; Maria Pintado for her support and encouragement, and assistance in analysis of the data and SEM expertise; Marilynn Erickson for her superb coordination of the Biomaterials Program; and Stuart Kemp for his many programming suggestions and witty ways.

Thanks also to my many friends and colleagues at Thames Polytechnic who were so hospitable and generous during my visits to London. Thanks especially to Mike Bramwell whose hospitality made the journeys to London so much more enjoyable and for his many suggestions regarding the manuscript and British methods, and to Peter Chow for all of his work on IFECS.

Finally, a project of this nature could not be accomplished without the love, support, and encouragement from my parents, Lou and Hatsy, who have always supported my academic pursuits, and from my wife, Nancy, whose love, support, patience, and encouragement made this project bearable.

To these people and many others, I thank you. Cheers!

RLS

Inver Grove Heights, Minnesota

September, 1988.

Table of Contents

Abstract

A Biophysical Analysis of the Occlusal Wear of Dental Materials

Ronald L. Sakaguchi

An artificial oral environment was used to clinically simulate the dental wear process and surface friction between opposing maxillary and mandibular elements. Measurement of surface friction between occlusal surfaces of natural premolar teeth demonstrated large variation. High viscosity lubricants and surfactant containing lubricants were capable of reducing the surface friction. The enamel appeared otherwise insensitive to natural and artificial salivary fluids. Orientation of opposing enamel prisms was critical for reduction of interocclusal friction. A critical choice of prosthetic dental materials evaluated for wear included amalgam, porcelain, and composite opposed by a natural third molar palatal cusp. The wear of amalgam was slight (volume loss 0.0307 ± .0036 mm^3 and depth .072 ± .0017 mm at 300K masticatory cycles) and wear of the opposing enamel was not measurable. SEM demonstrated smearing between the amalgam and the enamel cusp, thus supporting an adhesive wear mechanism. The wear of porcelain (volume .165 ± .037 mm^3, depth .127 ± .02 mm at 300K masticatory cycles) demonstrated a ploughing effect on the surface supporting an abrasive wear mechanism. The composite wear was intermediate (volume .046 ± .007 mm^3, depth .059 ± .01 mm). Posterior composites are thought to wear by an abrasive as well as fatigue mechanism. The artificial mouth demonstrated a high correlation (0.98) with clinical studies. Wear of enamel opposed by enamel demonstrated a high degree of variability. The physiologic occlusal orientation between enamel pairs appeared important. A finite element model of a natural and crowned premolar tooth was developed consisting of 586 triangular elements and 343 nodes using ANSYS and IFECS finite element analysis software. Validation of the model was achieved via a physical model of a natural premolar tooth with strain gages. A new full coverage restoration design employing layering of composite restorative materials was proposed and tested. The model predicted a problem of fatigue crack propagation through the restoration which was confirmed in preliminary clinical trials. This provided further evidence for the fatigue mechanism of wear in composite restorations. On the basis of the wear studies conducted, recommendations for restorative treatment design were presented.

1 Introduction

1.1 Concepts of clinical dental wear

The wear of dental materials is a gradual process which contributes to aging due to its effects on function and aesthetics. Natural and artificial materials coexist within a harsh oral environment which subjects the materials to a variety of insults: high localized stresses when materials are in occlusion, abrasion from foods and toothpastes, erosion and corrosion from oral fluids, and disease processes such as dental caries.

Rates of wear and mechanisms of loss are of clinical interest because proper selection of materials for restoration of lost natural tooth structure can preserve normal function and occlusal harmony. These findings also promote development of new materials which should be aimed at preserving natural structures, i.e., strengthening existing tooth structure and preventing loss of opposing surfaces.

The relationship between the maxilla and mandible as they approximate each other is determined by the anatomic form of the occlusal surfaces of the teeth. As these surfaces wear, the occlusal vertical dimension, or degree of closure, is reduced, thereby diminishing the performance of the stomatognathic system. Facial distortion is more noticeable as the chin appears to be closer to the nose, the commissure of the lips turn down, and the lips lose their fullness. The face appears flabby instead of firm and full. The temporomandibular joint is forced to rotate beyond its normal limit leading to potential damage and the mandible closes in a slightly prognathic position. Parafunctional disorders may result, including pain, tension and fatigue of the facial and masticatory musculature, clicking of the temporomandibular joint, headache, and phonetic impairment.

Although several mechanisms lead to loss of natural and restorative materials, it is the occlusal and lateral excursive contacts between arches which result in reduced occlusal vertical dimension. Attrition is the term associated with natural tooth loss when tooth-to-tooth contact occurs. The mandibular teeth approach and contact the maxillary teeth in a centric occlusal position when swallowing occurs, but there is no lateral excursive component. Mastication of a bolus of food results in periodic penetration of the food bolus usually on inclined planes of the posterior teeth. The approximating inclined planes serve to crush the food in preparation for swallowing. The tongue repeatedly lifts the food bolus onto the occlusal table for processing until a sufficient number of strokes has reduced the bolus adequately. There is a masticatory path of motion which is described by eccentric contact of the mandibular buccal cusps with the inner inclines of the maxillary buccal cusps, followed by a working movement to centric occlusion. This continues through centric occlusion to a balancing movement before the mandible is repositioned for the next cycle.[1] The length of contact in lateral excursion is determined by the type of guidance that exists, i.e., canine guidance, where the canines disclude the posterior teeth lateral to centric occlusion, or group function, where the posterior teeth are in occlusion throughout the lateral movement. The magnitude of the forces generated during mastication are in the 2-40 lb (9-180 N) range with a duration from 0.25 to 0.33 sec.[2] Bruxism extends the lateral contact time because of the characteristic reciprocating grinding that is produced.

1.2 Methods for studying dental wear

A number of methods have been employed for studying the process of dental wear which range from simple laboratory methods, to sophisticated simulation techniques, to measurement of in vivo wear. Laboratory methods are advantageous because they minimize the problem of biologic variability. Patients exhibit a wide variation of occlusal forces, contact times, dietary materials, occlusal alignment, restorative materials, and anatomy, making clinical evaluations extremely complex. In vitro methods offer the opportunity to test materials under various conditions that would not be well tolerated by live subjects and can offer accelerated turnaround of results. However, long term clinical studies with large patient samples provide the requisite validation of any in vitro method.

1.2.1 In vitro dental wear evaluation systems

Obviously the primary requirement for a test is to duplicate clinical findings. The method should be capable of ranking the performance of well established and clinically tested materials in the same order in which they are ranked clinically. The test should be able to accommodate a variety of material types without bias by the different wear mechanisms that might be involved.

Laboratory wear systems have ranged in sophistication from simulation methods which involve recreation of physiologic oral conditions, to simple screening methods. Simulation methods provide application of oral fluids and occlusal loads through enamel antagonists simulating the masticatory cycle. Their drawback is high equipment cost. Simple screening methods have the advantage of simple set up and lend themselves readily to inclusion in standard specifications. However, the validity of the results obtained from these and other non-simulatory tests is often open to doubt.

Any test method which produces wear, must also have a method of measuring it as it progresses. This may be a mechanical profiling method which is capable of quantifying the wear or an optical method for qualitative assessment which might include light or scanning electron microscopy.

Most popular of the non-stimulatory screening tests for wear are the pin and disk or pin and plate methods.[3-6] Here, the disk or plate is rotated or reciprocated against a pin under a constant load and the wear rate expressed as a decrease in volume of the pin, or the track width or depth in the disk or plate. Generally the pin is composed of an enamel sample and the disk is the material being studied. However other configurations have used the test material for the pin with the plate/disk formed by a supported sheet of carborundum paper[7] or an abrasive slurry.[8-10] Other variations have simulated two body wear and three body wear by revolving pins of test material against a slurry comprising a mixture of glass beads (two body wear) and fine aluminum oxide powder (three body wear).[11,12] Generally, the pin and disk methods are capable of ranking categories of materials, i.e., amalgam, composite, and porcelain and can simulate adhesive wear characteristics in enamel vs. amalgam testing.[4,13]

Sliding mechanisms have been used for screening materials which incorporate some of the physiologic factors of the human masticatory cycle.[13-15] These have simulated both sliding and impact contacts with human enamel. Thermocycling has also been included using hot and cold water jets.[15] The ranking order for wear using sliding contacts was the same as that experienced clinically.[14] The single pass abrasion test using a hemispherical diamond employed by Powers, et al.[16] and Roberts, et al.[17] provided information on frictional resistance and abrasive wear but lacked any consideration of fatigue.

Abrasion testing of test material against silicon carbide paper has been used to simulate contact stress, contact time, sliding distance and stroke speed.[5,8,18,19] This method found the wear for a conventional composite to be significantly lower than that for amalgam, which contradicts clinical findings. Recently a rotating cam device has been used with a millet seed/PMMA bead mixture for abrasive testing[20,21] which has proven useful for simple screening and ranking of wear of materials.

Toothbrush-dentifrice studies[22-24] simulating abrasion are used to mimic brushing cycles of patients and may be useful in predicting abrasive wear of materials used to restore abrasion or Class III lesions. These are unlikely, however, to give meaningful data for posterior restorations. Vibratory wear tests employing vibration of a specimen in a capsule containing an abrasive slurry[25,26] or vibration of a specimen in a capsule lined with abrasive paper[27] have demonstrated results contradictory to clinical findings.

DeLong and Douglas[28] have employed closed loop servohydraulics in a simulation instrument to produce an artificial oral environment. This allows precise control over applied load, contact time, lateral excursion and fluid environmental control when coupled with a thermocycler. One of the main advantages of such a system is the ability to reproduce the parameters of functional and parafunctional oral physiology with the capability of studying mechanisms of wear and interocclusal friction.

1.2.2 Clinical wear assessment methods

Long-term clinical tests are the most reliable wear studies[29] however they require accurate methods for measuring wear. Clinical evaluations have problems associated with quantifying the wear, interpreting the results in terms of the mechanism, and identifying the contribution of the individual parameters controlling wear. Also, direct clinical evaluation is insufficiently sensitive to identify wear of restorations, particularly in the early stages of wear.[30]

Conflicting findings occur with various methods of clinical measurement. For instance, the rate of wear of composite resins tended to decrease as a function of time using indirect assessment methods.[52] In direct contrast, the clinical evaluations showed an accelerated rate of wear over time.[32] Different evaluation methods are associated with different levels of sensitivity. Whereas indirect methods have a resolution of 50μm or better, direct clinical observation is effective only in the detection of discrepancies greater than 150μm which is the maximum loss of contour per year specified by the ADA specification for wear of composite materials.[33]

Several clinical measurement methods have been developed using direct or indirect techniques.[34] The test methodology which assesses wear in vivo is of fundamental importance in determining the usefulness or longevity of composites and other materials as posterior restoratives.[35-37]

The United States Public Health Service (USPHS), or Ryge criteria[38] direct assessment method for composite restorations includes evaluation of anatomic form, marginal adaptation, color match, cavosurface marginal discoloration, and caries.[39-42] Criteria are based on judgments or decisions that are compatible with the typical clinical observations of a dentist. The objective of the criteria is to provide a relatively complete picture of the clinical performance of a restoration. Anatomic form is used for the wear assessment. The problems with the system include the subjectivity of the findings, the qualitative nature of the assessment and the difficulty in evaluating tooth colored restorations.

Several investigators have made modifications to the USPHS criteria. Heights of the exposed cavity wall on epoxy casts made from silicone impressions have been measured with a stereomicroscope fitted with an ocular measuring scale.[43] Dennison, Powers and Charbeneau[44] modified the Ryge criteria by adding an additional division in the category of anatomic form.

In vivo wear has been evaluated by placing restoratives into the artificial teeth of removable prostheses.[45-48] This permitted several materials to be tested within the same arch of an individual but may not experience the occlusal forces and movements present in an intact dentition.

At least one study[49] suggested that the determined rate of wear depends on the method of evaluation. Criticism of the direct assessment method include inferior resolution, limited marginal detection because of bevels placed on the cavosurface angle, and difficult detection of small discrepancies due to similarity of color and refractive indices between the restorative material and the tooth structure. Uniform sharpness of the explorer tip is also a problem for this system.

A method of comparing casts (Leinfelder method) has been developed[50-53] consisting of six standard casts of differing amounts of wear ranging from not observable to severe. This is not a quantitative method. The six distinctive casts represent about 100μm of progressive wear, however the casts do not represent a true linear scale. The technique is subjective and only as discriminating as the evaluators can reproduce it.

Stereo cameras and a reference system incorporating the use of a bite splint and mirrors attached directly to the cameras[54] have been used for clinical measurement and SEM methods used for qualitatively studying abrasion resistance of posterior composites.[55]

Several researchers[56-59] have developed methods for digitizing occlusal surfaces by optical or mechanical means. A computer driven 3 coordinate-axis table is used to position the object to be measured against a measuring stylus coupled to a switch to determine the z axis position. Using a light microscope, replicas of the samples are aligned and the area to be scanned is defined by manual control of the stepper motors. Others[45,46,60] have used similar profilometer configurations. Lambrechts, et al.[61] and Braem, et al.[62] developed a three-dimensional measuring method requiring a highly accurate replica technique which is the prerequisite for quantitative wear studies.

The profiling system of DeLong and Douglas employs a mechanical stylus coupled with a strain gage extensometer to control vertical movement of a closed loop servohydraulic actuator. Vertical measurements are made via a linear variable differential transformer (LVDT) while two stepmotor controlled tables position the sample in the horizontal plane. This method will be discussed more fully in Chapter 2.

1.3 The wear of a critical choice of dental materials

The three restorative materials selected for this study, amalgam, porcelain, and composite, are the most common dental materials used in clinical dentistry (Fig. 1-1 and 1-2). They are very distinct in their composition and physical properties from each other and from natural tooth structure.

Biomechanically, the natural tooth is comprised of four elements: enamel, dentinoenamel junction, dentin, and the pulp (Fig. 1-3). Although the pulp provides no direct contribution to the strength of the tooth, it provides the innervation and vasculature for the tooth, without which the tooth becomes brittle, as seen clinically in endodontically treated teeth. The tooth can be considered a biolaminate with the most wear resistant component, enamel, on the outer surface. This hard, wear resistant layer provides for precise intercuspation of the tooth and its antagonist. However, it must be adequately supported by healthy dentin. The internal structural arrangement provides adequate resistance to fracture under normal stresses produced by the occlusion of the maxillary and mandibular teeth. Structurally, enamel is a biocomposite composed of crystals of calcium hydroxyapatite in a continuous protein matrix. Enamel is anisotropic with a preferred orientation to the crystals arranged in prisms running approximately at right angles to the enamel surface. Beneath the 2-3 mm thickness layer of enamel lies the dentin which is a relatively soft material, having approximately 20-25% the

Fig. 1-1. Amalgam and porcelain restorations. Porcelain fused to metal crown on #3 (maxillary right first molar); amalgam restorations on premolars and molars

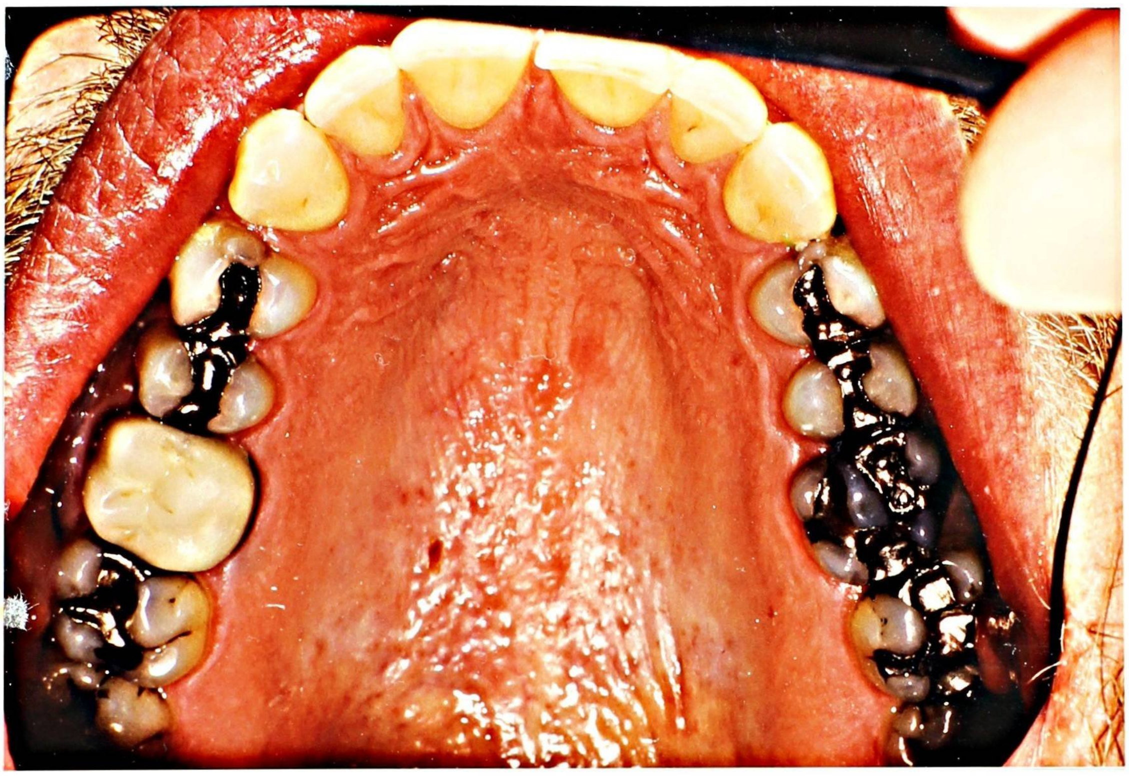

Fig. 1-2. Amalgam, gold and composite restorations. Amalgam in mandibular right second molar; composites in right and left molars; gold crown on mandibular left first molar

hardness of enamel. The dentin consists of hydroxyapatite in a collagenous matrix. Dentin is penetrated throughout by tubules which are oriented perpendicular to the dentinoenamel junction where the dentin is intimately bonded with the enamel. Once the enamel is penetrated, wear progresses rapidly through the softer dentin.

Dental amalgam is an alloy of mercury with silver, tin, copper, and sometimes zinc. When mixed, or amalgamated, it has a plasticity that permits it to be conveniently packed or condensed into a prepared tooth cavity. They are generally used in the posterior segments because of their silvery gray metallic color and subsequent darkening under corrosion. Amalgam is very strong in compression but much weaker in tension and shear. It tends to exhibit creep or flow when subjected to a continuous compressive force even after the mass has completely set. When subjected to a rapid application of stress either in tension or in compression, amalgam functions as a brittle material, subject to fracture with little deformation or elongation. Amalgam has been one of most serviceable restorative materials for over 100 years.

As a crown veneering material, dental porcelain is widely used because of its aesthetics. It is comprised of feldspar, quartz, kaolin, and pigments which are blended together, fused, then sintered to form a powder. Although they have been used as inlay materials, porcelain is generally considered a full coverage, or crown, material. The basic designs of the restoration include the full porcelain jacket without a metal backing or core, and porcelain fused to metal (PFM) crown which utilizes the metal core for strength. Porcelain is tolerated well by the gingival tissues because of its smoothness and inertness when glazed. However, it is quite brittle and hard, resulting in fracture if inadequately supported when a load is applied. The material is very resistant to oral fluids and capable of only very slight cold flow.

Dental composite restoratives are classified as direct aesthetic restorative materials because they are generally placed directly into a prepared tooth cavity, as amalgam, without the need for an intervening replication technique, and because they are tooth colored. They consist of

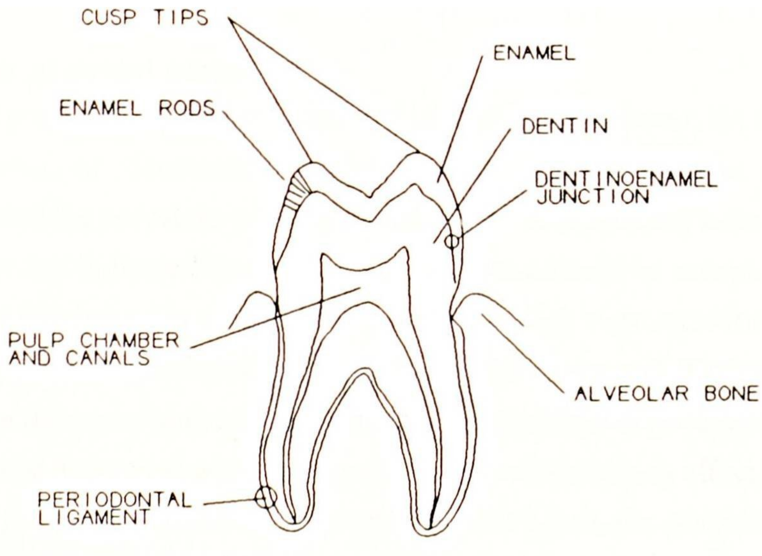

Fig. 1-3. Structure of the natural tooth

an organic resin such as Bis-GMA (bisphenyl glycidyl methacrylate) into which is incorporated a dispersed inorganic phase consisting of several inorganic materials such as quartz, borosilicate glass, lithium aluminum silicate, barium aluminum silicate, barium fluoride, and many other inorganic materials. These filler materials are treated with organic silanes, called coupling agents, to enhance the bond between the inorganic and organic phases. The indentation hardness of the material is approximately 15% of the hardness of enamel and approximately one-half that of amalgam. One of the major benefits of the material is its ability to be bonded to enamel and dentin, promoting reinforcement of existing natural tooth structure and a marginal seal.

1.3.1 The wear of dental amalgam

Dental amalgam is one of the oldest dental restorative materials and has been used with success in most regions of the mouth. Although it has been criticized for its mercury content and poor aesthetics, it is very resistant to occlusal wear. This property makes it a material of choice for stress bearing areas in the posterior segment of the dental arch. Lambrechts[61,63] found in clinical studies that dental amalgam typically lost 200 micrometers in contact areas after 4 years in the mouth. Non-contact wear of amalgam was very small and, in the same clinical study, only 24 micrometers were lost. Powell, et al.[64] tested amalgam, composites, and composite resins under enamel pins and were able to rank amalgam and conventional composites according to clinical experience of occlusal wear. They found that enamel wear against amalgam was very small and noted considerable amalgam transfer onto enamel but concluded that the dominant wear process was abrasion. Bailey and Rice[65] found that amalgam wear was essentially independent of contact stress, although they concluded that stress was important in ranking comparisons involving amalgam and other materials which might be contact stress sensitive. Amalgam appeared to smear against its antagonist during wear experiments and lost surface contour by a process of transfer. Single-pass experiments by Roberts[17] indicated smearing of amalgam phases by a diamond slider. Rice[66] also noted heavy amalgam transfer during wear experiments. This finding was confirmed by Mueller[4] in enamel/amalgam wear studies. Further, these workers could not identify calcium or phosphorus on the amalgam, and could offer no support for the 3-body abrasive model of wear of amalgam.

1.3.2 The wear of dental porcelain

The use of dental porcelain is popular because of its aesthetics, however, the design of the restoration and location of placement is critical because of its brittle and abrasive nature. Mahalick[67] regarded the porcelain-porcelain combination as producing severe attrition under high occlusal force, but indicated that the same combination would be acceptable under lower occlusal force as experienced in a removable prosthesis. High wear rates for enamel-enamel and the enamel-porcelain combinations were found. Monasky and Taylor,[68] studying the finishing effects on the porcelain surface, found that the wear rate of porcelain against enamel was high initially but decreased with time, possibly due to a polishing effect that the enamel produced on the porcelain surface. They suggested that where the porcelain surface glaze was broken it should be repolished. Miller et al.[69] studied the wear mechanism of porcelain under single pass sliding experiments and found that track width was accounted for by elastic deformation of porcelain. Any adhesion between porcelain and its antagonist was found to be unlikely. However, small grooves were noted within the tracks that were attributed to a ploughing out effect by the asperities on the diamond slider. Further, these authors noted brittle failure of the porcelain surface, and considered the pressure at which the onset of brittle failure occurred as important.

1.3.3 Dental composites

Composites have been recently developed for restoration of the anterior and posterior segments. They have been used extensively, primarily because of their aesthetics. The pattern of composite clinical wear is in sharp contrast to that of amalgam restorations.[70] The problem of wear is an inherent characteristic of the material[52] appearing as uniform loss of material over the entire occlusal surface. Several studies have shown that the occlusal surface undergoes relatively little wear during the first 12-18 months after insertion; comparison of equal numbers of amalgam and composite resin restorations in posterior teeth after one year disclosed no significant differences in the amounts of wear. However, at the end of the second and third years the loss of anatomic form shown by the composite resin restoration was greater than that of the amalgam restorations.[14,35]

There appears to be disagreement with the rate of wear of composite restorations. The works of Braem[71] and Lutz[60] indicate that the progress of wear and the occlusal contact area is linear with time, with little or no flattening of the wear rate. The clinical studies of Leinfelder[72] and Vrijhoef, et al.[73] indicated that the vertical loss of occlusal height showed a high wear rate initially which reduced with time giving a characteristic curved appearance to the wear curve. They attributed the high initial wear of posterior composites to the problems associated with the establishment of an ideal occlusion. Others have also found that the greatest rate of wear occurred during the first three to six months after placement.[30,70,74,75] Several investigators[32,48,50,52] also noted the decrease of wear rate over a period of time. This early wear could be a result of microcracks formed in the surface and subsurface during finishing procedures.[52] As the occlusal surface is contoured and finished, energy is created which may be sufficient to generate microcracks on and below the surface of the restoration.

Microfilled composite resins appear to be more wear resistant and demonstrate nearly a linear wear rate.[45,46,59,63] However, microfilled composite resins are characteristically susceptible to localized wear.

Certain aspects of the wear process for macrofil and microfil composites are well understood. In macrofils, loss of resin through wear exposes particles which are left standing proud of the resin matrix. These particles are subsequently exfoliated from the composite. In microfils, occlusal contact stresses result in localized microcracking and debonding of the prepolymerized particles. Localized defects are initiated by small cracks. This results in a volumetric loss of contour and the development of a surface roughness, which leads to a high friction which sus-

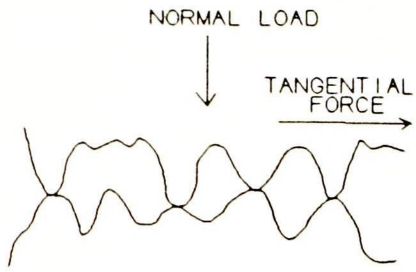

Fig. 1-4. Two microscopically rough surfaces contact only at the tips of their asperities.

tains the rate of wear and can be responsible for the accumulation of plaque and stain. Bulk fracture can occur in areas of high stress concentration.

1.4 Engineering wear of dental materials

The wear of restorative materials may be evaluated in terms of the four general types of engineering wear (adhesive, abrasive, fatigue, and chemical) as they occlude and slide against other restorations or natural enamel. The rate at which material is removed depends on the working conditions, e.g. loading, lubrication, and environment. No universal law exists for wear phenomena; each wear situation is very individual in character and is generally dependent upon the nature of the materials that oppose each other.

1.4.1 Adhesive wear

Macroscopically smooth surfaces are rough on an microscopic scale and when two such surfaces are brought together contact is made at relatively few isolated asperities (Fig. 1-4). As a normal load is applied the local pressure at the asperities becomes extremely high. The yield point stress is exceeded, and the asperities deform plastically, until the real contact area has increased sufficiently to support the applied load (Fig. 1-5). In the absence of surface films the surfaces would adhere together, but very small amounts of contaminant prevent adhesion under purely perpendicular loading. However, relative tangential motion at the interface acts to disperse the contaminant films at the points of contact, and cold welding of the junctions takes place. Continued sliding causes the junctions to be sheared and new junctions to be formed. If shear takes place deep to the interface then material is transferred from one surface to the other. With further rubbing some of the transferred material is detached to form loose wear particles (Fig. 1-6).

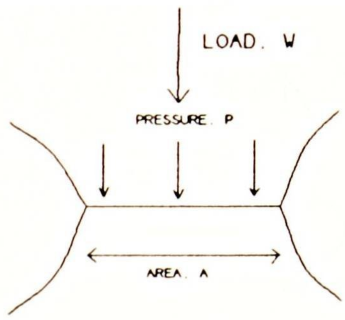

Fig. 1-5. Asperities deform until load is supported

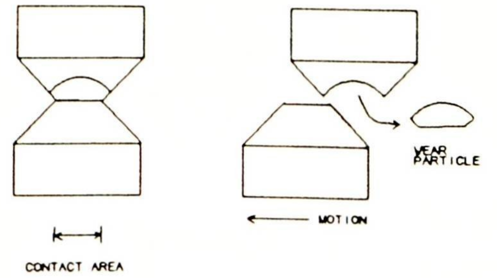

Fig. 1-6. Formation of an adhesive wear particle

Law of adhesive wear

If V is the volume of material removed, and L is the distance of sliding, V/L represents the volumetric rate of wear per sliding distance (Fig. 1-7). Assuming that the contact is made up of a number of similar spherical asperities each of radius, r, the area of each contact is πr^2 and each contact supports a load of $P\pi r^2$ where P is the yield pressure. The surfaces will pass completely over each asperity in a sliding distance of 2r and it is assumed that the wear fragment produced at each asperity is hemispherical in shape and of volume $2/3\ \pi r^3$. Then the total wear volume per sliding distance, V/L, is given by

$$V/L = \Sigma\,(2/3\ \pi r^3)/2r \qquad (1.1)$$

$$= 1/3\ \Sigma\ \pi r^2$$

$$= n\pi r^2/3 \qquad (1.2)$$

where n is the total number of contacts. But each contact supports a load of $P\pi r^2$, therefore

$$\text{total load, } W = nP\pi r^2 \qquad (1.3)$$

$$\text{or } n\pi r^2 = W/P \qquad (1.4)$$

therefore

$$V/L = W/3P \qquad (1.5)$$

This assumes that all asperity encounters produce a wear particle. If only a fraction K of all encounters produce wear particles then the equation becomes

$$V/L = KW/3P \qquad (1.6)$$

where K is the probability of an asperity contact producing a wear particle. K must be found for different combinations of sliding materials and for different conditions of rubbing. This is

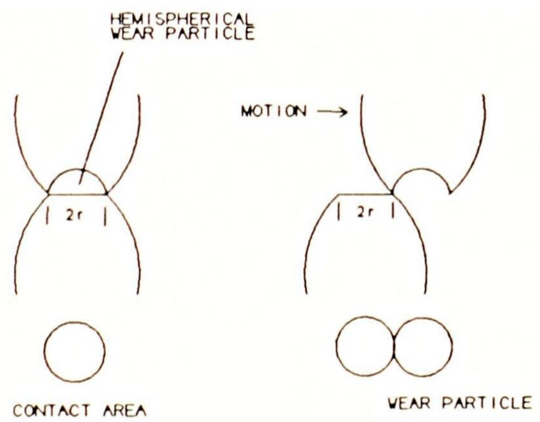

Fig. 1-7. Mechanism of adhesive wear

the basic equation of adhesive wear.[77] K is known as the coefficient of wear and is dimensionless. The factor of 3 in the denominator comes from the assumption of circular areas of contact and hemispherical wear particles. It is a shape factor that can change if different geometries are assumed.

Three laws of wear can be derived from this equation:[78]

1. the volume of wear material is proportional to the distance of travel.
2. the volume of wear material is proportional to load.
3. the volume of wear material is inversely proportional to the yield stress, or the hardness, of the softer material.

1.4.2 Abrasive wear

Abrasive wear can occur as a result of two situations. A rough hard surface sliding against a softer surface will plough out the softer material. This is a two body interaction. Abrasion could also be caused by loose hard particles sliding between rubbing surfaces. This is considered a three body interaction.

If the harder material consists of an array of hard conical asperities all with the same included angle of 2θ and the opposing surface is softer and flat, then the hard asperity will produce a track through the softer surface (Fig. 1-8).

When the conical indenter is pressed into a material of hardness, H, by a load, W, with the radius of the circular impression, r then

$$H = W/(\pi r^2) \qquad (1.7)$$

$$r^2 = W/(\pi H) \qquad (1.8)$$

In traversing distance, L, at a depth of d, the asperity displaces a volume of material (2rd/2)L.

$$d = r \cot \theta \qquad (1.9)$$

so

$$V = r^2 \cot \theta \, L \qquad (1.10)$$

therefore the volume displaced by one asperity in distance, L, is

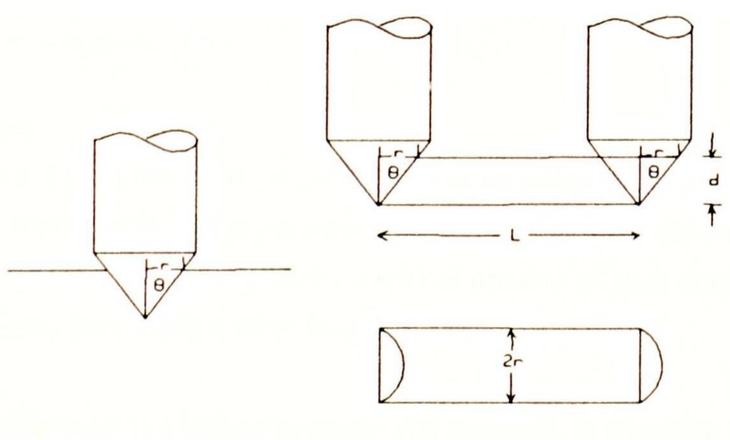

Fig. 1-8. Mechanism of abrasive wear

$$r^2 \cot \theta \, L \qquad (1.11)$$

then

$$V/L = r^2 \cot \theta \qquad (1.12)$$

$$= (W/\pi H) \cot \theta \qquad (1.13)$$

This equation has the same general form as the adhesive wear equation determined previously. The rate of wear is therefore proportional to the load on the indenter and to the sliding distance but inversely proportional to the hardness of the material scratched.

A more universal, but empirical relationship is

$$V/L = KW/H \qquad (1.14)$$

where H is the hardness of the softer material, and K is the abrasive wear constant which covers a wider range of abrasive conditions and indenter geometries.

This equation is applicable for two or three body interactions with K lower in the three body situation where many of the particles tend to roll rather than slide.

As wear due to abrasion proceeds, some blunting of the hard asperities or particles will occur, thus reducing the wear rate. However, an abrasive grit, which is brittle, can fracture causing a resharpening of the edge of the particle and an increase in wear rate.

Several investigators have confirmed that hardness is the most important parameter in abrasive wear.[79-81] The wear volume of a workpiece can be studied as a function of the ratio of the hardness H_w/H_a where H_w is the indentation hardness of the workpiece surface and H_a is the hardness of the abrasive. The wear volume is adequately described by equation 1.14 as long as H_w is less than 0.8 H_a. For intermediate surface hardness, i.e., $0.8 < H_w/H_a < 1.25$, the wear rate is given by

$$V/L = kW/5.3H_w \, (H_a/H_w)^{2.5} \qquad (1.15)$$

When $H_w/H_a > 1.25$, the abrasive wear becomes very small.

Young's modulus of elasticity may have a direct relationship on abrasion resistance however the work of Oberle[82] which suggested that abrasion resistance was related to low elastic moduli is in disagreement to Spurr and Newcombe[83] who suggested that wear resistance increased with increasing elastic modulus.

1.4.3 Fatigue Wear

When sliding surfaces make contact via asperities, wear by adhesion and abrasion can take place. However, it is conceivable that asperities can become plastically deformed during sliding but not be removed from the surface. After a critical number of such contacts an asperity would fail due to fatigue, producing a wear fragment.

It can be speculated that wear is a fatigue process. The factor, K, in equation 1.6 can be interpreted by assuming that a wear particle is produced when an asperity has experienced a sufficient number of contacts and deformations to produce a fatigue fracture. A loose wear particle is produced and this explains the production of wear particles from both the harder and the softer of the two rubbing surfaces. The fatigue mechanism does not exclude the possibility of transfer by an adhesive mechanism and therefore it appears that most of the wear phenomena can be explained at least qualitatively in terms of fatigue.

1.4.4 Chemical Wear

Chemical wear usually operates simultaneously with adhesive or abrasive wear. Interaction of the environment with the sliding surfaces produce reaction products which are found on one or both surfaces. The reaction products are usually poorly attached to the surface and rubbing removes these products.[77] Erosive dental wear mechanisms caused by chemical insults fall into this category and progress when chemical agents alter the surface of the enamel by promoting dissolution of the mineral enabling accelerated adhesive or abrasive wear mechanisms to progress.

1.5 Mechanisms for minimizing wear - friction and lubrication

Since wear depends on the nature of the surface asperity interactions, a substance which modifies this interaction may potentially decrease the amount of wear. Friction, described as the resistance to motion which is experienced whenever one solid body slides over another,[78] accompanies this surface to surface interaction. The resistive force, which is parallel to the direction of motion is called the frictional force. The value of the tangential force required to initiate sliding is the static frictional force and the force required to maintain sliding is the kinetic (or dynamic) frictional force, which is generally lower than the static frictional force.

Amontons,[84] in 1699, observed two phenomena regarding friction which are obeyed over a wide range of conditions: 1) the frictional resistance, F, is proportional to the weight, W, of the object which is being moved, and 2) the frictional force is independent of the apparent area of contact. These two laws of friction are referred to as Amontons' Laws. Coulomb added a third law which states that the interfacial resistance between two surfaces is independent of the velocity of sliding. This appears to hold only over a limited range of speed.[85]

The first law of friction allows the definition of a coefficient of friction, μ. The law states that the friction force, F, is proportional to the normal load W.

$$F \propto W \qquad (1.16)$$

therefore

$$F = \mu W \text{ or} \qquad (1.17)$$

$$\mu = F/W \qquad (1.18)$$

It is important to note that μ is not an intrinsic property of a material but depends primarily on the solids constituting the friction couple.

1.5.1 The adhesion theory of friction

The theory of Bowden and Tabor[86] was based on the fact that surfaces contact only at the tips of the asperities when loaded, as was seen in the adhesive wear theory. In fact measurements have shown that as little as 1/10,000 of the nominal contact area may be in actual contact.[87]

The relationship describing the real area of contact, A, in terms of the yield pressure of the surface, P, and the normal load, W, can be written as

$$AP = W \qquad (1.19)$$

The area of real contact is dependent neither on the size nor the shape of the area of apparent contact, but relies only on the yield pressure and load. Strong adhesion takes place at regions of intimate surface-to-surface contact and junctions "cold weld." If one surface is made to slide over the other, the welded junctions will ultimately fail by shearing which takes place at the weakest junction, whether it is in the bulk of one of the materials, thus producing a wear particle, or the junction itself. An abrasive component could also be included which accounts for hard surface asperities ploughing grooves in a softer material, however this may be regarded as insignificant in the adhesive theory. If S is the force per unit area of contact necessary to shear the junctions, then AS represents the shear force.

$$F = AS = WS/P \qquad (1.20)$$

and

$$\mu = F/W = S/P \qquad (1.21)$$

= shear strength of the junctions/yield pressure of the softer material

Since shearing usually takes place in the softer material, Bowden and Tabor suggest that μ may be defined as

μ = shear strength of the softer material/yield pressure of the softer material (1.22)

This relationship indicates that μ can remain approximately the same for a wide range of materials since it is defined as the ratio of two strength properties of the same material.

The yield pressure of the softer material is the same as that occurring around a conventional hardness indenter, therefore P may be taken to be equal to the indentation hardness of the softer material.

1.5.2 The contribution of abrasion to friction

In situations where hard asperities penetrate into the softer opposing surface, the ploughing term can become significant. The friction force is obtained by considering the total projected area of material which is displaced by plastic flow. The coefficient of friction always equals one half the vertical projected area of the asperity divided by the horizontal projected area of the asperity. On rough surfaces, the ploughing term can be comparable to the adhesion term.[78]

1.5.3 The effect of lubrication

The laws of friction and the theories of friction expounded so far apply to boundary conditions where there is direct contact between solid interfaces. Introduction of a lubricant between these sliding surfaces strongly modifies the frictional behavior by serving to (1) prevent interacting surfaces from coming into direct contact, (2) provide an easily sheared interfacial film, and (3) carry away any heat evolved in lubricated contacts. A lubricant is able to support a load only if there is relative movement between the surfaces. Thus, at the time of startup, there is direct contact between the surfaces which is diminished when the speed is sufficient for the lubricant to support the load.

Friction between lubricated surfaces can be described by the degree of relative separation of the sliding surfaces. Boundary friction occurs when the film thickness of the lubricant is very small and the films are adsorbed on the surface. Some boundary lubricants are capable of producing molecular layers which prevent welding of contacting asperities. Thin film friction is determined by the nature of the lubricant and the asperity contacts due to the roughness of the surfaces that are separated by it. Thick film friction occurs when the films are thick enough to suppress the effect of the surface finish. In general, thin film friction may be expected with low speeds and heavy loads, whereas thick film friction requires high speeds and light loads.[88] As indicated earlier, a slider system may encounter thin film friction on starting or stopping and thick film friction when the velocities are sufficient to maintain a thick film. Saliva has been shown to demonstrate lubricating qualities[89] and may reduce interocclusal friction between natural teeth.

1.6 Significance of the study of dental wear

Although dental wear is a natural part of the aging process, the accelerated or selective wear of dental materials disrupts the occlusal balance resulting in pain and decreased performance of the stomatognathic system. The degree of tension or relaxation of the masticatory musculature is dictated by the occlusal vertical dimension which in turn is defined by the occlusal surfaces of the teeth. Small localized areas of wear can affect the entire masticatory physiology because of changes in biting force and excursive contacts.

The artificial mouth referred to previously, provides the platform from which to conduct an in depth study of dental materials. The problems of in vivo studies, i.e., biologic variability, lengthy study times, and sample attrition, are minimized while the main parameters of mastication and physiologic articulation are preserved. Occlusal load, lateral excursion, and contact time are rigidly controlled, although modifications are easily made. Use of a human palatal cusp as the opponent to the prosthetic materials and thermocycling of natural and artificial salivas and fluids provide an accurate simulation of the oral environment. Precise surface measurement techniques complete the system for the study of friction and wear of dental materials.

The availability of clinical data on composite[71] and amalgam[61,63] wear is timely for the retrospective correlation with artificial mouth studies. These will provide insights into the predictive capabilities of the artificial mouth and accuracy of the simulation.

The study of dental wear is of paramount importance not only to be able to quantify the wear of various dental materials but also to elucidate the mechanisms of wear such that synthetic restorative materials may be designed for optimum performance and protection of the existing dentition.

A critical choice of dental materials, dental amalgam, dental porcelain, and composite, will be studied in the artificial mouth for the determination of characteristic qualitative and quantitative wear, and associated mechanisms of wear. A study of dental enamel will be made concerning its performance against itself and the dental materials chosen. Also, strain gage methods and finite element analysis will be used to explore the dissipation of energy that results from occlusal contact and mastication. A significant database will be developed to which other dental materials can be compared which will permit predictions of wear on the basis of mechanisms involved. Also, methods for reduction of wear or selective wear may be developed for the optimization of future dental materials.

2 Experimental methods for simulation and evaluation of dental wear and friction

2.1 The artificial mouth

In Chapter 1, the benefits of in vitro, or laboratory, testing of dental materials were discussed: lower variance, precise control of physiologic parameters, and greater reproducibility. However, the simulation will be physiologically accurate only if three basic areas are coordinated: 1) the forces and movements found during mastication must be duplicated, 2) a fluid environment must be developed which provides equivalent lubrication and surface interactions as saliva, and 3) temperature fluctuations, aeration, and humidity control must mimic the conditions found in the natural environment.[90] The artificial mouth developed by DeLong and Douglas[90] reproduces the main parameters of mastication while maintaining a fluid environment that mimics the oral cavity. This instrument is the basis for the current study of friction between dental materials and the wear that is produced.

The artificial mouth (Fig. 2-1) is based on an M.T.S. Series 812 Testing Instrument (MTS Systems Corporation, Eden Prairie, MN). It incorporates two closed servo-hydraulic loops controlling two actuators, one operating vertically, and one operating in the horizontal direction. The three dimensional motion of mastication is reproduced by two dimensional control by rotating the planes of motion so that straight line motion of the horizontal plane lies parallel to the long axis of the horizontal actuator. Load cells are used for both load measurement and control, and linear variable differential transformers (LVDT) are used for stroke (positional) measurement and control. The vertical plane is run in load control, and the horizontal plane in stroke control. Each of the mechanical closed loops consist of a testing fixture, a load cell, a hydraulic actuator mounted in a rigid frame, a limit detector associated with integration control, a function generator, and command and controller module.

A constant occlusal force can be generated from 1 to 1000 lb (4.45-4450 N) and can follow any shape of occlusal anatomy. The portion of the masticatory cycle during which no forces are generated is truncated to increase the cycling time to four cycles per second. The typical pattern of movement in the vertical plane is a truncated "teardrop" form in the shape of a trapezoid. The error in motion is only as great as the approximation of the working motion in the horizontal plane as a straight line rather than an arc.

A thermocycler (Fig. 2-2) was added to the system to allow circulation of natural and artificial salivas and their components. The temperature control permits hot and cold fluids to be pulsed through four jets mounted in an environmental chamber which conveys fluids onto the occluding surfaces of the teeth and test material. The position and flow rate of the ducts can be accurately controlled. The environmental chamber consists of an acrylic cylinder which encompasses the test materials and provides temperature, humidity, and chemical control.

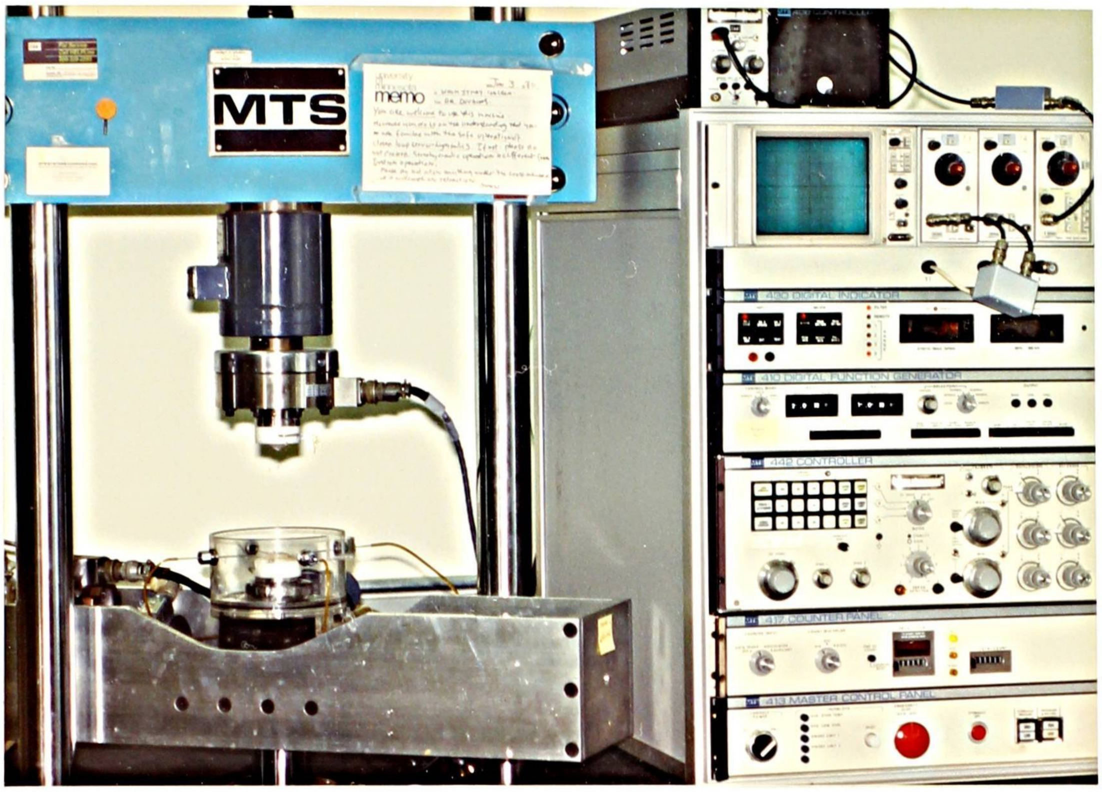

Fig. 2-1. The Artificial Mouth. Above: load frame with maxillary and mandibular element, electronics control panel. Below, acrylic environmental chamber with four fluid ducts, natural premolar teeth in opposition

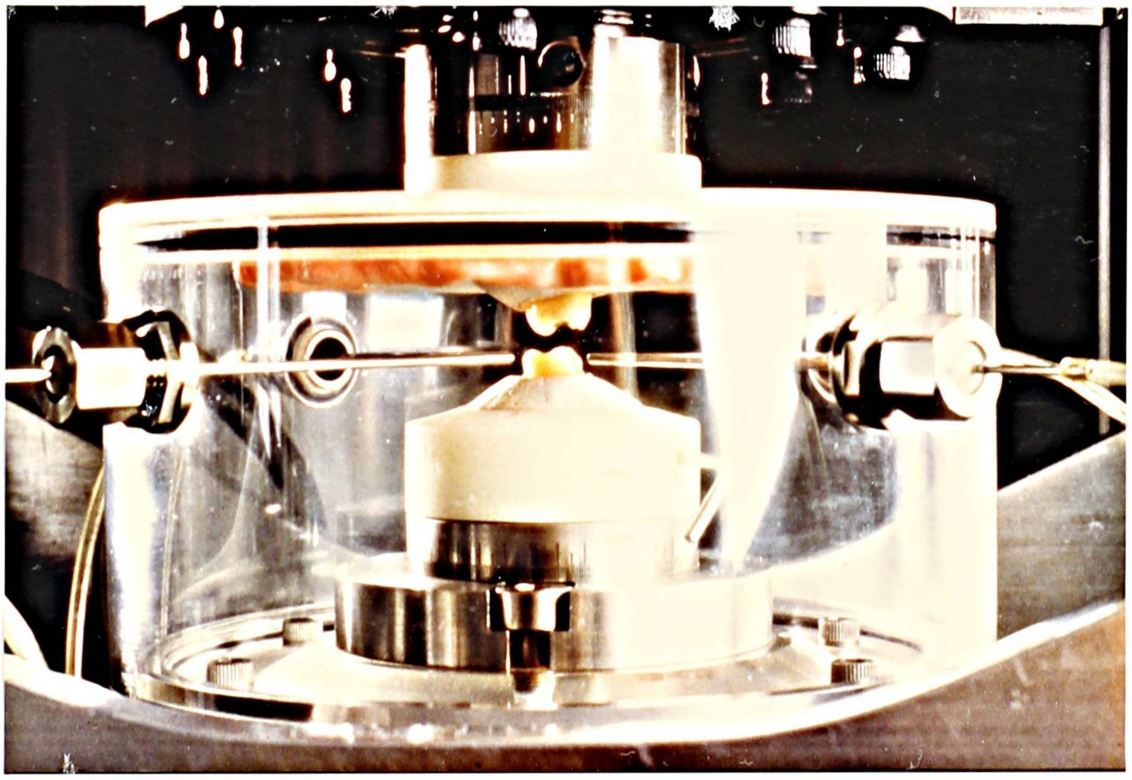

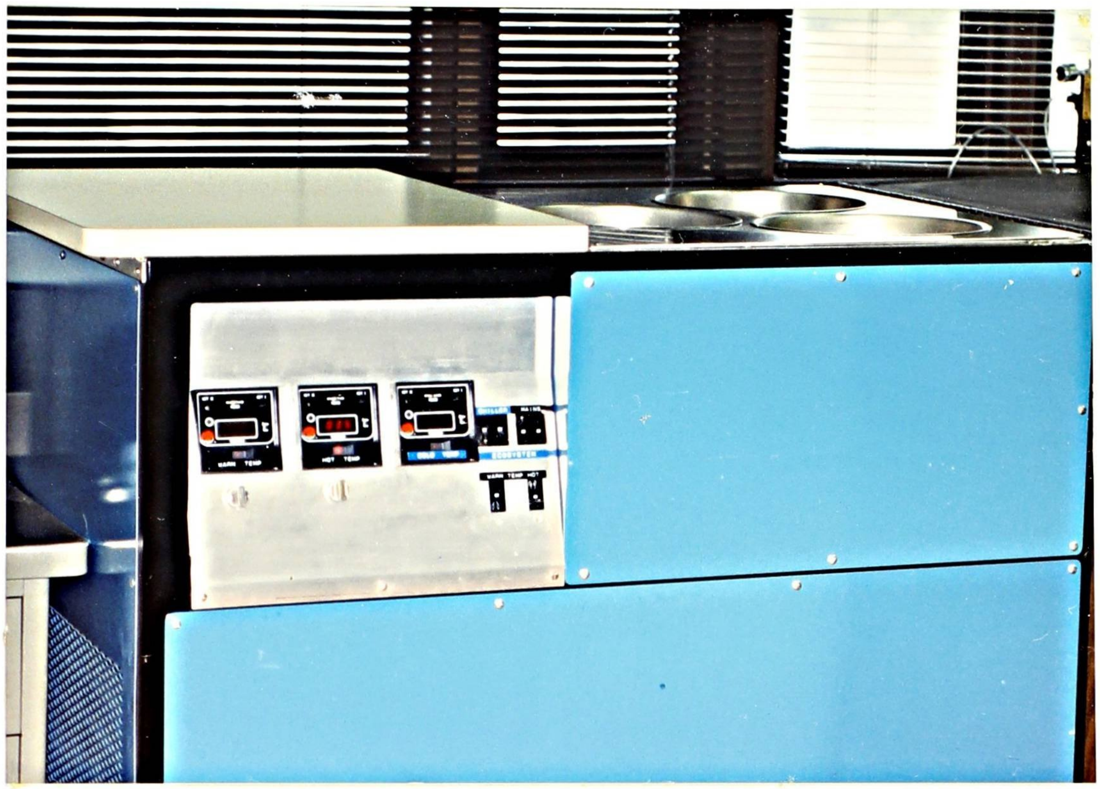

Fig. 2-2. Thermocycler. Three stainless steel reservoirs hold fluids for circulation within the environmental chamber. These fluids may be heated or refrigerated.

Temperature control is particularly important for measurement of surface anatomy because of temperature related expansion and contraction of the materials. The apparatus will tolerate corrosive or cariogenic fluids and is capable of pumping fluids with the viscosity of syrups.

2.2 Anatomic measurement

Anatomic measurement was also added to the system using profilometry in combination with computer graphics (Fig. 2-3).[91] A tungsten carbide stylus with 10° included angle was connected to an extensometer with the tip of the stylus in contact with the surface to be investigated. The system is capable of measuring a variety of geometries, ranging from a flat disk to the occlusal surface of a natural tooth or replica. The tooth is positioned on 2 sliding tables which are mounted on the vertical piston of an MTS servohydraulic testing instrument. The tooth position is controlled in three dimensional space under the tip of the stylus using two stepmotors for the horizontal control (X & Y) with the servohydraulics controlling the vertical or Z axis position.

The stylus follows the anatomy of the tooth and the coordinates of 256 points along its traversal are fed into an array through an analog to digital (A/D) converter in the microcomputer. Each pass across the surfaces requires 10 seconds and constitutes one profile. Generally, 100 micron steps are made between profiles. A large number of profiles generated at known intervals can be assembled by computer graphics to provide a 3D image of the surface on the computer screen consisting of up to 30,700 data points for a typical molar tooth.

A software program has been written to analyze the profile data by fitting two images ("pre-wear" and "post-wear") together. This is essential if progressive clinical wear is to be evaluated at future recall visits. A least squares fit algorithm is employed on a profile by profile basis. The goodness of fit is determined by the root mean square (RMS) of the difference between the images. When the best fit is achieved the profiles can be visually inspected on the computer screen to identify areas of change in surface contour. These areas can be limited by the screen cursor and calculations of mean depth and maximum depth of change of contour can be done. If a number of profiles are involved, the change of contour can be integrated using Simpson's Rule to arrive at the volume of the change in surface contour. The data analysis software was originally implemented on an Apple IIe (Apple Computer, Cupertino, CA) microcomputer. Recently the program has been ported to a PC/AT class microcomputer and 32 bit superminicomputer (Masscomp, Massachusetts Computer Corporation, Westford, MA) with significant enhancements in graphics resolution, speed, and ease of use.

The accuracy of measurement of the system was determined by profiling an objective reference of known volume in the range of a clinically realistic volume change. A small case hardened ball bearing was pressed into a much softer polished aluminum surface. Two depressions were produced in this way of appropriate volume and with a good approximation to the segment of a sphere. By gauging the diameter and greatest depth, which can be done to 1 micron accuracy, the volumes of contour change can be calculated using mensuration formulae. The two depressions were profiled using 15 individual profiles. By using Simpson's integration, the volumes of the two depressions could be measured. The volume of 0.0281 mm^3 was measured with 2.5% error. The smaller volume of 0.006 mm^3 was measured with 12% error. This probably

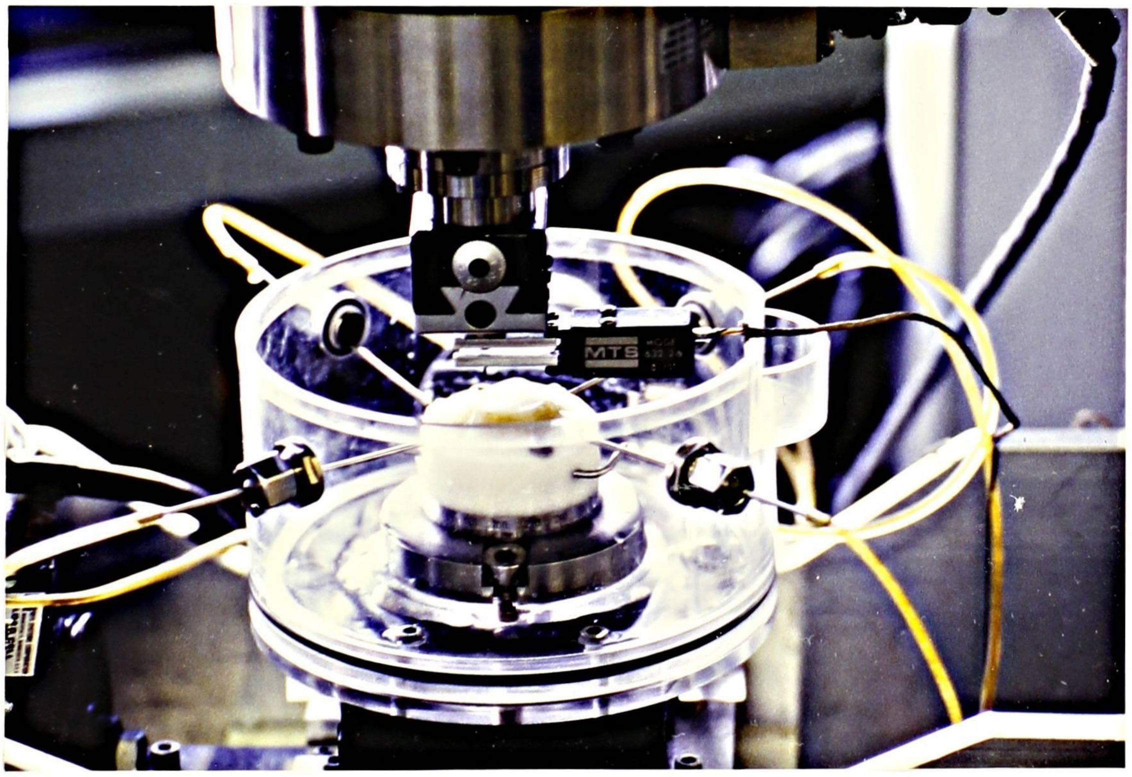

Fig. 2-3. Profiler. A tungsten carbide stylus is mounted in a strain gage extensometer under which the sample is passed. Constant temperature is provided by circulating fluids.

represents the threshold volume that can be measured by the computer graphic measurement system described.

2.3 Enhancements and contributions to existing technology

A systems approach was used to optimize testing procedures and to maximize reproducibility through standardization of the testing configuration. Profiling increments were established to maximize throughput of the system which permitted completion of over one year's masticatory effort in less than 24 hours. Defaults were installed into the software controlling the profiling system. A series of 30 profiles spaced 100 micrometers apart was found to be adequate for encompassing the wear facet on both the test sample and opposing cusp.

A mounting system was developed to provide uniform placement of the test material and palatal cusp opposing the sample (Fig. 2-4). Specifications were made for the uniform size of the test sample and a split ring mounting system was developed for simple mechanical retention of the test disk eliminating the need for any mounting media. This mount provided for uniform placement of all sample disks with the sample plane oriented parallel to the horizontal axis of movement. Custom silicone molds were fabricated for mounting the palatal cusp quickly with chemically cured composite which was found to endure thermocycling of various fluids. The mounting material needed to be sloped away from the enamel cusp without any undercuts to allow for profiling of the sample.

A computer network written in the Pascal programming language was developed to permit rapid and error free transfer of data between the Apple IIe, PC/AT, and Masscomp com-

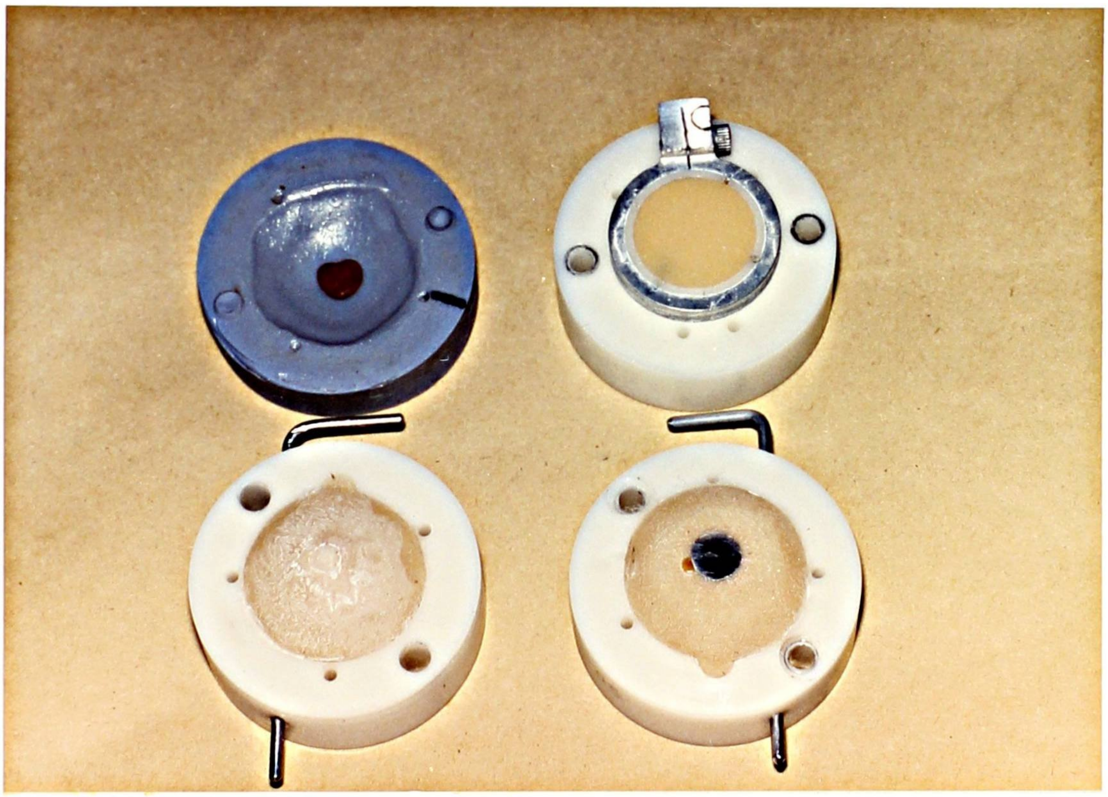

Fig. 2-4. Mounting system. Left: silicone mold for the natural palatal cusp with mounted cusp in composite below. Right: split ring mount for sample disk. Alloy mounted in composite below.

puters. Networking was performed through hardwiring of the serial ports of the machines. Transfer rates of 19,200 baud were achieved with error checking. This allowed data collected via the Apple II computer to be transferred to either the PC/AT or Masscomp for rapid data analysis. The PC/AT and Masscomp computers were linked to a Tektronix 4696 color ink jet printer (Tektronix, Beaverton, OR) and Hewlett-Packard PaintJet printer (Hewlett-Packard, Palo Alto, CA) for screen prints in color.

Software was written with Dr. Ralph DeLong utilizing the rapid data acquisition system of the Masscomp computer for friction measurements during wear experiments on the artificial mouth. Sampling rates up to 1 MHz for 16 channels are possible. The FORTRAN program opened the appropriate analog to digital (A/D) acquisition channels and then triggered collection of lateral force, lateral excursion stroke, vertical load, and vertical stroke which was synchronized with the function generator on the artificial mouth. The data arrays were passed to the Masscomp graphics processor which displayed frictional force as a function of lateral excursion. A particular lateral excursion could be tagged interactively with a mouse or joystick to determine the coefficient of friction.

A microchamber was developed to allow recirculation of small volumes of fluids, such as natural saliva. Two hypodermic syringe needles were used for the ducts and the fluids were recirculated with a peristaltic pump. The total volume of the microsystem was approximately 10 ml. Databases were developed to provide quick correlations to other studies. A comprehensive systems manual with diagrams and photographs was developed permitting standardized operation of the instrument.

2.4 Experimental procedure

2.4.1 Wear simulation and assessment

A series of experiments were designed using the servohydraulic based artificial mouth for testing of a critical choice of dental materials: dental amalgam, composite and dental porcelain. These materials were chosen because they represent the most commonly used materials in clinical dentistry. Recently published clinical studies were used to test retrospectively the correlation between the clinical wear of amalgam and composite with results obtained in the artificial mouth.

Opposing maxillary and mandibular elements were mounted in the artificial mouth. Recently extracted human maxillary third molars were stored in deionized water at $4^{o}C$ until use. The palatal cusp was isolated and sectioned, and served as the natural enamel antagonist for the study materials. The mandibular element in each case was a disk of test material of standard diameter and thickness. The maxillary and mandibular elements were mounted in nylon rings using the mounting jigs described earlier with a laboratory prepared chemical-cured composite containing 50/50 (w/w) ground quartz (Fig. 2-5). The inhibition layer of the cured composite mounting material was removed and voids were filled with a light cured composite.

Before each masticatory test, the apparatus was configured to record the occlusal anatomy of both the mandibular and maxillary elements as previously described. The occlusal surfaces were mapped and digitally recorded onto 5" floppy disks using a microcomputer. This procedure was followed at the beginning and end of each masticatory test, enabling the change in occlusal contour to be determined quantitatively and visually in terms of computer graphics.

During each masticatory cycle, the following parameters were maintained (Table 2-1): a lateral excursion of 0.82 mm; occlusal force at 13.35 N (3 lbs.) with a force profile in the form of a half sine wave; time of cuspal contact 0.23 sec; and a chewing rate at 4 cycles/sec. Deionized water was circulated at 37°C during mastication and conveyed through ducts onto the occluding surfaces.

Three replications were carried out for each experiment. Generally, the experiment was interrupted and occlusal measurements were made at 30,000; 100,000; 200,000; 300,000; and 500,000 masticatory cycles. For the composite, early wear was of interest, therefore, the chewing cycle was interrupted at 30,000, 85,000, and 300,000 cycles. The recorded profile data was analyzed and occlusal change was recorded in terms of depth and volume.

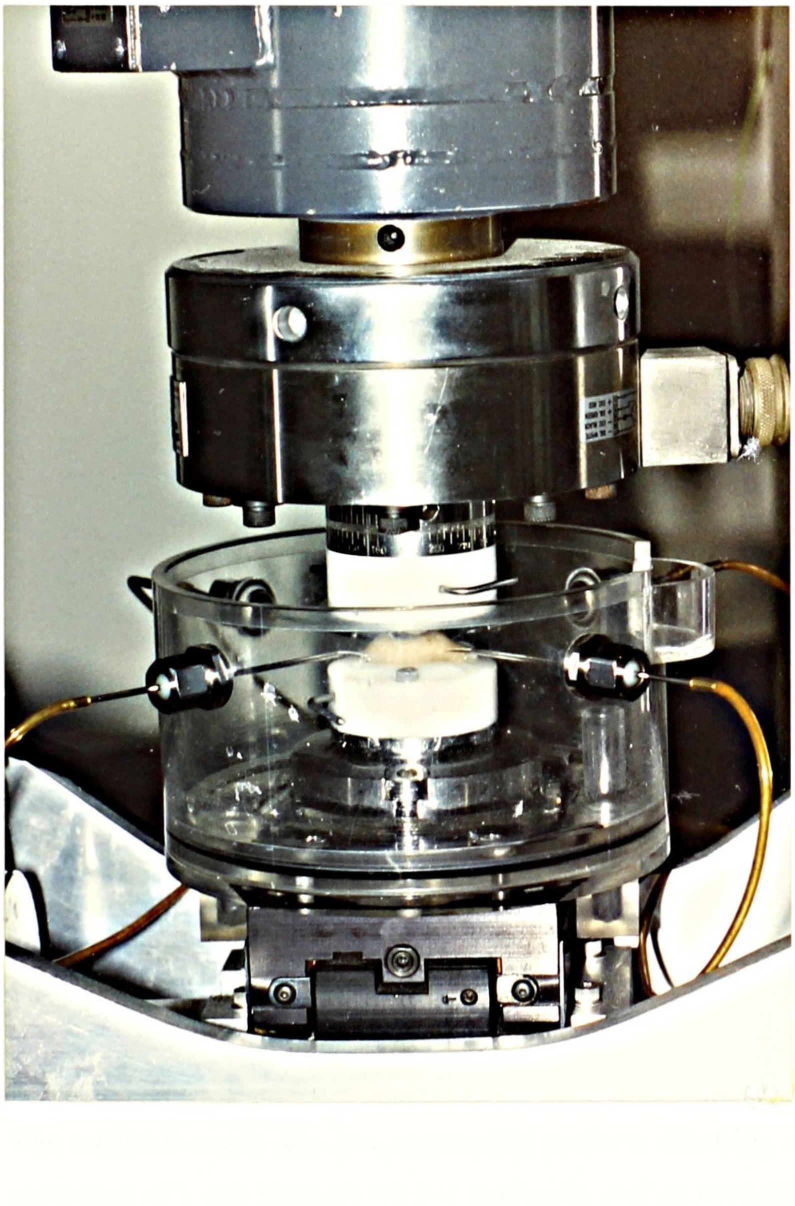

Fig. 2-5. Test configuration in the artificial mouth

Table 2-1. Parameters for mastication

Maximum occlusal force	13.35 N (3 lbs)
Force profile	half sine wave
Lateral excursion	0.82 mm
Masticatory rate	4 Hz
Environmental temperature	37°C

The maxillary enamel cusp and mandibular sample disk were sectioned with a diamond wheel and mounted onto SEM stubs with quick set epoxy. These specimens were gold sputter coated (EMS 76, Fulham) for 2 minutes at 35 volts then placed into a scanning electron microscope (Hitachi S450, Hitachi Electronics, Japan). The energy dispersive attachment was used to identify chemical species on the surfaces. A low magnification orientation view (50X) was

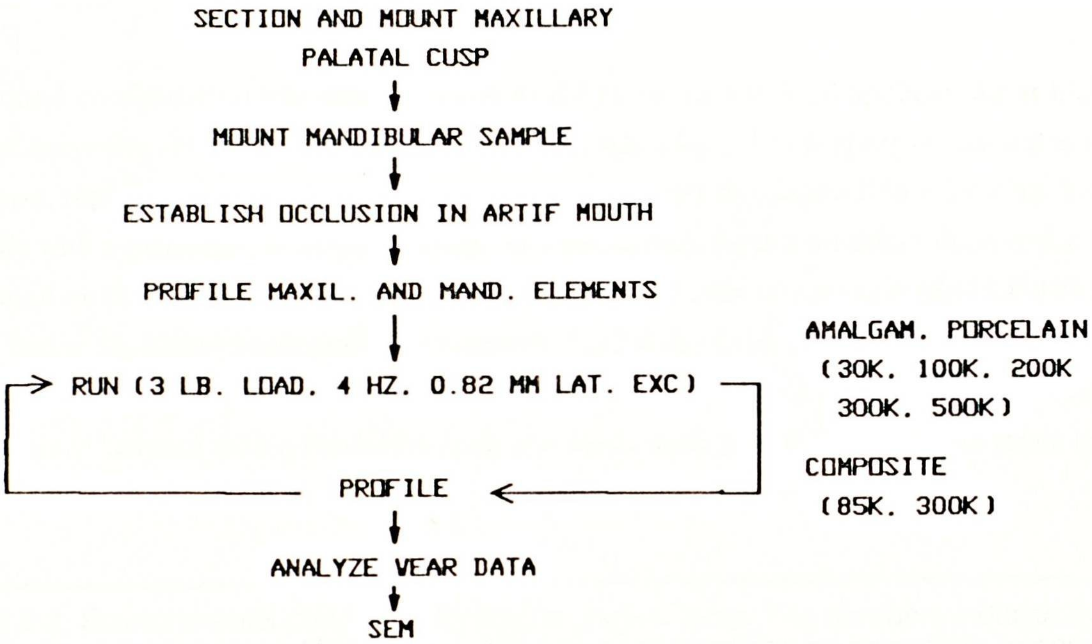

Fig. 2-6. Experimental procedure

taken followed by higher magnification (900-4000X, 15-20 KV) views of the center of the wear facet and edge at each side of the facet. Figure 2-6 lists the experimental procedure in flow-chart form.

2.4.2 Measurement of friction

A series of experiments examined frictional dependence on fluid environment. Opposing pairs of human premolars from the same patient were stored in de-ionized water at 4° C. The teeth were mounted in nylon rings using a laboratory prepared, chemically cured composite. The physiologic relationship between the maxillary and mandibular premolars was established with the mandibular buccal cusp in contact with the lingual incline of the maxillary buccal cusp. In this manner, 4 pairs of human premolars were established successively in the artificial mouth. The artificial mouth was programmed to perform a bruxing motion (Table 2-2) with a lateral excursion of 1 mm through centric occlusion and an occlusal force of 13.35 N (3 lbs) on the

Table 2-2. Bruxing parameters for friction experiments.

Maximum occlusal force	13.35 N (3 lbs)
Lateral excursion	1 mm
Velocity	2 mm/sec
Environmental temperature	37°C

single tooth pair. The velocity of the lateral excursion was 2 mm per second. A physiologic oral environment was simulated by circulating fluids maintained at 37° C onto the occluding surfaces. A coefficient of friction, μ, was derived from both the buccal and lingual excursions. Environmental conditions were changed by altering the circulating fluids (H_2O, dry, Xerolube, human pooled centrifuged saliva). The following procedure for changing the environmental fluids was employed: occlusal surfaces were cleaned with ethanol and acetone, and dried with oil-free compressed air (Table 2-3). The surface was wetted with the new fluid, and bruxing was continued until equilibrium was achieved.

A second configuration was desired which would allow for low load applications at higher lateral excursive velocities. A phonograph tonearm was adapted by keeping the gimbal mount and arm, replacing the cartridge with an aluminum cylinder that tapered to a flat plate in the middle with a platform for weights on top. An enamel cusp from a maxillary third molar was mounted on the end of the cylinder with epoxy. Semiconductor strain gages (S/U LP-120-160 gage factor 55, Kulite Semiconductor Products, Inc., Ridgefield, NJ) were bonded onto the flat of the aluminum plate in opposition using the manufacturer's recommended adhesive. These were covered with a Bis-GMA resin and leads were attached. The entire strain gage

Table 2-3. Environmental conditions for friction experiments. The numbers indicate the sequence of environmental fluids used. All tooth pairs were natural premolars opposing natural premolars. All fluids were circulated at 37° C.

Intervening environmental fluid	tooth pair number				
	1	2	3 run 1	3 run 2	4
H_20	1	1	1	1	1
Saliva, centrifuged	2	2	3	2	4
Xerolube	3	4	4	3	2
Dry	4	3	2	4	3
H_20	5	5	5	5	5
Petrolatum gel		6			
Other environmental conditions					
H_20		7			
H20 on roughened enamel		8			
Petrolatum gel		9			
Cleaned, H_20		10			
H_20 on roughened enamel		11			
Lubricant, oil		12			
Cleaned, H_20		13			

Table 2-4. Substrates and lubrication regimes

enamel on glass	enamel on enamel
loads: 2, 10, 20 gms velocities: 1.5, 3, 5, 10, 15, 20 mm/sec	loads: 2, 10, 20 gms velocities: 1.5, 3, 5, 10, 15, 20 mm/sec
lubricants glycerol glycerol and surfactant	lubricants none (dry) water glycerol glycerol and surfactant

network was covered with a vinyl polysiloxane impression material to protect it from environmental effects (Figure 2-7).

The MTS Bionix 858 Testing Instrument (MTS, Eden Prairie, MN) (Figure 2-8) is a second generation "artificial mouth" with four station capability, although two stations are currently installed. (The two machines will be referred to as Bionix and the artificial mouth). The philosophy of this machine is slightly different from the artificial mouth in that it utilizes a vertical actuator for vertical movement of the maxillary member and a horizontal actuator for the mandibular member. Thus, lateral excursion is provided by the mandibular member and the vertical motion by the maxillary member. In contrast, the artificial mouth provides vertical and horizontal movement through two actuators on the mandibular element alone. No motion is produced by the maxillary element.

The Bionix was configured for a bruxing lateral excursion from 0.3 mm to 4.0 mm at a rate of 1 cycle/0.2 sec. The strain gages were configured in a half Wheatstone bridge amplified by a strain gage conditioner (Micromeasurements 2120, Measurements Group, Inc., Raleigh, NC) then output to an XY recorder (Omnigraphic 2000DX, Houston Instruments, Austin, TX). The circuit was zeroed before each run.

The substrates and lubrication regimes are listed in Table 2-4. An optically flat glass slide, bovine enamel, human enamel, and restoratives were used as substrates. The lubricant was placed onto the surface with the cusp immersed and fully bathed in lubricant. The palatal cusp was acid etched and dried prior to each experiment. Brass balance weights of 2, 10, and 20 grams placed onto the platform served as the occlusal loads.

In summary, the artificial mouth was utilized for the wear simulation and assessment (profiling) of the dental materials chosen. Recently, an independent profiler has been developed solely for the purposes of assessing wear. The concepts of this new instrument are similar to that of the artificial mouth. The MTS Bionix, although quite capable of wear simulation in its own right, was utilized only for lateral excursive movements in friction and lubrication studies.

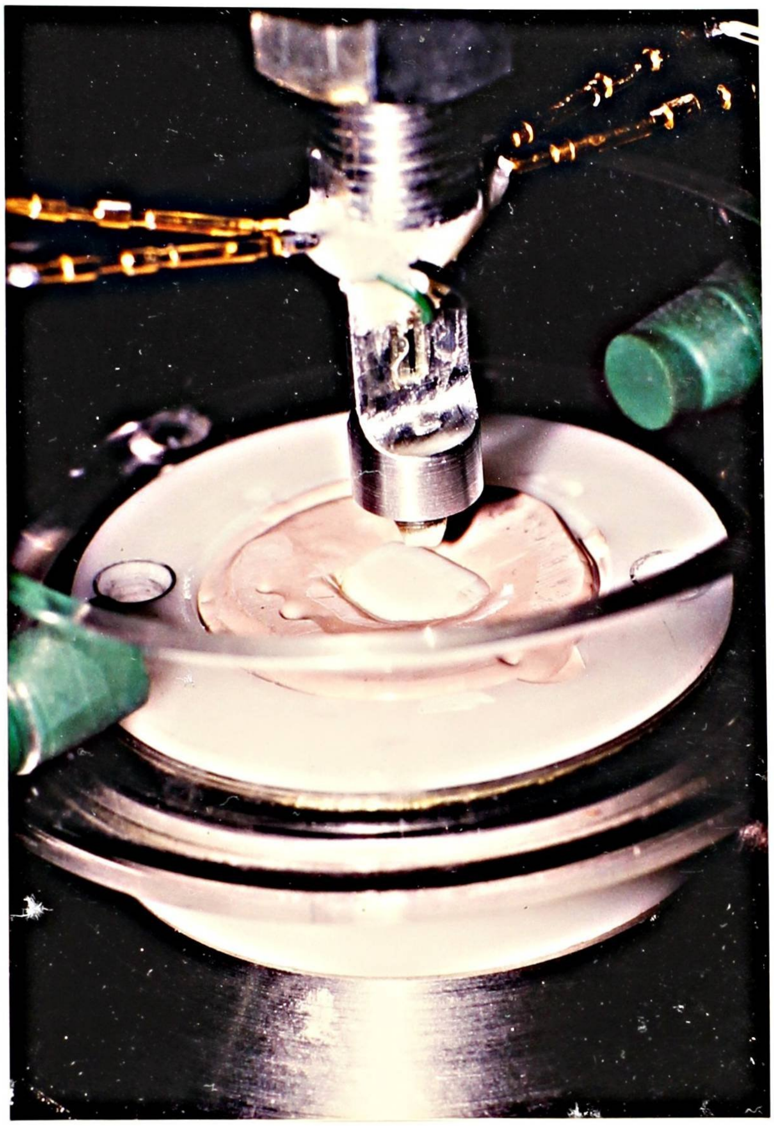

Fig. 2-7. Maxillary friction instrument with semiconductor strain gages.

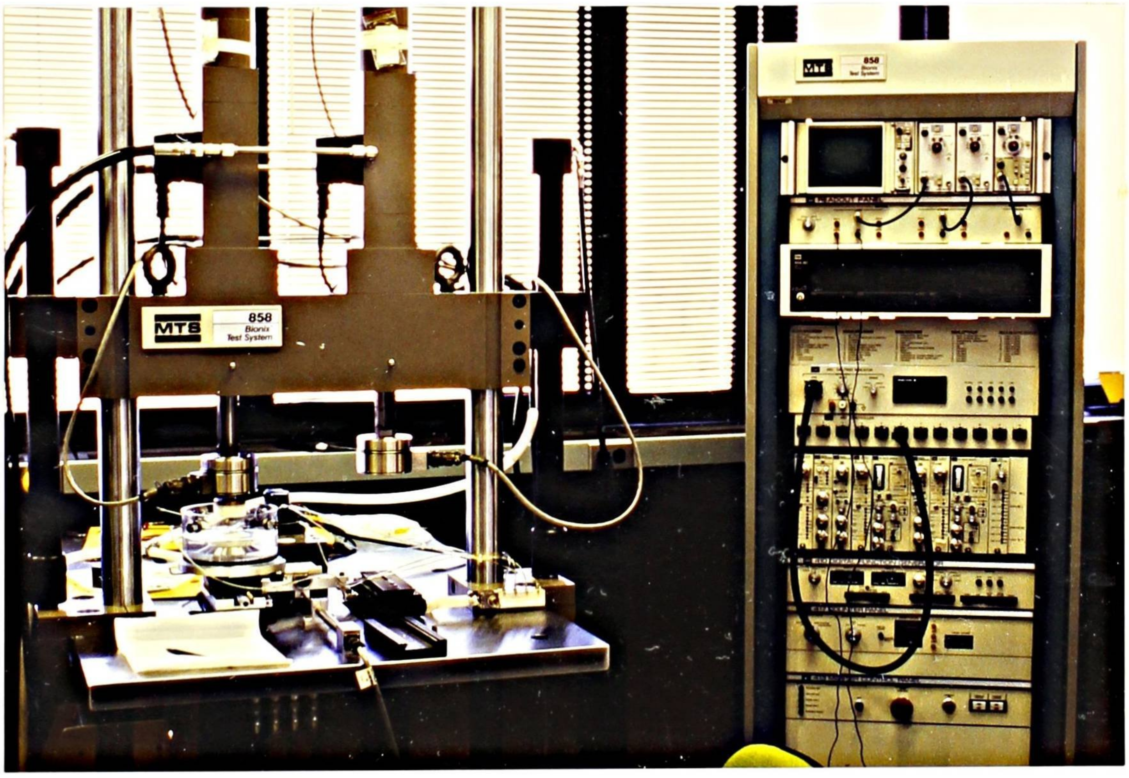

Fig. 2-8. MTS Bionix Test Instrument

3 Influence of environmental control

One of the requirements for successful simulation of the oral environment, as indicated in Chapter 2, is incorporation of a fluid which mimics saliva in the modification of occlusal surface interactions. If the fluid has lubricating qualities, a reduction will be seen in the interocclusal friction at the point of contact in lateral excursions of the mandible.

Friction between occluding teeth produces two main consequences. First, a side thrust is induced onto the periodontal membrane. The vertical occlusal load in conjunction with the lateral movement of the opposing tooth in function creates this lateral component of force. The periodontal ligament is designed to absorb depressive forces along the long axis of the tooth crown and root, however, lateral forces on the occlusal table are damaging because they direct lateral stresses into the supporting alveolar structures. The second sequel to interocclusal friction is occlusal wear of dental materials. The role of saliva may be to serve as a lubricant for the reduction of interocclusal friction and wear. It is of primary importance, therefore, to determine whether saliva provides any advantage over other fluid media for the reduction of friction between dental materials under defined biomechanical conditions.

A load cell was included in the path of the lateral excursion so that the side thrust or the resultant horizontal force on the mandibular element could be accurately monitored. Since the artificial oral environment is capable of measuring the horizontal and vertical forces, if it is assumed that the only force in the horizontal direction is the frictional force, then the coefficient of friction can be calculated from

$$\mu = F_h/F_v \qquad (3\text{-}1)$$

where F_v is the occlusal force measured by the vertical load cell and F_h is the frictional force, or side thrust, measured by the horizontal load cell. This equation is true only for motion in the horizontal plane. For teeth, the path of motion is usually along an incline on the cuspal surface. Therefore, the normal forces no longer equal the occlusal force. However, the magnitude of the normal force at any point on the surface can be calculated from

$$N = F_v \cos\theta \cos\phi \qquad (3\text{-}2)$$

where θ is the angle of inclination of the tangent to the surface parallel to the path of motion at the point of contact. ϕ is defined similarly, except it is perpendicular to the path of motion (Fig. 3-1). During bruxing or chewing it is possible to find a path of motion where ϕ is approximately zero. Then $\cos\phi = 1$ and $N = F_v \cos\theta$. The coefficient of friction can be determined from the geometry by

$$\mu = (F_h \cos\theta + F_v \sin\theta) / (F_h \sin\theta - F_v \cos\theta) \qquad (3\text{-}3)$$

where F_h, F_v, and θ are measurable parameters.

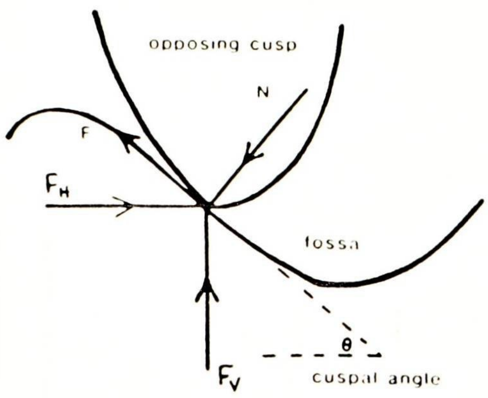

Fig. 3-1. Geometry for determination of coefficient of friction. θ = cuspal angle; F_v = vertical (occlusal) force; F_h = horiz. force (side thrust); F = friction; N = normal force

Figure 3-2 illustrates a typical X-Y record of the side thrust measured by the horizontally positioned load cell. The tracing generated during bruxing motion shows the zero side thrust line through the middle of the record. The distance of the tracing from the zero horizontal load component is determined by the direction of the friction forces and the angle of the cuspal incline. Thus, the coefficient of friction, μ, can be determined under functional conditions.

The results for tooth pairs 1, 2, and 3 are shown in Fig 3-3 with the sequence of environmental fluids used. Fig. 3-4 shows the results for 2 further matched pairs of teeth. One of these was a second run on matched pair 3. The results in Fig. 3-4 are grouped because they show an essential difference from the results in Fig. 3-3. The influence of a number of surface effects are shown on a second run of tooth pair 2 in Fig. 3-5. The arrows and dotted lines in these figures indicate the direction in which the magnitude of the coefficient of friction is moving and the initial and stabilized coefficient magnitudes.

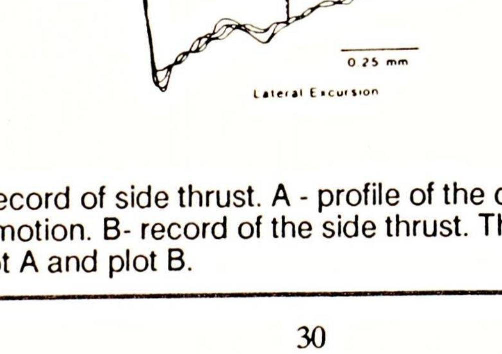

Fig. 3-2. Typical X-Y record of side thrust. A - profile of the contact area showing the shape of the bruxing motion. B- record of the side thrust. The dashed line corrdinates identical points on plot A and plot B.

Fig. 3-3. The coefficients of friction for 3 different premolar pairs with different intervening fluids.

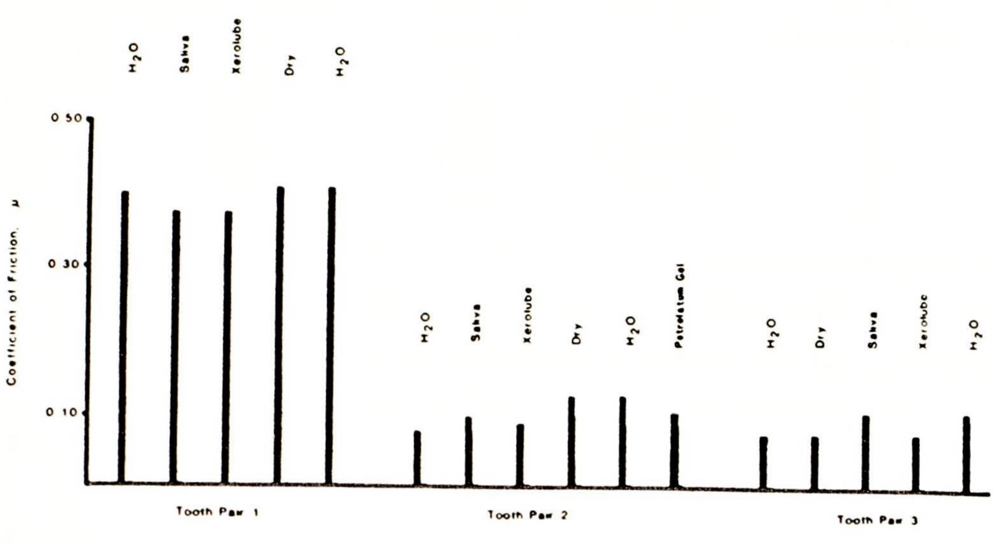

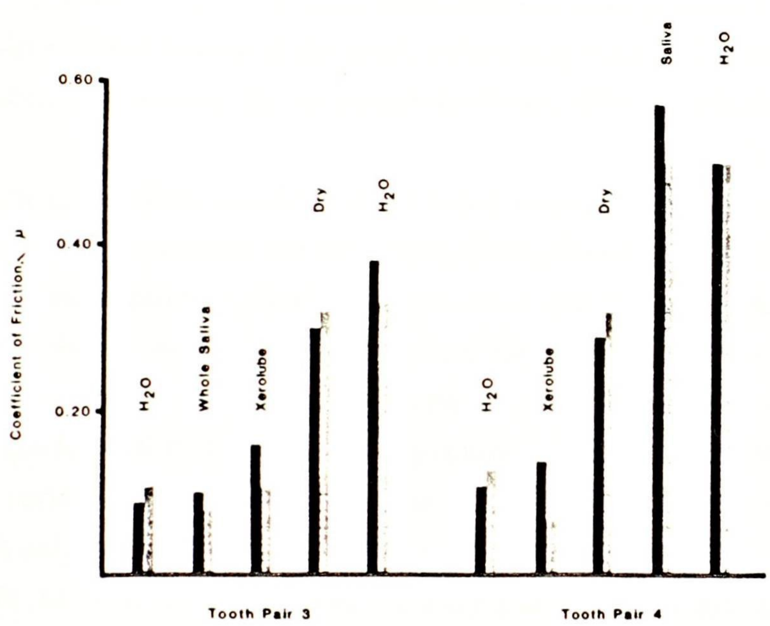

Fig. 3-4. The coefficient of friction for 2 different premolar pairs with different enamel surfaces.

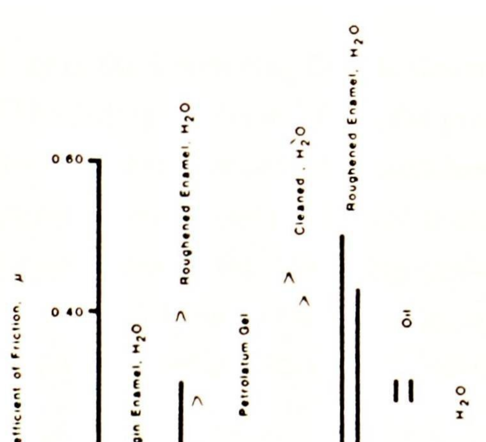

Fig. 3-5. Variation of the coefficient of friction between a premolar pair under different enamel surface conditions

Table 3-1. Coefficients of friction, μ, averaged over all conditions for tooth pair

mean coefficient of friction, μ	coeff. of variation	tooth pair	no. of measurements
0.418	7%	1	20
0.097	18%	2 (run #1)	24
0.1	15%	3 (run #1)	20
0.20	55%	3 (run #2)	20
0.313	58%	4	20

The calculated coefficients of friction averaged over all conditions are shown in Table 3-1 for all sample pairs. This table includes the coefficients of variation and the number of measurements performed. Each measurement in Table 3-1 represents an equilibrium value achieved after 20 lateral excursions.

One of the first observations is the variability of friction on enamel. Within groups, the trends were similar, however the magnitude of the coefficient of friction varied considerably. Although the premolar pairs of teeth were from the same patient, it was not possible to verify the environmental history of the teeth before they were collected. Observations under low power stereomicroscopy did not reveal significant differences in the surface enamel.

Although μ varied for enamel from 0.1 to 0.4, it was difficult to account for it either in terms of chemistry or viscosity of the circulating fluids. However, it should be pointed out that the saliva was subjected to a high centrifugal force and only the supernatant was used. As the velocity of sliding decreases and the occlusal force increases, the teeth are likely to penetrate the intervening fluid and establish true enamel to enamel contact. Under these conditions, μ is the same for all liquids and for the dry condition and is determined by the biophysics of dry enamel surface. The friction under these conditions is independent of the lubricant and dependent only the nature of the contacting surfaces. This was demonstrated by a two-fold increase in the coefficient of friction when the enamel was roughened with an abrasive wheel (Fig. 3-5).

This insensitivity to the intervening fluid is altered by two types of lubricants: high viscosity lubricants and boundary lubricants. Thus, the presence of petrolatum gel on the roughened enamel led to a twofold reduction in the coefficient of friction (Fig. 3-5). The application of a fine lubricating oil also produced a reduction in the interocclusal friction of enamel to enamel contact. Attempts to remove the lubricating qualities with various solvents failed, which is a result of surfactants which form a tenacious film on the enamel surface. This effect is known as boundary lubrication and is quite unrelated to the viscosity of the lubricant.

Table 3-2. Coefficients of friction for amalgam, composite, and porcelain opposed by enamel

amalgam	$0.2 \pm .05$
composite	$0.5 \pm .1$
porcelain	$0.6 \pm .1$
enamel (unmatched pairs)	$0.4 \pm .3$

The results for frictional measurements between enamel and amalgam, composite, and porcelain are shown in Table 3-2. The variability of enamel to enamel friction was much larger than the frictional variability between artificial dental materials and enamel. Friction on amalgam was low while the highest friction was measured between enamel and Ceramco porcelain.

The anisotropic nature of enamel was evident when friction between enamel pairs was evaluated as a function of orientation. Frictional measurements were made at four different orientations between the two enamel contacts functioning on inclines of the cusps (Table 3-3). Rotation of the sample through 90^{o} and 180^{o} from the preferred physiologic orientation resulted in elevated friction coefficients. Returning the sample to the original orientation restored the original frictional value. This is consistent with the orientation of the enamel rods at the enamel surface. The rods are oriented relatively perpendicular to the occlusal surface but have a definite inclination at the surface. Reversing the orientation would change the incidence between the opposing enamel rods from a physiologic sliding contact where the rods slid over each other to that where the rods opposed each other. Normal mastication would not cause this effect, however, bruxing produces preferential and counter-preferential sliding in its reciprocating motion. The coefficient of friction was seen to rise in this "counter-physiologic" mode and could contribute to the elevated wear seen in bruxism. A stick-slip phenomena is also seen in bruxing characterized by a "sawtooth" friction profile. This could be explained by the surface asperities engaging and disengaging as lateral forces are applied resulting in an oscillation between static and kinetic friction.

Although the previously discussed friction measurement system was adequate for examination of friction during bruxing or mastication under average physiologic loads, the study of friction under low loads (8.8 N) and higher velocities was necessary to determine whether fluids were capable of developing adequate film thickness to support the occlusal load. The Bionix configuration described in Chapter 2 with the gimbal mounted arm and maxillary strain gage element eliminated the need for the servohydraulic actuator for load application and

Table 3-3. Coefficients of friction for enamel to enamel at rotations from physiologic orientation in 90^{o} increments

	0^{o}	90^{o}	180^{o}	270^{o}	0^{o}
Coefficient of friction	0.1	0.13	0.18	0.14	0.08

only the servohydraulic driven horizontal tables were employed. This afforded a convenient method for application of low loads (2-30 gms) at velocities higher than those available on the artificial mouth. The geometry of the system was controlled through use of optically flat microscope slides and flat ground sections of bovine enamel opposed by a human palatal third molar cusp.

The friction measurements between enamel and glass recorded on the Bionix experimental configuration is listed in Table 3-4. In general, the application of water intervening between the cusp and substrate resulted in higher coefficient of friction values. Several references[92-94] indicate similar findings. This increased friction has been suggested to be due to the polarity of the fluid and the material being tested influencing the friction. The surfactant with glycerol resulted in the lowest friction values.

Table 3-4. Friction between enamel/glass and enamel/enamel under various environmental conditions

substrate	load (N)	fluid	velocity (mm/sec)	lateral force (N)
enamel on glass	0.015	glycerol	1.5	0.017
			3	0.014
			5	0.004
			10	0.003
			15	0.003
			20	0.004
	0.073		1.5	0.060
			3	0.041
			5	0.029
			10	0.021
			15	0.019
			20	0.020
	0.146		1.5	0.094
			3	0.085
			5	0.062
			10	0.046
			15	0.044
			20	0.041
enamel on glass (#2)	0.015	glycerol	1.5	0
			3	0.011
			5	0.004
			10	0.004
			15	0.004
			20	0.004
	0.073		1.5	0.026
			3	0.026
			5	0.018
			10	0.013
			15	0.011
			20	0.011
	0.146	glycerol	1.5	0.076
			3	0.076
			5	0.052
			10	0.032
			15	0.026
			20	0.026

Table 3-4 cont'd

enamel on glass	0.015	glycerol + surfact	1.5	0.002
			3	0.001
			5	0.001
			10	0.001
			15	0.002
			20	0.002
	0.073		1.5	0.055
			3	0.038
			5	0.012
			10	0.009
			15	0.008
			20	0.008
	0.146		1.5	0.050
			3	0.035
			5	0.026
			10	0.019
			15	0.018
			20	0.018
enamel on enamel	0.015	dry	1.5	0.009
			3	0.012
			5	0.018
			10	0.026
			15	0.018
			20	0.021
	0.073		1.5	0.014
			3	0.029
			5	0.047
			10	0.052
			15	0.048
			20	0.059
	0.146		1.5	0.109
			3	0.124
			5	0.079
			10	0.009
			15	
			20	
enamel on enamel	0.015	water	1.5	0.020
			3	0.029
			5	0.032
			10	0.032
			15	0.032
			20	0.026
	0.073		1.5	0.042
			3	0.085
			5	0.115
			10	0.129
			15	0.135
			20	0.144
	0.146		1.5	0.076
			3	0.106
			5	0.100
			10	0.129
			15	0.159
			20	0.165
enamel on enamel	0.015	glycerol	1.5	0.006
			3	0.011
			5	0.012
			10	0.015
			15	0.014
			20	0.015
	0.073		1.5	0.032
			3	0.038
			5	0.044
			10	0.059
			15	0.050
			20	0.049
	0.146		1.5	0.094
			3	0.072
			5	0.081
			10	0.079
			15	0.100
			20	0.103

Table 3-4. cont'd

enamel on glass	0.015	dry	1.5	0.002
			3	0.002
			5	0.002
			10	0.002
			15	0.003
			20	0.003
	0.073		1.5	0.016
			3	0.020
			5	0.029
			10	0.026
			15	0.027
			20	0.037
	0.146		1.5	0.056
			3	0.038
			5	0.035
			10	0.059
			15	0.056
			20	0.085
enamel on glass	0.015	whole pooled saliva	1.5	0.011
			3	0.011
			5	0.011
			10	0.009
			15	0.012
			20	0.012
	0.073		1.5	0.044
			3	0.047
			5	0.048
			10	0.049
			15	0.047
			20	0.054
	0.146	20	1.5	0.214
			3	0.207
			5	0.149
			10	0.174
			15	0.176
			20	0.180

The data was organized in the McKee format[95] with the coefficient of friction, μ, plotted as a function of $\eta S/P$ where η is the viscosity of the fluid, P is the occlusal load, and S has been modified to represent the sliding speed (Fig. 3-6). The advantage of this format is the ability to distinguish between various lubrication regimes, i.e., boundary, thin film, and thick film. At large values of $\eta S/P$, the friction coefficient is low and proportional to $\eta S/P$ (Petroff's Law). This is the area of thick film or hydrodynamic lubrication. On decreasing $\eta S/P$, the friction passes through a minimum value which distinguishes between thick film and thin film lubrication. The minimum point shifts to the left and becomes more sharply delineated for smoother surfaces. For even smaller values of $\eta S/P$ the coefficient of friction increases rapidly, marking the complete penetration of the lubricant film, denoting a boundary lubrication regime. In general, the shapes of the curves for a particular pair of materials remained constant for different fluids with a shift toward increased coefficient of friction for the systems operating with water or saliva as the fluid (Fig. 3-7).

Although saliva is generally thought of as a lubricant, the coefficient of friction was elevated when saliva intervened between glass and enamel compared to dry conditions. Water had a similar effect with greater magnitudes of the coefficient of friction. It appears that the adhesion of oppos-

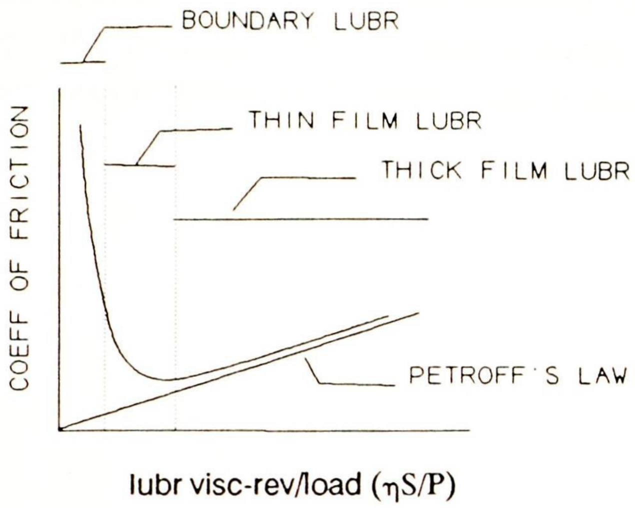

Fig. 3-6.
McKee format for plotting coefficient of friction vs. lubricant viscosity-revolutions/ load in journal bearings

ing asperities under these conditions is greater in the presence of saliva and water resulting in a higher subsequent force necessary for their rupture. Other investigators have found similar findings in the friction of artificial teeth.[96]

The assumption of increased lubrication as a result of increased lubricant viscosity underlies the work of Nordbo, et al.[97-99] and is implied in the mixed lubrication regime, i.e., to the left of the μ-ηS/P minima. Levine[89] could not demonstrate this assumption in a series of experiments on saliva and salivary substitutes.

Lubrication depends not only on the structural chemistry of the lubricant, but also on the biophysical conditions, which may vary from patient to patient. Mixed lubrication may operate in a patient under normal masticatory conditions. However, under heavy masticatory load boundary lubrication may be the only mechanism for reducing friction. Further, certain salivary molecules may provide enhanced thick film lubrication and offer no boundary lubrication. Conversely, other salivary molecules, with strong hydroxyapatite binding sites may offer superior boundary lubrication and little or no thick film lubrication. The two most obvious clinical factors likely to influence the interocclusal friction, therefore, are the lubricity of saliva and the surface texture of the occluding surfaces.

Saliva offers the materials and environment from which pellicle can be formed on the enamel surfaces. Pellicle may be strongly bound onto the surface of hydroxyapatite and may serve as a boundary lubricant. The tests conducted examined freshly etched enamel surfaces stripped of pellicle. The total lubricating effect of saliva may have been masked by removal of the contribution by pellicle. It may therefore be necessary to "incubate" the tooth samples in saliva at physiologic temperatures to promote growth of pellicle prior to frictional measurements. The problem is to limit the bacterial growth which tends to degrade the saliva. Future studies will need to address this factor.

On the basis of this study, a significant difference in the frictional characteristics in enamel couples was not observed when saliva or water intervened. Considering the convenience of water over saliva as the circulating fluid in the artificial mouth, deionized water circulated at physiologic temperature (37°C) was used for the subsequent wear studies.

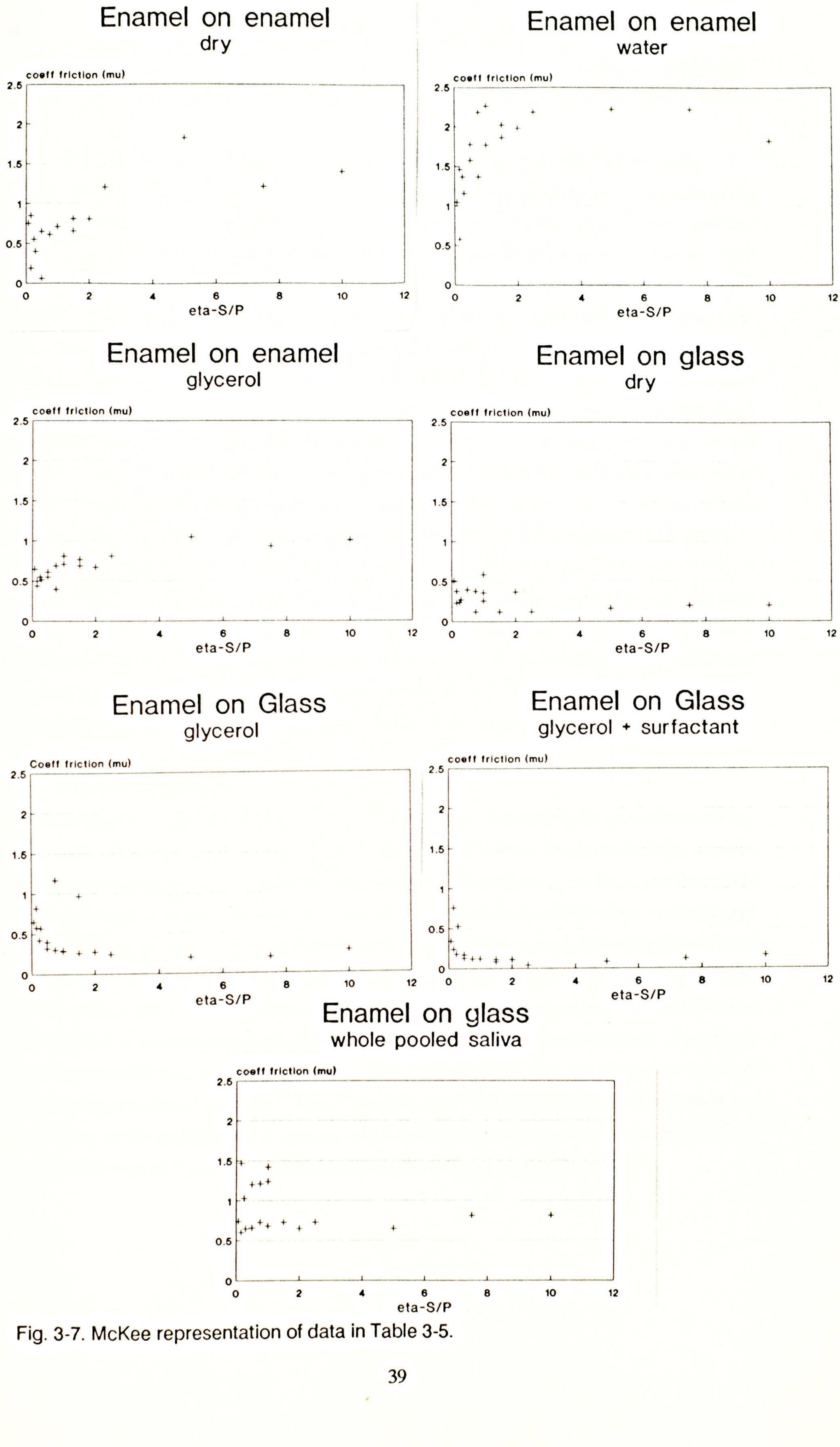

Fig. 3-7. McKee representation of data in Table 3-5.

4 The Wear of a Critical Choice of Dental Materials

4.1 Development of clinical parameters in the artificial mouth

The correlation of artificial mouth studies to clinical studies required the determination of the clinical equivalence of an artificial mouth masticatory cycle. Coffey, et al.[100] used artificial teeth for this pilot study in occlusal wear. Artificial teeth are uniform in occlusal form which facilitated establishment of an occlusion in the artificial mouth. A parallel clinical study[101] permitted comparison of clinical years to artificial mouth masticatory cycles. An average occlusal force of 2.5 pounds (5.0 pounds maximum) was employed, with a lateral excursion of 0.5 mm and cuspal contact time of 0.25 secs. Calculations indicated that 300,000 masticatory cycles gave a clinical equivalence of 16 months for acrylic teeth and 8 months for IPN teeth (interpenetrating network; highly cross linked improved resin). It was evident that the difference in wear resistance between the two materials was overemphasized which was seen in simpler wear machines which developed too much abrasive effort. A reduction in occlusal force and slight lengthening in lateral excursion corrected this discrepancy. The ability to change physiologically recognizable parameters interactively is a major advantage of the artificial mouth. A study of dental amalgam was conducted to verify the premise that the masticatory parameters of 3 lbs occlusal load (1.5 lb mean), 0.82 mm lateral excursion, and use of deionized water as the circulating fluid produced one year of clinical wear at 250,000 cycles. A recent clinical study on amalgam by Lambrechts, et al.[61,63] allows a retrospective comparison with artificial mouth data which will verify the assumption.

4.2 Dental amalgam

Dental amalgam is distinguished from many other direct restoratives by a resistance to occlusal wear. This property makes it one of the materials of choice for stress-bearing areas in the posterior segment of the dental arch. The inclusion of dental amalgam for any in vitro study of occlusal wear is necessary, since it is one of the standards by which other materials are judged. The loss of contour of dental amalgam is quite small in comparison with other dental materials such as composite. Lambrechts[63] found that dental amalgam typically loses 200 μm in contact areas after 4 years in the mouth and 24 μm in non-contact areas. Non-contact wear of composites amount to over 40% of the total occlusal attrition. The mechanism of amalgam wear appears to be that of smearing and transfer of the material onto the antagonist as found in sliding experiments of Roberts,[17] Rice,[66] and Mueller.[4] Although there is considerable understanding of the amalgam wear process when opposed by enamel, there is no clear indication why the wear of this couple should be so small in clinical experience.

Table 4-1. Amalgam loss of contour by volume

years (250,000 cycles = one year	masticatory cycles in thousands	volume changes (mm^3)
.12	30	.00425 ±.0049
.4	100	.0136 ±.0048
.8	200	.0136 ±.004
1.2	300	.0307 ±.0036
2	500	.052 ± .0063

Table 4-2. Amalgam loss of contour by depth in an artificial mouth

Years (250,000 cycles = one year)	Masticatory cycles in thousands	Maximum depth in microns (μm)
.12	30	20±11
.4	100	39±3.9
.8	200	57±1.7
1.2	300	72±1.7
2	500	94±2.5

Using the techniques and instrumentation described in Chapter 2, amalgam disks (Dispersalloy, Johnson and Johnson, NJ) were prepared to a size of 12 mm in diameter by 3 mm in thickness. Three spills of alloy were amalgamated and condensed into split steel molds. The amalgam was carved, and after 24 hours storage in water at 37°C, one face was finished and polished, precisely following clinical procedures.

The loss of surface contour of amalgam due to wear is shown by volume in Table 4-1. In Table 4-2, amalgam wear is recorded by maximum depth of the wear facet. A plot of the raw data in Table 4-2 is shown in Fig. 4-1, with the clinical data of Lambrechts[61,63] superimposed. The regression constants for these 2 sets of data are shown in Table 4-3. The clinical data has been recalculated using the clinical regression line as shown in Table 4-4.

In the scientific literature, there is no generally agreed method of reporting wear. Volume loss may be a more fundamental measurement than depth of loss because it is less dependent on the morphology of the opposing cusp. However, clinically, it is usually the depth of loss of the occlusal surface due to wear, that is assessed. Table 4-3 shows that the wear of amalgam in the artificial mouth gave a near linear relationship with respect to the depth of loss. The wear depth is curvilinear near the zero (time of placement), however, a linear relationship is quickly established. A linear relationship is also shown for the clinical study in Table 4-3 and Fig. 4-1.

Fig. 4-1. Graph of the artificial mouth and clinical wear data.

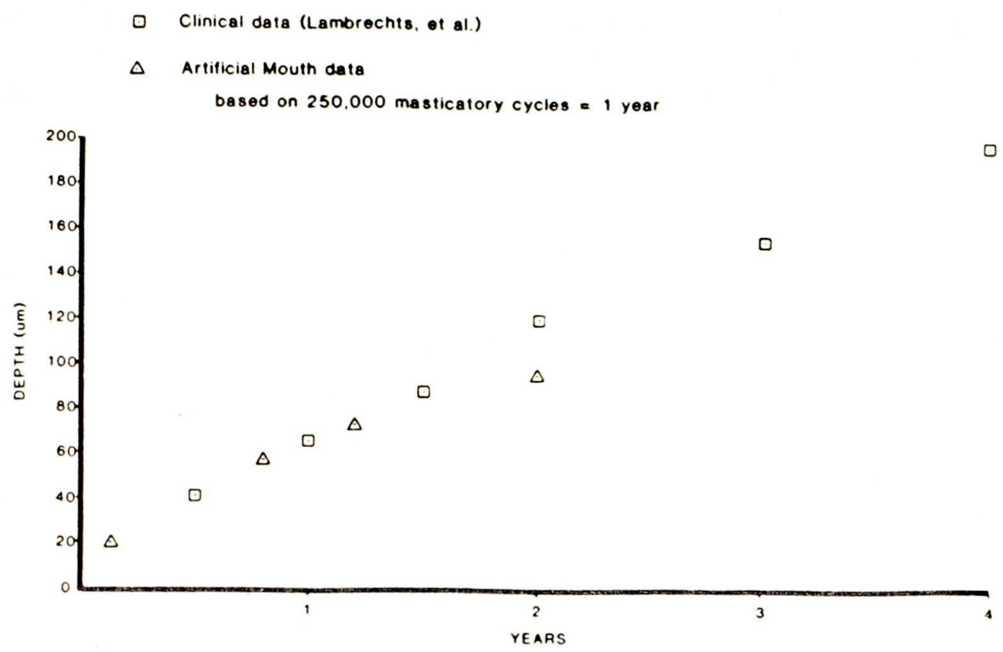

4.2.1 Clinical Correlation

The linear correlation between clinical wear and artificial mouth wear was very close at 250,000 masticatory cycles which is equivalent to one clinical year. The correlation coefficient was 0.938 for two years of clinical wear.[63] The typical coefficient of variation for the artificial mouth study (20%) was significantly lower than that for the clinical study (50%). The small coefficient of variation and the high correlation with clinical results indicate the ability of the artificial mouth to simulate clinical mechanisms and to predict clinical wear rates.

4.2.2 Mechanism of wear

The transfer of material from the amalgam surface to the opposing enamel cusp is characteristic of an adhesive wear mechanism (Fig. 4-2). These adhesions are clearly shown on the SEM photomicrograph. Energy dispersive analysis showed in every case that the adhesions were dental amalgam.

If adhesive wear is hypothesized then the coefficient of wear can be calculated on the basis of wear volume, occlusal load, and indentation hardness. As shown in chapter 1,

Table 4-3. Regression constants for wear studies on amalgam against enamel

	Slope	Y intercept	Correlation coefficient
Clinical* study	44.71	21.43	.997
Artificial mouth study	38.31	21.77	.98

* Lambrechts et al.

Table 4-4. Recalculated clinical data using the clinical regression line.

Time years	Clinical studies* (regression line) µm	Artificial mouth (raw data) µm	Correlation coefficient between artificial mouth and clinical studies
.12	26.8	20±11	
.4	39.3	39±3.9	
.8	57.2	57±1.7	
1.2	75.1	72±1.7	
2	110.8	94±2.5	0.938

* Lambrechts et al.

Fig. 4-2. Scanning electron micrograph of enamel cusp after 500K masticatory cycles againist amalgam. The edge of the contact area is shown with amalgam adhesions.

$$V/L = K\,W/3P \qquad (1.6)$$

assuming circular areas of contact and hemispherical wear particles. Given the parameters under which the artificial mouth studies were performed, $W = 13.3$ N, $P = 1079$ MN/m^2, $L = 0.82$ mm times the number of cycles, the mean wear rate for all runs, $V/L = 1.07 \times 10^{-7}$ mm^3/mm, then

$$K = 2.6 \times 10^{-5}$$

K can be considered a probability coefficient and indicates that approximately 10^5 asperity interactions must be made before a wear particle is produced. This suggests an explanation for the wear resistance of amalgam and suggests the fatigue process operating in conjunction with an adhesive wear mechanism.

Once a transferred layer of a soft metal is formed on a harder surface, cold welding of the surfaces is no longer possible.[77] Therefore, the transfer of amalgam to the opposing enamel cusp limits further asperity adhesion. The effective surface area available for asperity interaction is controlled by the rate of removal of transferred material and formation of loose wear particles. A fresh enamel surface will have amalgam transferred to it at a faster rate than a surface that has been partially contaminated with amalgam smears. After the surface has received an initial transfer coating, further transfer and release of the smeared material continues at a relatively constant rate. This would explain the early elevated wear rate that subsequently reaches a steady state.

The coefficient of friction may be calculated using published values for shear strength and yield pressure.

$$\mu = S/P = \text{shear strength/yield pressure} \qquad (1.21)$$

$$\mu = 188/1079 = 0.17$$

The yield pressure used in the above equation is that of the softer of the two opposing materials (amalgam) and can be taken as the indentation hardness of the softer material.[102] The calculated coefficient is quite close to reported experimental values of 0.1 to 0.18 [92] and those determined experimentally using the artificial mouth (0.2). When the calculated coefficient of friction (equation 1.21) and the measured coefficient begin to approximate each other, it is a characteristic indication of an adhesive friction and wear mechanism.

It is apparent from the values of the coefficient of friction, wear rate, and coefficient of wear that the primary mechanism of wear operating between amalgam and enamel is that of adhesion. The characteristic transfer of material from the softer amalgam to the enamel cusp can be seen on the SEM photomicrographs. The resistance of amalgam to wear is due to the moderately high fatigue strength under the clinical simulated conditions, which required approximately 10^5 flexions of an enamel/amalgam surface junction to produce a wear particle. This supports the theory of shear and slippage at the interface resulting in transfer or wear particle production caused by adhesion between opposing asperities during sliding contact.

Gross amalgam transfer in the form of silver and mercury to the enamel pin was also noted by Mueller, et al.[4] who also concluded that the wear progressed by shear and welding rather than by abrasion.

4.3 Posterior composite

Although the early composites were designed for aesthetic restorations in the anterior segment, modifications of the resin and filler improved the material for use in occlusal stress bearing areas, i.e., the posterior segment. Improved aesthetics is of questionable advantage in the molar region, however the benefit of bonding to remaining tooth structure and integration of the restoration to the natural tooth is attractive.

Although composites satisfy most of the requirements for an acceptable filling material, they are prone to wear.[36] The wear is a very specific and characteristic loss of surface resulting in a 'dished out' appearance which is the chief criticism of these materials. The publication of quantitative clinical data for wear in the occlusal contact area[62] make retrospective clinical correlations with artificial mouth studies possible. Because of the nature of current clinical measurement methods as discussed in Chapter 1, most of the discussion centers on depth of wear in the occlusal contact area (OCA) wear.

The particular composite studied was P10 (3M Company, St. Paul, MN, USA), a fine grind quartz/BisGMA resin type material. Disks of material 12 mm in diameter by 3 mm in thickness were prepared and cured under pressure between plastic sheets. The material was mixed and finished according to the manufacturer's instructions. The maxillary member was the palatal cusp of a maxillary third molar and the mandibular member was the autocured composite disk. The maxillary and mandibular elements were mounted in nylon rings and stored in deionized water at 37°C until installation in the artificial mouth. The protocol was identical to the previous amalgam study in all occlusal and environmental factors, however, different time intervals were chosen because of the clinical interest in the shape of the early wear curve. The experiment was stopped at 85,000 and 300,000 cycles and the maxillary and mandibular surfaces were profiled. These two profiling intervals were chosen because (1) consideration

Table 4-5. Depth and volume of wear in the occlusal contact area of a posterior composite in an artificial mouth

	depth of wear mm		volume of wear mm^3	
masticatory cycles sample I.D. no.	85k	300k	85k	300k
57	.0313	.0463	.016	.037
65	.047	.068	.023	.049
80	.035	.052	.021	.047
61	.053	.072	.027	.057
71	.038	.057	.018	.040
mean (standard deviation)	.041 (± .008)	.059 (± .01)	.021 (± .004)	.046 (+ .007)

Fig. 4-3. Occlusal wear curves for artificial mouth results with Braem clinical results superimposed.

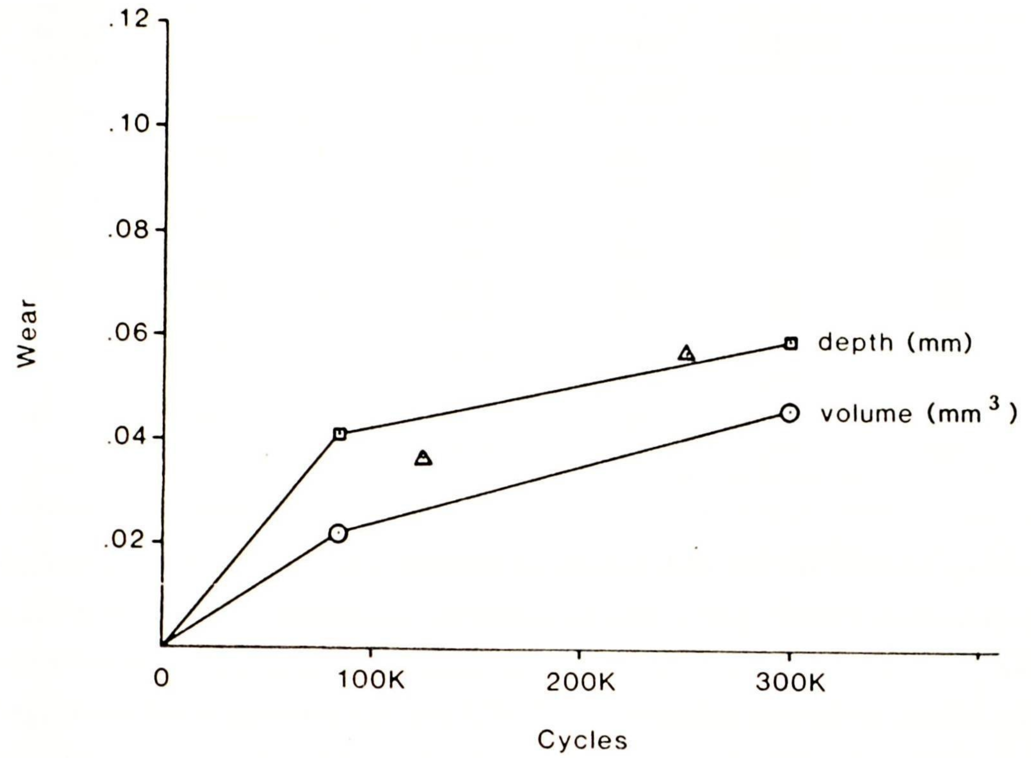

Occlusal wear curves for artificial mouth depth □ and artificial mouth volume ⊙ and clinical depth △ Braem calculated as one year equals 250,000 masticatory cycles.

of the wear curve indicated that these two points would be indicative of the wear rate and (2) a fast reproducible test was required which was capable of screening a large number of candidate composite systems.

The wear results for loss of contour by depth and volume are shown in Table 4-5. The results are shown in graphical form in Figure 4-3 with the results of the one year report of Braem, et al.[62] superimposed.

Table 4-6. Correlation of clinical regression line to artificial mouth raw data

Time years masticatory cycles	Clinical data recalculated for artificial mouth time intervals Braem µm	Artificial mouth data from Table 1 µm	Correlation coefficient of artificial mouth raw data to clinical regression line
0	0	0	
0.34 (85 k)	22.5	41±8	
1.2 (300 k)	67.4	59±10	0.84 (at the 95% level of confidence, coefficient lies in the interval 0.57, 0.94)
3 years (750 k)	161.4	142	

Table 4-7. Parameters of the wear facets of a posterior composite in occlusal contact area in the artificial mouth

Sample I.D. #	*l*	m	masticatory cycles	measured depth mm (raw data)	calculated volume mm^3	measured volume mm^3 (raw data)
57	.056	.173	85 k	.031	.0152	.0158
			3000 k	.046	.035	.037
65	.057	.36	85 k	.047	.025	.023
			300 k	.068	.050	.049
61	.069	.21	85 k	.053	.033	.027
			300 k	.072	.071	.057
71	.047	.27	85 k	.038	.020	.018
			300 k	.057	.045	.040
80	.045	.173	85 k	.035	.023	.021
			300 k	.052	.047	.047

On the basis of linearity, a correlation between the clinical data and the artificial mouth data is shown in Table 4-6 with a correlation coefficient of 0.84. Using Fisher's method the 95% confidence limits indicate that the correlation coefficient for artificial mouth raw data to the clinical regression line is between 0.57 and 0.94. This correlation coefficient applies only up to one year of wear. Although this linear relationship appears to hold true for early wear, further results suggest a parabolic relationship between depth of wear and time.

4.3.1 Relationship between depth of wear and volume of wear

It is appropriate to examine the relationship between volume and depth of wear because depth is the parameter that is measured in most clinical studies. The depth of wear also contributes directly to occlusal vertical dimension. The wear facet that is generated on a flat surface by a convex cusp is generally paraboloid. In addition, the worn area of the flattened cusp is also parabolic in shape. The wear facet thus can be described by two parabolas with the origin at the deepest point Z of the occlusal contact area (Fig. 4-4):

$$Z = my^2 \text{ and } Z = lx^2 \qquad (4.1)$$

Thus at any depth Z,

$$x = \sqrt{(Z/l)} \text{ and } y = \sqrt{(Z/m)} \qquad (4.2)$$

where l and m are the shape factors of the occlusal contact. The projected area of the wear facet in Fig. 4-4

$$\text{area of the ellipse} = \pi xy \qquad (4.3)$$

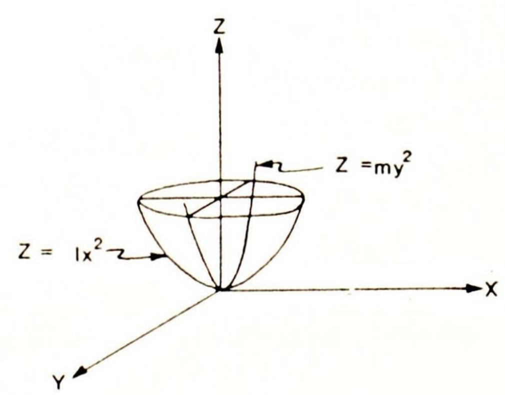

Fig. 4-4. Geometry of wear facet

$$\text{Area at depth } Z = \pi\sqrt{(Z/l)}\sqrt{(Z/m)} = \pi Z/\sqrt{(lm)} \qquad (4.4)$$

The volume of the wear facet in Fig. 4-7

$$\text{Volume, V at depth, } Z = \pi/\sqrt{lm} \int Z\,dZ \qquad (4.5)$$

$$= (\pi/\sqrt{lm})\,(Z^2/2) \qquad (4.6)$$

This defines the relationship between the volume and the depth of a wear facet as a parabola.

The values of l and m change very little in Table 4-7 from sample to sample. This is an interesting observation since the wear facets were developed under the palatal cusps of different maxillary third molars which were subject to biologic variation of occlusal anatomy. The measured depth in Table 4-7 was used to calculate the volume, and the very close agreement between measured volume and calculated volume in that table indicates that the artificial mouth supports the premise that the depth of wear has a parabolic relationship with time (i.e. a high initial wear rate, followed by a decline in wear rate). Conversely, the depth can be calculated from a known volume of wear.

Since the theoretical and experimental studies in the artificial mouth support the parabolic nature of the wear facet in a posterior composite, the same relationship can be used to develop the ratio of wear at two different periods. This is a useful predictive tool and is shown in Table 4-8, where several ratios at different time intervals are shown, worked out on the basis that one year of clinical masticatory effort is equivalent to 250,000 defined masticatory cycles in the artificial mouth. The ratio of 6 months to three years is of particular importance, and may be compared to two clinical studies as shown in Table 4-8. It would appear that the artificial mouth studies support the Leinfelder study as far as the shape of the wear curve is concerned. However, it also supports the Braem clinical study[62] as far as the mean wear values are concerned at 6 months and 1 year as shown in Table 4-6. The predictive power of in vitro and in

Table 4-8. The ratio of depth of two time intervals based upon the parabolic relationship between volume and depth of the wear facet.

Ratio of time intervals $\frac{T_1}{T_2}$	Square root of ratio of no. of masticatory cycles in the artificial mouth $\sqrt{\frac{N_1}{N_2}}$	Ratio of depth of wear for the two time intervals $\frac{D_1}{D_2}$	Clinical study Leinfelder	Clinical study Braem
$\frac{0.5 \text{ years}}{3 \text{ years}}$	$\sqrt{\frac{125{,}000}{750{,}000}}$	0.41 (41%)	49%	23%*
$\frac{0.5 \text{ years}}{5 \text{ years}}$	$\sqrt{\frac{125{,}000}{1{,}250{,}000}}$	0.32 (32%)		
$\frac{0.5 \text{ years}}{7 \text{ years}}$	$\sqrt{\frac{125{,}000}{1{,}750{,}000}}$	0.27 (27%)		
$\frac{0.5 \text{ years}}{7 \text{ years}}$	$\sqrt{\frac{125{,}000}{1{,}750{,}000}}$	0.65 (65%)		

* The three year value is extrapolated on the basis of a linear relationship.

vivo screening tests is an important goal for future research as indicated by Phillips.[109] If this is to be realized, the shape of the wear rate curve, as well as the initial rate itself must be known. While the difference between the mean depth of wear for the linear rate and that for the parabolic rate may not be too serious at three years of clinical wear, the difference between these two wear curves and hence their predicted values will be very different in long term performance. The percentage differences for two clinical studies are shown in Table 4-8. It is important to establish, therefore, whether the parabolic or the linear rates reflect the true clinical performance. At the moment, the evidence favors the parabolic rate.

The wear pattern of posterior composite resins is substantially different from those of amalgam restorations.[36] Uniform loss of material occurs over the entire occlusal surface, resulting in a 'dished-out' appearance to the worn surface. Occlusal stresses are transmitted into the surrounding resin matrix creating small cracks or fractures resulting in localized areas of material loss. The greater the size of the particle and the harder the particle, the greater the amount of wear.

Most workers agree that there is an abrasive element due to the filler. Wear of posterior conventional composite restorations is a process where exfoliation of the inorganic filler particles occur as the resin matrix is continually worn away. The microabrasion of the polymer matrix occurs under stress and the actions of abrasive food, causing the filler particles to be deposed and increasingly subjected to mechanical stress. At a critical point of exposure, dislodgment of the particles occurs. The inorganic filler particles are only abraded when the abrasive is harder than the filler itself.[103]

If the abrasive wear coefficient is calculated for composites, then

$$k_a = 3.15 \times 10^{-5}$$

when $H = 9.8 \times 10^8$ N/m, $W = 6.6$ N, $V/L = 2.12 \times 10^{-7} \text{mm}^3/\text{mm}$. The coefficient of friction for the composite/enamel couple with intervening water was 0.2-0.3. Although friction may not be directly related to wear, the relatively low abrasive wear coefficient considered with a low coefficient of friction suggests that the volumetric wear rate should be lower than that measured. Fatigue mechanisms are suspected to be operating together with abrasion in the wear of composite restorations.

Several investigators have attributed the elevated early wear rate to microcracks generated in the surface and subsurface during finishing procedures.[72] McCabe[27] had reported bulk fracture of clinical restorations necessitating replacement. Subsurface and surface microcracks are thought to yield to wear through fatigue.[53,104] Cyclic stresses, due to loading and unloading of the surfaces during mastication, can initiate and propagate microscopic fatigue cracks.[75,105] Also tensile stresses between the matrix and filler initiated by large differences in the thermal expansion coefficients can generate fine cracks. Fatigue studies by

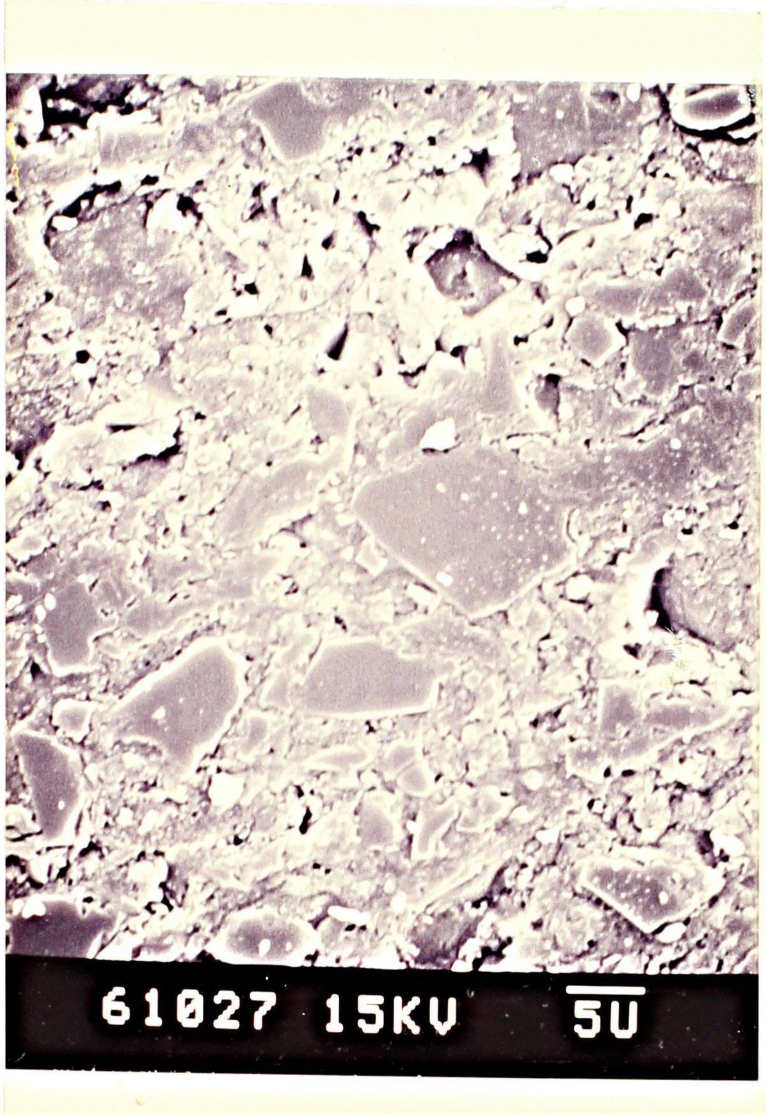

Fig. 4-5. Scanning electron micrograph of the composite wear facet

Draughn[107,108] indicate that for a wide variety of composite products, the cyclic compressive stress below which failure would not be expected to occur in 5000 stress cycles is only 0.66 of the ultimate compressive strength.

SEM photomicrographs (Fig. 4-5) show the nature of the surface degradations after 300,000 masticatory cycles in the artificial mouth. Although some wear tracks are evident, the predominate appearance is that of microfracture and chipping. Interparticulate resin, including the smaller particles are lost prematurely from the mass. The masticatory effort is borne by the larger particles until they are exfoliated because of excessive loss of resin and microcracks within the resin. Further investigation into the nature of crack propagation in composites will be presented in Chapter 6.

The degradation and wear of composites are apparently due to abrasion and resin fatigue. Experimental and clinical evidence together with SEM analysis support this claim. Also, good correlation of the artificial mouth studies with clinical studies indicate that the mean depth of wear curve for the posterior composite studied is parabolic in shape.

Table 4-9. Wear of dental porcelain opposed by a maxillary palatal cusp in terms of volume and depth

Years of simulated clinical service*	No. of masticatory cycles	Volume loss of contour/mm³	Depth loss of contour/mm
0.12	30,000	.0185±.004	.0365±.009
0.4	100,000	.064 ±.015	.079 ±.016
0.8	200,000	.116 ±.028	.107 ±.018
1.2	300,000	.165 ±0.37	.127 ±.02
2	500,000	.238 ±.06	.157 ±.022

*based on 1 year of clinically simulated wear is equal to 250,000 masticatory cycles

4.4 Dental porcelain

The wear of dental porcelain is included in this study because it represents a different category of dental materials from amalgam or composite, i.e. a material that is used for aesthetic full coverage restorations. Porcelain fused to metal crowns are the most common form of porcelain used in dentistry[110] and are considered to be extremely successful. Although general guidelines have been implied for the use and design of porcelain and porcelain fused to metal restorations, aesthetic requirements often override these guidelines. Because of the brittle and abrasive nature of ceramic materials, the high rate of attrition of the opposing natural dentition is of primary concern. Christensen's[110] survey found that the most desired improvement for porcelain fused to metal (PFM) restorations was less wear on opposing teeth.

The protocol for this study was similar to that for the dental amalgam study. The maxillary member consisted of a palatal cusp of a maxillary third molar opposed by a porcelain fused to metal disk (Ceramco II, Ceramco, Inc., New York, NY). A nonprecious metal disk (Talladium, Talladium, Inc., Los Angeles, CA), was sandblasted with aluminum oxide, then oxidized in a porcelain furnace according to the manufacturer's instructions. A thin opaque layer was formed and fired, followed by a layer of body porcelain which was subsequently fired. The surface was not stained, but was autoglazed per the manufacturer's instructions. The samples were mounted in nylon rings and stored in deionized water at 37°C prior to installation in the artificial mouth. All environmental and occlusal factors were the same as in the amalgam and composite study. Profiling intervals were established at 30K, 100K, 200K, 300K, and 500K masticatory cycles.

Loss of contour by volume and depth of the mandibular porcelain disk are listed in Tables 4-9. The plot of depth loss (Fig. 4-6) is once again curvilinear as was seen in the amalgam study. Volume loss due to wear in Fig. 4-6 shows good linearity as confirmed by the regression constants (correlation coefficient 0.94) in Table 4-10. Nevertheless, the volume curve in Fig. 4-6 does show a little flattening at the higher masticatory level (500,000 cycles). Mulhearn and Samuels[111] suggested that the dropping off of the wear rate was due to the blunting of the abrasive particles, which agreed with the observation of Monasky and Taylor.[68] This finding suggests that porcelain surfaces which have been adjusted for occlusal reasons should be repolished or glazed. The depth of wear curve in Fig. 4-6 shows a pronounced deviation from

Figure 4-6. Graph of loss of contour by volume and by depth and number of masticatory cycles. Triangles represent volume in mm^3 and circles represent depth in mm

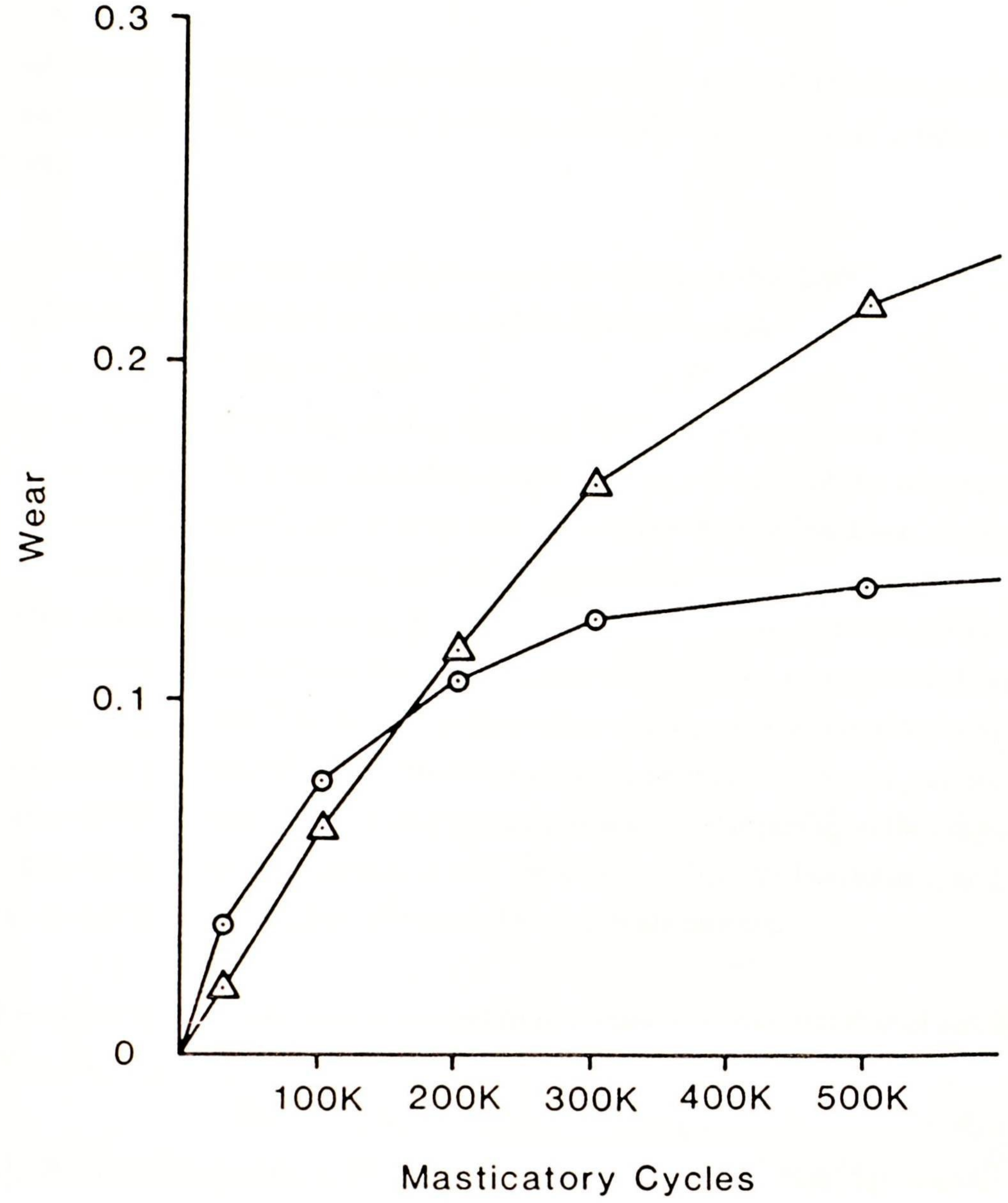

Table 4-10. Regression constants for volume loss of contour

Intercept mm^3	Slope mm^3/ masticatory cycle	Correlation coefficient
.01	4.79×10^{-7}	.99

Table 4-11. Shape factors of the porcelain wear facet after 500K masticatory cycles

Sample I.D.	*l*	*m*	Measured depth (raw data)	Calculated volume	Measured volume (raw data)
63	.098	.221	.179	.341	.287
64	.094	.205	.131	.194	.197
91	.089	.177	.139	.245	.163
59	.091	.197	.178	.372	.305
Mean	.093	.2	.157	.288	.238
Standard deviation	±.004	±.018	±.025	±.083	±.069

linearity, i.e. a flattening of the wear rate with time. The results in Table 4-11 show that this rate of depth of wear is a parabolic curve as explained by the geometry of the wear facet as was seen in the composite study.

SEM photomicrographs (Fig. 4-7) show parallel wear tracks through the facet produced by enamel/porcelain contact. The edges of the wear facet exhibit smooth wear grooves with little chipping.

The equation for abrasive wear and adhesive wear are similar in that both incorporate a factor of W/H, normal load divided by hardness of the softer material:

$$V/L = K_a W/H \qquad (1.14)$$

where V/L is the volume loss per sliding distance, also known as the wear rate; K_a is the abrasive wear constant; W is the normal load; and H is the hardness of the softer material. This equation applies to two-body abrasive wear. In three-body abrasion, loose abrasive particles cause wear on rubbed surfaces, and although the same form of equation will hold, K_a will be lower, representing lower wear, since many of the particles will tend to roll rather than slide.[78] The wear produced by three body abrasion is usually an order of magnitude lower than that in a two body situation.[85] In two body abrasion, as wear proceeds, some blunting of the hard asperities or particles will occur, thus reducing the wear rate. However, the wear rate can be increased by fracture of brittle particles resulting in a resharpening of the edges of the particle. Also, if one of the components is soft, abrasives can become buried in it, and if they protrude, wear of the opposite face can occur by a two body process.

Inspection of the wear pattern seen in enamel to porcelain wear suggests that of an abrasive mechanism. Assuming this to be the case,

$$V/L = K_a W/H \qquad (1.14)$$

V/L for artificial mouth studies $= 5.9 \times 10^{-7}$, $W = 6.6N$, $H = 4.5 \times 10^{9}\ N/m^2$ for enamel

$$K_a = V/L * H/W$$

$$= 4.02 \times 10^{-4}$$

By this analysis, the coefficient of wear for porcelain is greater than that for amalgam by one order of magnitude.

The coefficient of friction for the porcelain/enamel couple was measured to be 0.57. The friction started at a lower value then increased until a steady state value was reached. This equilibrium value might be explained by a decrease in particle size or sharpness.[85] It is reasonable to conclude that the primary mechanism of wear for the porcelain/enamel couple is that of abrasion. The high coefficient of friction and elevated coefficient of wear in addition to the evidence brought forth from the SEM photographs support this theory.

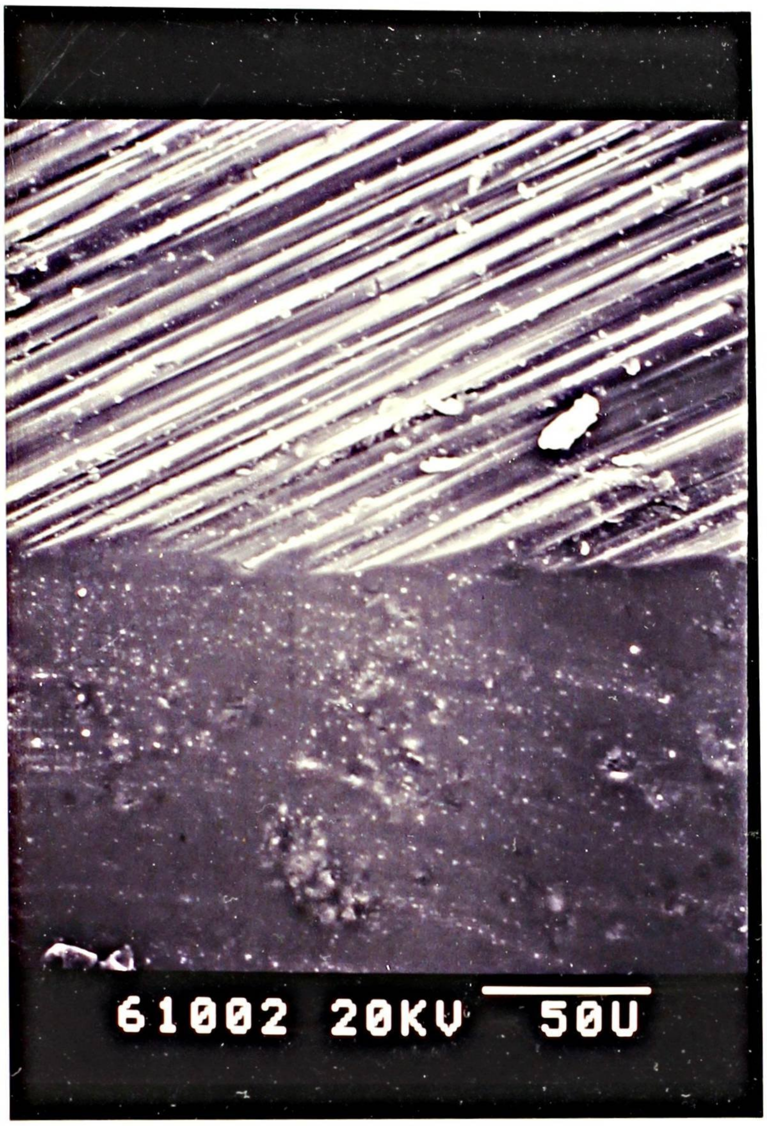

Fig. 4-7. Scanning electron micrograph of porcelain wear grooves at the edge of the wear facet.

In summary, amalgam was found to wear by an adhesive wear mechanism with amalgam particles transferring to the opposing enamel cusp. The wear of amalgam was very low. The wear of composite was intermediate, suspected to be a result of abrasive and fatigue wear. The wear of porcelain was the highest and demonstrated an abrasive wear pattern (Fig. 4-8 and 4-9).

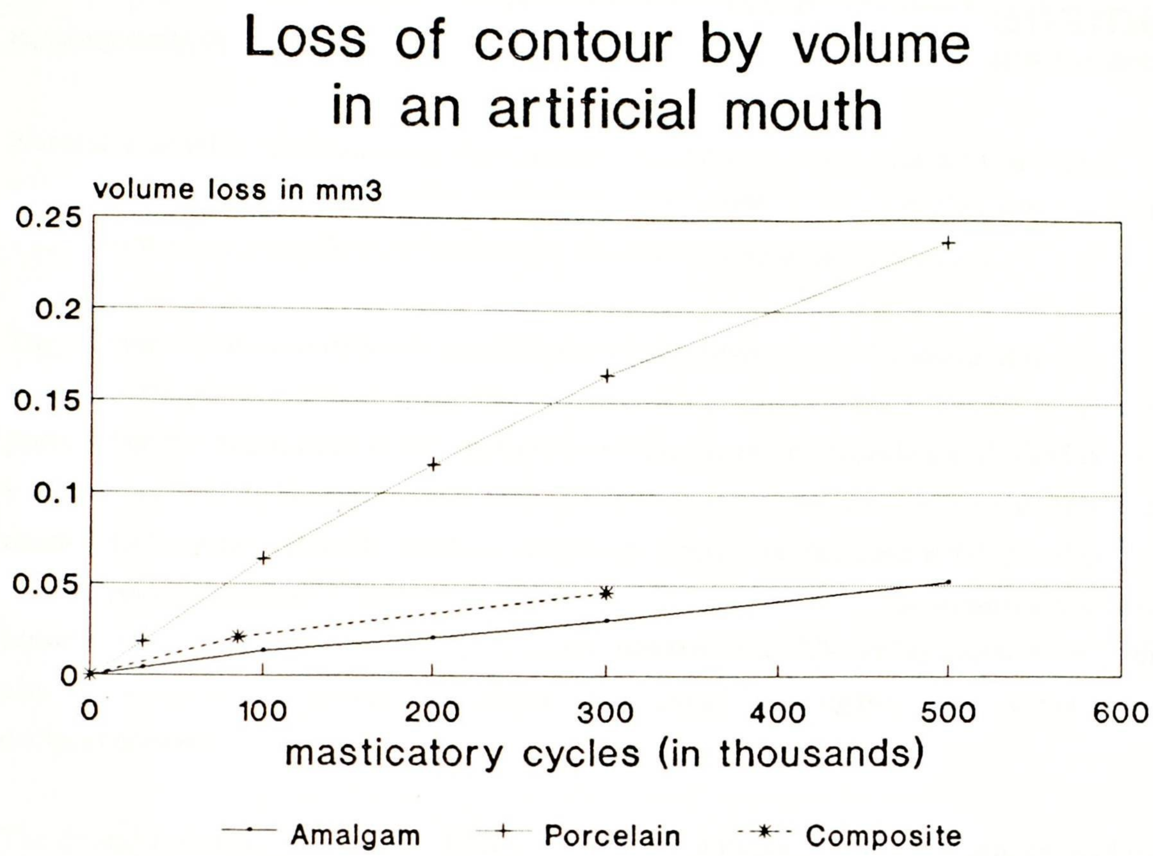

Fig. 4-8. Loss of contour by volume

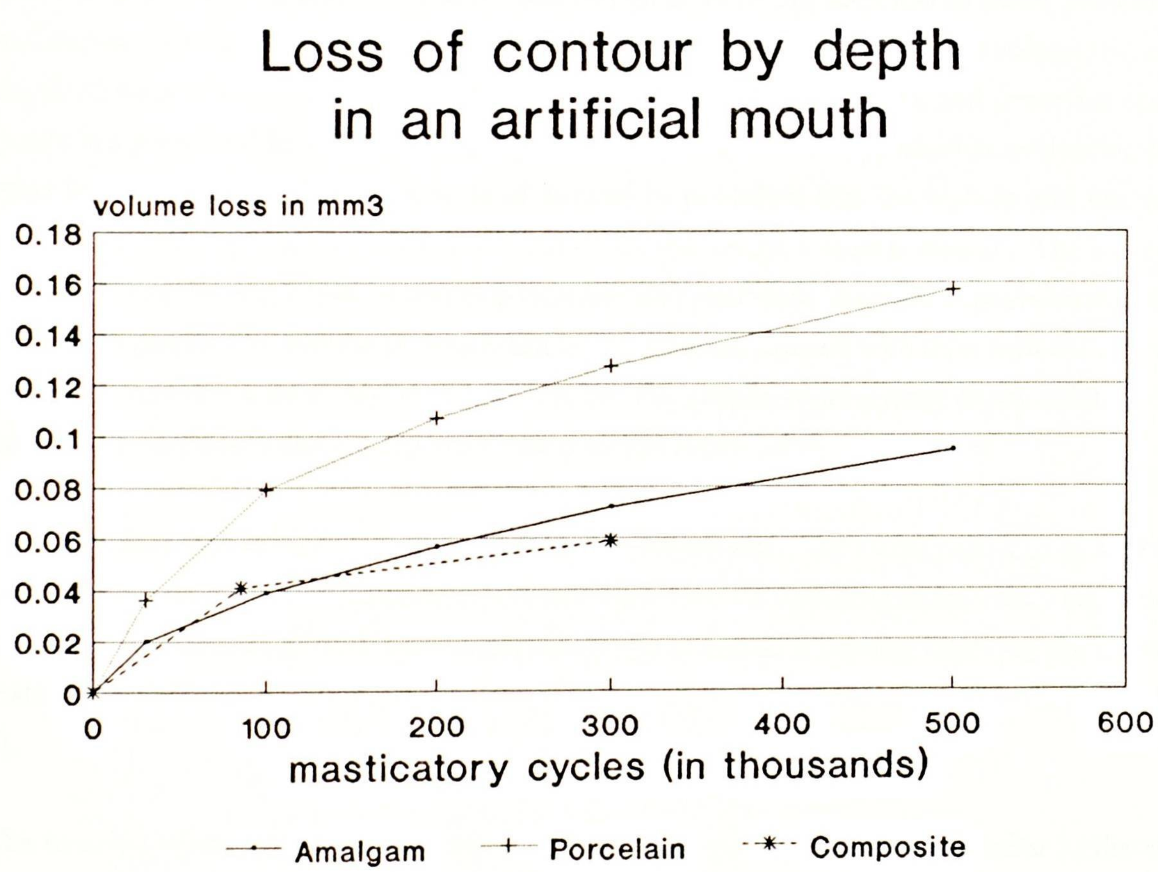

Fig. 4-9. Loss of contour by depth

5 The wear of natural enamel

Natural enamel is distinguished from the restorative materials presented in that it is an anisotropic biocomposite of enamel crystallites with a preferred orientation within a matrix. The anisotropy is most likely reflected in its friction and wear characteristics.

The structure of the natural tooth maximizes its ability to withstand high occlusal stresses while demonstrating little occlusal wear. The wear resistant enamel layer is brittle when unsupported, but the orientation of the crystallites within the matrix together with the high bond with the underlying dentin prevent bulk fracture. Laboratory studies have demonstrated enamel to have considerable fracture anisotropy producing fracture paths parallel to the general prism direction.[111a] Microcracks or craze lines are not uncommon within the enamel however these rarely result in through-and-through fractures. The saliva and salivary pellicle also play a role in diminishing interocclusal friction, thus reducing the surface damage under occlusal contact.

The dental materials presented in Chapter 4 have been opposed with a natural enamel palatal cusp. This provides a large database from which to evaluate the behavior of enamel wear under various conditions. Also, enamel wear was evaluated against an enamel antagonist which allows comparative studies between the prosthetic materials and the natural physiologic standard. The experimental conditions and study design is therefore identical to those presented in Chapter 4 except that only the wear of enamel is presently considered. The volumetric and depth of wear of natural enamel opposing amalgam, porcelain, enamel, and posterior composite are presented in Table 5-1 and Figures 5-1 and 5-2. Generally, whether evaluating the wear by depth or by volume, the wear of enamel by porcelain was the highest and was not detectable when opposed by amalgam. Wear by the composite was intermediate. The wear of enamel to enamel was between that of composite and porcelain. As seen in previous volume and depth graphs, the volume generally tended to increase linearly with time with the exception of a decrease in wear rate at 500,000 cycles. The graphs representing depth exhibited a curvilinear shape with decreasing wear rate over the course of the experiment.

The first clear fact to emerge is the variability of enamel wear, both within groups as well as between groups. Porcelain produced more extensive wear on opposing enamel than any other material. The smooth, glazed layer on porcelain was penetrated rapidly, exposing the coarse textured underlayer and this textured layer is responsible for extensive enamel wear (Fig. 5-3).

The wearing effect of the posterior composite on the opposing enamel was similar to the effect of enamel opposing enamel, which was surprising, considering the coarser texture of the composite (Fig. 5-4). Embong, et al.[112] also found the opposition of enamel by composite acceptable.

Table 5-1. Wear of enamel opposed by enamel, amalgam, porcelain, and composite

material	samples	cycles	volume (mm^3)	depth (mm)
enamel	7	30	.016 ± .014	.060 ± .043
		100	.034 ± .043	.074 ± .050
		250	.046 ± .040	.092 ± .051
		350	.065 ± .058	.104 ± .058
		500	.093 ± .080	.114 ± .070
amalgam	3	30	0	0
		100	0	0
		250	0	0
		350	0	0
		500	0	0
porcelain	5	30	.055 ± .017	.097 ± .011
		100	.122 ± .045	.137 ± .013
		250	.246 ± .122	.180 ± .029
		350	.369 ± .114	.229 ± .023
		500	.422 ± .075	.234 ± .022
P10 comp.	5	85	.038 ± .019	.081 ± .024
		300	.085 ± .039	.124 ± .036

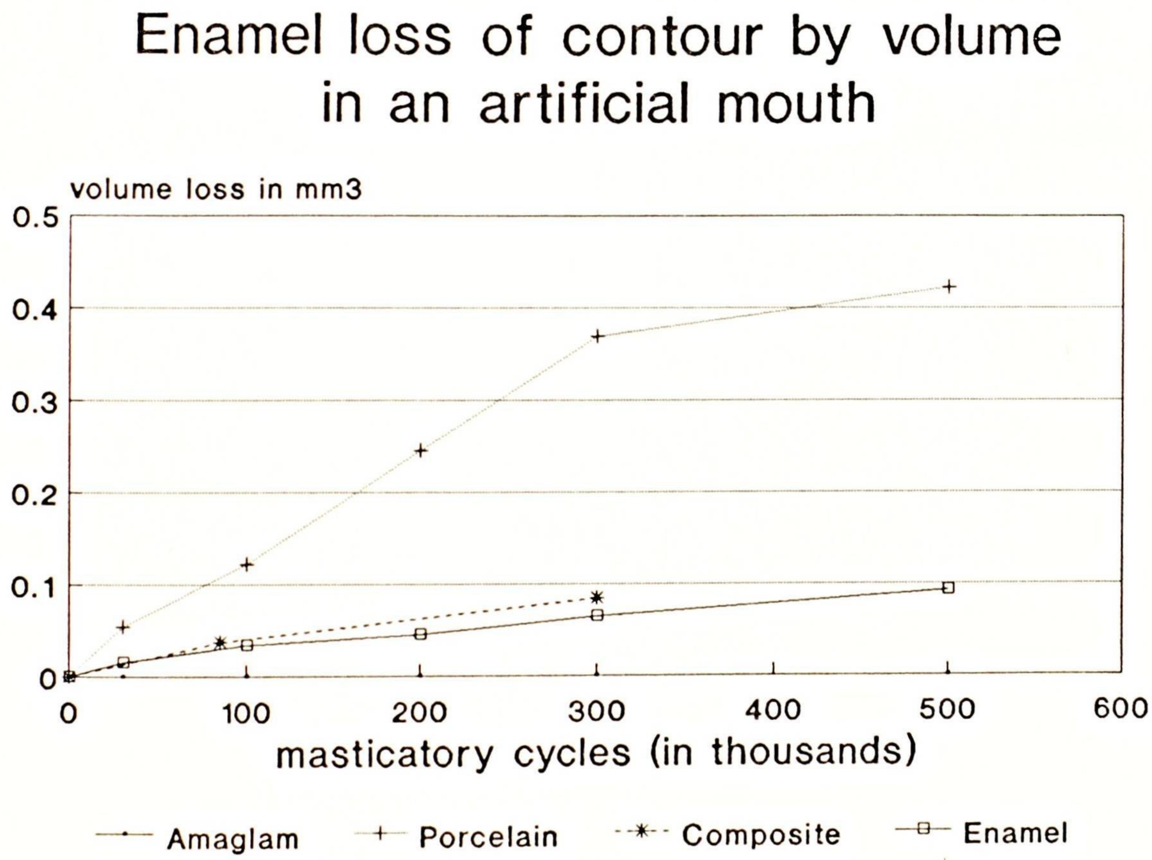

Fig. 5-1. Loss of contour by volume for enamel opposed by enamel, amalgam, porcelain, and composite

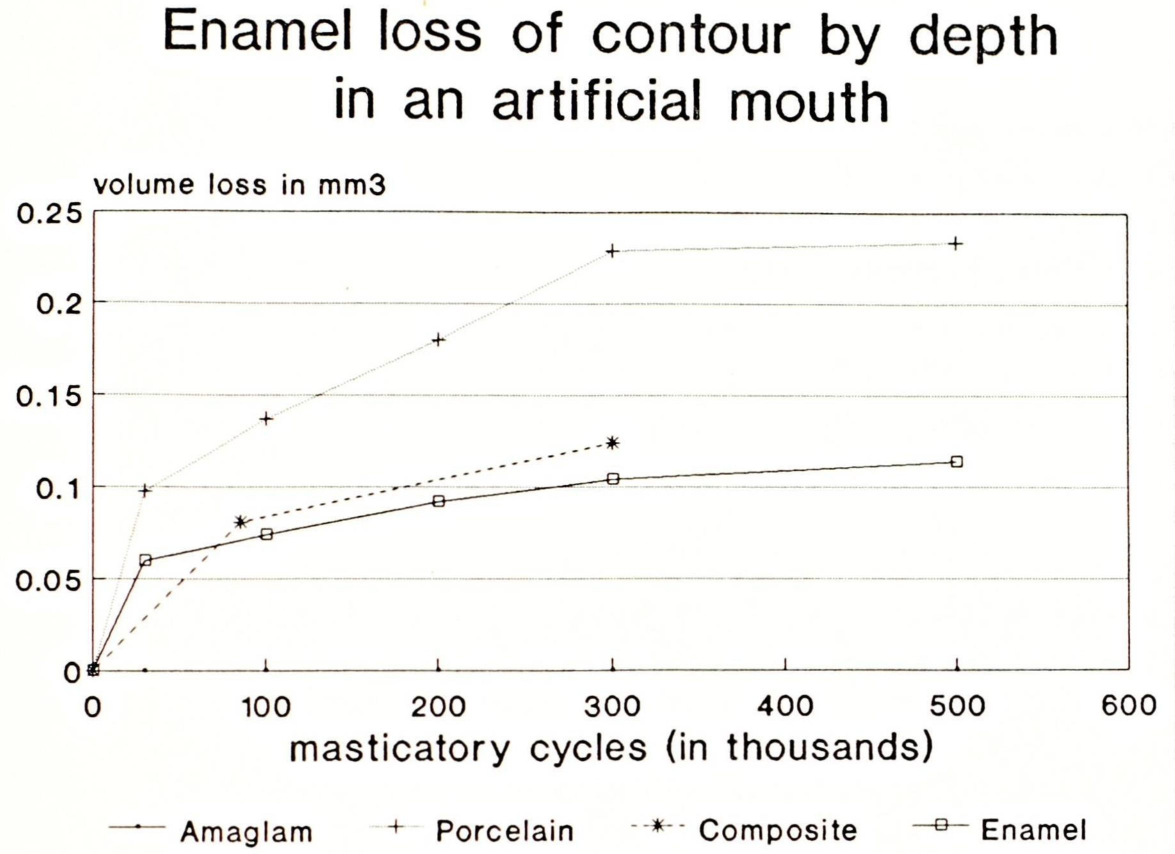

Fig. 5-2. Loss of contour by depth for enamel opposed by enamel, amalgam, porcelain, and composite

The wear of enamel against amalgam is remarkable in that is it essentially not measurable. This is a direct consequence of the adhesive wear mechanism as shown earlier, where shallow slips take place within the amalgam. Thus, the amalgam is essentially transferred to the enamel cusp, with the cusp itself experiencing very little abrasion (Fig. 5-5). Mueller, et al.[4] also noted gross amalgam transfer to enamel pins. It appears that among all materials in this study, amalgam is the least damaging to the opposing dentition.

A clear relationship between friction and wear volume is difficult to determine. Certainly amalgam demonstrates a low frictional coefficient that is coincident with its low wear behavior. The friction of enamel appears to be variable and appears to be related to surface effects, such as prism direction. Porcelain demonstrates a rapidly increasing level of friction with repeated masticatory strokes. The coefficient of friction also appears to rise with the wear volume. Norman[113] found the highest frictional resistance in the combination of porcelain against porcelain, and the lowest between chrome cobalt alloy pairs. The friction between the enamel pairs was intermediate.

With the enamel opposing enamel, the variability of the wear from sample to sample was compounded, which made conclusions difficult to reach. Further, scanning electron microscopy revealed that different wear mechanisms were operating, with a strong suggestion that enamel rod orientation at the point of contact favoring adhesive (smearing) or abrasive wear, even within the same occlusal contact area (Fig. 5-6). However, it is important to note that enamel does show measurable wear. A small amount of wear may be regarded as physiological and probably has important biological roles to play such as harmonizing the fully developed occlusion in lateral excursion. Lambrechts, et al. [61] found enamel/enamel wear rates of 52 (6 months), 68 (1 yr), and 82 micrometers (1.5 yrs) which may be regarded as the physiologic norm.

Clearly, human enamel is a unique material. The anisotropic nature of the material determines the friction and wear characteristics. The saliva and pellicle appear to provide lubrication for occlusal contacts. Although the role of saliva as a lubricant has not been clearly determined, it is probable that it serves to reduce interocclusal friction while working together with the pellicle which is tightly adhered to the enamel surface. Strong binding sites may be present allowing the pellicle acts as a boundary lubricant. The great variability of enamel both in its structure and environment as well as its pivotal importance in ail that is related to occlusion and the human masticatory process, makes it a subject that requires a great deal of attention in further studies.

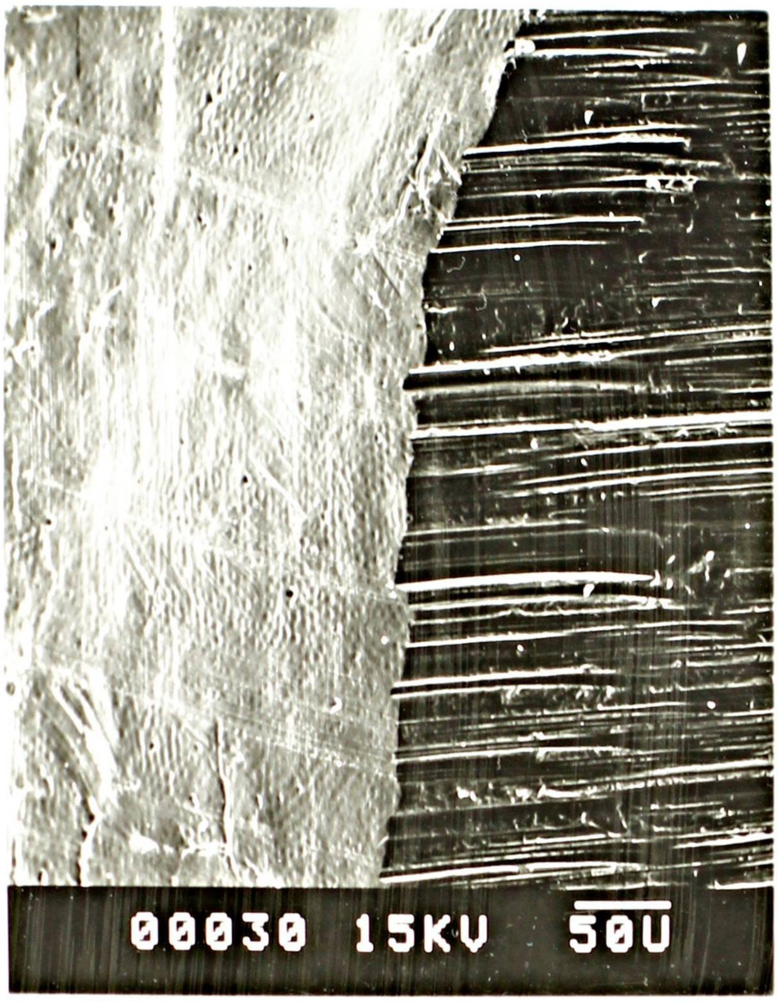

Fig. 5-3. Abrasive wear experienced by enamel when opposed by porcelain

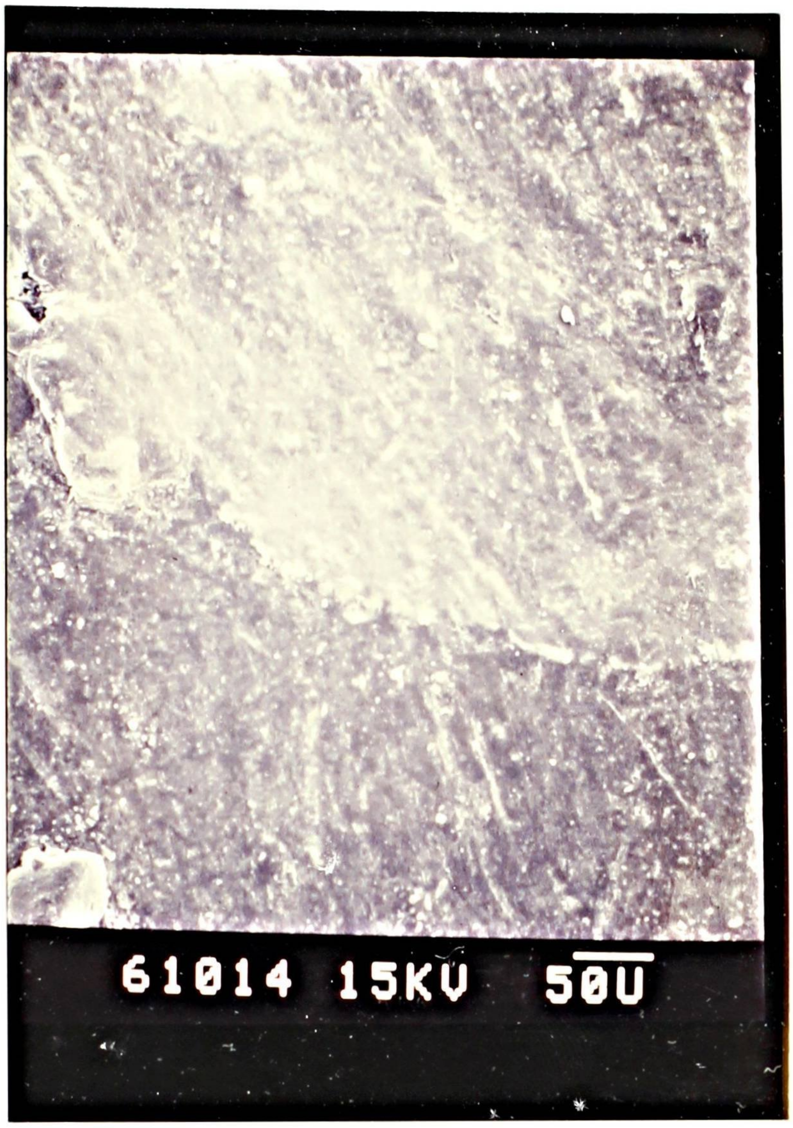

Fig. 5-4. Enamel opposed by posterior composite

Fig. 5-5. Enamel opposed by amalgam. Amalgam is transferred to the enamel cusp

Fig. 5-6. Enamel opposed by enamel

6 Stress analysis of natural teeth and fixed prosthetics

6.1 Introduction

There is no restorative material which mimics the aesthetics, wear and fracture resistance of enamel that is also capable of bonding to natural tooth structure. Material candidates for full coverage fixed restorations include porcelain, porcelain fused to metal, composite veneered on metal, and gold or other metal alloys. Gold or metal alloys can be eliminated as a choice if aesthetics are critical and porcelain has been shown to produce significant wear of the opposing enamel. Microfil composites veneered onto a metal substructure have not been clinically satisfactory because of fracture, as alluded to earlier in the discussion of composites.

As natural teeth age, the surface texture of the enamel becomes smoother and craze lines become evident (Fig. 6-1). These microcracks rarely result in bulk fracture of the tooth unless the dentinal support has been lost to caries or large restorations. Although composite restorations and porcelain crowns sometime fracture under occlusal loads, the natural tooth handles this same load without resulting in failure. The distribution of occlusal stress undoubtedly explains this discrepancy.

6.2 A layered design for restorations

Considering the problems of existing restoratives as described above, it would be beneficial to place a wear resistant material on the occlusal surface which is supported by a stiffer core of material that is bonded to the existing tooth structure. Such a system would have the advantages of (1) bonding to remaining tooth structure, (2) good aesthetics, (3) good wear resistance, and (4) protection of the opposing dentition. A layered design for a full coverage restoration was proposed utilizing a wear resistant outer "enamel" layer (microfil composite) bonded onto a higher modulus "body" core (hybrid composite). The rationale for this layered approach is to mimic the laminated natural dentition which is composed of a wear resistant enamel covering the more elastic dentin. The difference in this design from the natural tooth is in the stiffness of the materials. While natural enamel is high in elastic modulus, the artificial "enamel" is lower than the underlying material.

6.2.1 In vitro evaluation

A disk of the layered material was fabricated and opposed by a natural maxillary third molar cusp in the artificial mouth for study of the wear and fracture behavior of the "sandwiched" material. The experiment continued for 300,000 masticatory strokes which approximated 1.2 years of clinical wear. The testing procedure followed those listed in Chapter 2. The material demonstrated wear characteristics similar to enamel with a small amount of microcrack generation. The wear of the veneered composite material (volume loss 0.02 mm^3, depth .062 mm at 300K masticatory cycles) was similar to that of enamel and did not produce appreci-

Table 6-1. Material properties

material	Poisson's ratio	Mod. of elast (N/m2)
dentin	0.25	1.54 E10
enamel	0.30	4.69 E10

able wear of the opposing natural enamel cusp. Scanning electron microscopy (SEM) revealed a small amount of microcracking or embrittlement perpendicular to the path of lateral excursion.

6.3 Modelling the restoration design

The feasibility of the layered design for full coverage crown restorations was evaluated using the finite element method (FEM) for stress and strain analysis. As with any computational method, parallel experimental study is recommended to provide validation of the theoretical model. Thus, strain gage techniques were employed on a natural tooth loaded in the artificial mouth to achieve this end. A bruxing mode of load application was chosen to amplify the effects of oblique loads placed on the occlusal surface of the natural tooth. This is a severe test for a natural tooth because of the extended contact times in lateral excursion. While normal occlusal stresses are transient, bruxing applications tend to be longer in duration and higher in magnitude. The behavior of the natural tooth under these extreme parafunctional conditions will aid in the understanding of distribution of stresses under normal conditions and will also provide validation of the finite element model. From this foundation, tests can be performed on mathematical models of restorations to evaluate their behavior under similar conditions. It can then be determined whether any deviation in stress distribution compared to the natural tooth contributes to degradation of the restoration.

Techniques for modelling the natural dentition have included physical, photoelastic models and computer generated mathematical models. Noonan[114] conducted some of the first photoelastic studies analyzing the stress concentrations in silver-amalgam restorations. Several other investigators have used photoelasticity to evaluate intracoronal restorations and the effects of loading, design of the pulp chamber, and external shape of the tooth model.[115,116]

The finite element method (FEM) has been shown to produce results similar to those found by photoelastic and strain gage studies.[117-119] However, experimental techniques such as strain gage methods are still necessary for validating the results from theoretical, mathematical methods such as the finite element method. Morin[120,120a,120b] used strain gage techniques to analyze the strain distribution of natural virgin maxillary premolar teeth and premolars under a load at centric occlusion with a number of different cavity preparations and restorations. Comparison of the results to those produced by the finite element method produced significant correlation. Strain gages have also been used to study stress in other tooth related areas.[121-123]

6.3.1 Strain gage methods

Strain gage techniques are useful in the determination of strain, or relative bending, experienced by a surface. The concept is simple: when a wire is strained, its electrical resistance changes and within certain limits, this relationship is linear.

$$\text{strain} \propto \text{change of electrical resistance}$$

$$\text{strain}, \varepsilon = K\,\Delta R/R \qquad (6.1)$$

where K is the gage factor, R is the electrical resistance of the strain gage in ohms and Δ R is the change of electrical resistance of the strain gage (ohms) due to ε. As K is known, and R and Δ R can be measured, ε can be readily obtained from equation 6-1. These measurements are converted to a voltage signal through the use of a Wheatstone bridge which can be measured with a recording instrument. The Wheatstone bridge circuit can be used for both static and dynamic strain measurements since it can be initially balanced to yield a zero output voltage. The output voltage, ΔE, from the Wheatstone bridge is nonlinear with respect to resistance change, ΔR, which is usually not a problem in typical experimental stress analysis. An amplifier (or conditioner) is used in the circuit to produce a measurable signal to the recording device.

Foil strain gages are small, precision resistors mounted on a flexible carrier that can be bonded to a component part in a typical application. The gage resistance is accurate to 0.4 percent, and the gage factor is certified to 1.5 percent. This gage is capable of precise measurements of strain, but the results obtained are a function of the installation procedure, state of strain being measured, and environmental conditions during the test. This gage is etched out of flat metal foil so that its electrical resistance along its axis can be very large compared with its electrical resistance perpendicular to its axis.

If a strain gage is subjected to a change of temperature, it very often suffers a larger change in length than that caused by external loadings. To overcome this deficiency, it is necessary to attach another strain gage (a "dummy" gage) to a sample of identical properties as the structure itself, and to subject this sample to the same temperature changes as the structure, but not to "constrain" the "dummy" gage, or allow it to undergo any external loading.

A strain gage installation can be detrimentally affected by direct contact with water or by the water vapor present in the artificial oral environment. The water absorbed by both the adhesive and the carrier results in changes of the gage performance through a decrease in the gage to ground resistance, degradation of the strength and rigidity of the bond which reduces the effectiveness of the adhesive in transmitting the strain from the specimen to the gage, and electrolysis when current passes through the gage producing gage filament erosion and a significant increase in resistance. Careful isolation of the strain gage through the use of sealant resins and silicones are necessary for precise measurement. It is important that the elasticity of these materials are sufficiently lower than that of the sample to measured so as not to introduce additional stiffnesses into the system.

6.3.2 Strain gage methods and materials

Four freshly extracted, virgin maxillary second premolars were mechanically cleansed of all soft tissue and debris and stored in deionized water at 4^{o} C. Strain gages (Micromeasurements CEA-06-032UW-120, Measurements Group, Raleigh, NC) were positioned and bonded using the manufacturer's methods at the height of contour on the buccal and lingual surfaces of the tooth (Figure 6-2). The gage and exposed wire ends were coated with light cured Silux-Enamel Bond Resin (3M Company, St. Paul, MN). Pairs of teeth were mounted in nylon rings with clear Orthodontic Resin (LD Caulk Company, Milford, DE) apical to the cemento-enamel junction. Polyvinylsiloxane impression material (Express, 3M Company, St. Paul, MN) was placed around the strain gages and exposed wire ends for insulation from fluids. The system was placed into the mandibular member of the artificial mouth. The cuspal inclines were modified at the occlusal contact area to facilitate occlusal loading by a 4.4 mm spherical loading element along the buccal and lingual triangular ridges (Fig. 6-3).

A profile of the occlusal surface (buccolingual) was recorded before the loads were applied to determine the cuspal inclinations. Occlusal loads (5, 8, 10 pounds) were applied to the tooth in a bruxing pattern starting at one cusp tip through centric occlusion to the opposite cusp tip and back. The strain gages were connected to a Micromeasurements 2100 System Strain Gauge Conditioner (Measurements Group, Raleigh, NC) via a half Wheatstone bridge and output to an XY recorder (Houston Instruments Omnigraphic 2000DX, Austin, TX). Strains were measured at the buccal and lingual heights of contour as a function of varying occlusal forces and lateral excursion. The analog tracing was digitized at points located .35 mm apart on the occlusal surface.

6.4 The finite element method

The finite element method is a numerical method for solving problems of engineering and mathematical physics such as structural analysis, heat transfer, fluid flow, mass transport, and electromagnetic potential problems. For problems involving complex geometries, loadings, and material properties, numerical methods provide acceptable solutions, because analytical mathematical solutions are generally not possible. The finite element formulation of the problems results in a system of simultaneous algebraic equations for solution, rather than requiring the solution of differential equations. These numerical methods yield approximate values of the unknowns at discrete number of points in the continuum. By a process of discretization, the body is modelled by dividing it into an equivalent system of smaller bodies or units (finite elements) interconnected at common points (nodes). In the finite element method, instead of solving the problem for the entire body in one operation, one formulates the equations for each finite element and combines them to obtain the solution of the whole body. On making use of known stress/strain properties for the material making up the structure, one can determine the behavior of a given node or element in terms of the properties of every other element in the structure.

The solution for structural problems typically refers to determining the displacements at each node and the stresses within each element making up the structure that is subjected to applied loads. In nonstructural problems, the nodal unknowns may be temperatures or fluid pressures. The finite element method has several advantages over other modeling techniques:

1. Able to model irregularly shaped bodies easily
2. Handle general load conditions without difficulty
3. Model bodies composed of several different materials because the element equations are evaluated individually
4. Handle unlimited numbers and kinds of boundary conditions
5. Vary the size of the elements to make it possible to use small elements where necessary
6. Alter the model relatively easily

6.4.1 General steps of the finite element method[132]

1. Discretize and select element types

This involves dividing the body into an equivalent system of finite elements with associated nodes and choosing the most appropriate element type. The elements must be made small enough to give usable results and yet large enough to reduce computational effort. Small elements (and possibly higher order elements) are desirable in those areas where the results are changing rapidly and additional detail is desired. The choice of element types depends on the physical makeup of the body under actual loading conditions and how close to the actual behavior the analyst wants the results. For two dimensional problems, quadrilateral elements are generally suited for regular geometries composed of straight line segments or continuous arcs, whereas irregular geometries such as those of teeth are best divided by triangular elements or a combination of triangular and quadrilateral elements.

2. Select a displacement function

A displacement function within each element is chosen using the nodal values of the element. For a two-dimensional element, the displacement function is a function of the coordinates in its plane. The functions are expressed in terms of the nodal unknowns. The displacement through the body is approximated by a discrete model composed of a set of piecewise continuous functions defined within each finite domain or finite element.

3. Define the strain/displacement and stress/strain relationships

These are necessary for deriving the equations for each finite element. In the case of one-dimensional deformation, in the x direction, strain ε_x is related to displacement u by

$$\varepsilon_x = du/dx \qquad (6.2)$$

for small strains. Stresses must also be related to the strains through the stress/strain law (constitutive law). Hooke's law is often used in stress analysis and is given by

$$\sigma_x = E\varepsilon_x \qquad (6.3)$$

where σ_x = stress in x direction and E = modulus of elasticity.

4. Derive the element stiffness matrix and equations

Several methods are available for producing the stiffness matrix (direct equilibrium method, work or energy methods, methods of weighted residuals). Any of these methods will produce the equations to describe the behavior of an element. In matrix form,

$$
\begin{Bmatrix} f_1 \\ f_2 \\ f_3 \\ \cdot \\ \cdot \\ \cdot \\ f_n \end{Bmatrix} = \begin{bmatrix} k_{11} & k_{12} & k_{13} & \dots & k_{1n} \\ k_{21} & k_{22} & k_{23} & \dots & k_{2n} \\ k_{31} & k_{32} & k_{33} & \dots & k_{3n} \\ \cdot & & & & \cdot \\ \cdot & & & & \cdot \\ \cdot & & & & \cdot \\ k_{n1} & & & \dots & k_{nn} \end{bmatrix} \begin{Bmatrix} d_1 \\ d_2 \\ d_3 \\ \cdot \\ \cdot \\ \cdot \\ d_n \end{Bmatrix} \qquad (6.4)
$$

or in compact matrix form as

$$\{f\} = [k]\{d\} \qquad (6.5)$$

where $\{f\}$ is the vector of element nodal forces, $[k]$ is the element stiffness matrix and $\{d\}$ is the vector of unknown element nodal degrees of freedom or generalized displacements, n.

5. Assemble the element equations to obtain the global or total equations and introduce boundary conditions

The individual element equations generated in step 4 can now be added together using a method of superposition (the direct stiffness method) to obtain the global equations for the whole structure. Implicit in the direct stiffness method is the concept of continuity, or compatibility, which requires that the structure remain together and that no tears occur anywhere in the structure.

The final assembled or global equation written in matrix form is

$$\{F\} = [K]\{d\} \qquad (6.6)$$

where $\{F\}$ is the vector of global nodal forces, $[K]$ is the structure global or total stiffness matrix, and $\{d\}$ is now the vector of known and unknown structure nodal degrees of freedom or generalized displacements. The global stiffness matrix $[K]$ is a singular matrix because its determinant is equal to zero. To remove this singularity problem boundary conditions must be invoked so that the structure remains in place instead of moving as a rigid body.

6. Solve for the unknown degrees of freedom (or generalized displacements)

The previous equation, modified to account for the boundary conditions is a set of simultaneous algebraic equations that can be written in expanded matrix form as

$$
\begin{Bmatrix} F_1 \\ F_2 \\ F_3 \\ \cdot \\ \cdot \\ \cdot \\ F_n \end{Bmatrix} = \begin{bmatrix} K_{11} & K_{12} & K_{13} & \dots & K_{1n} \\ K_{21} & K_{22} & K_{23} & \dots & K_{2n} \\ K_{31} & K_{32} & K_{33} & \dots & K_{3n} \\ \cdot & & & & \cdot \\ \cdot & & & & \cdot \\ \cdot & & & & \cdot \\ K_{n1} & & & \dots & K_{nn} \end{bmatrix} \begin{Bmatrix} d_1 \\ d_2 \\ d_3 \\ \cdot \\ \cdot \\ \cdot \\ d_n \end{Bmatrix} \qquad (6.7)
$$

where n is the structure total number of unknown nodal degrees of freedom. These equations can be solved for the d's.

7. Solve for the element strains and stresses

Stress and strain values can be obtained because they can be directly expressed in terms of the displacements determined above. Typical relationships between strain and displacement and between stress and strain can be used.

8. Interpret the results

The final goal is to interpret and analyze the results for use in the design/analysis process. Determination of locations in the structure where large deformations and large stresses occur is generally important.

6.4.2 Development of the finite element model

The modelling phase of the study involved the development of a two dimensional, mathematical model representing the physical model. Two microcomputer based finite element analysis packages were employed: the ANSYS finite element package (Swanson Analysis Systems, Inc., Houston, PA) and IFECS (interactive finite element computing system, Lewis and Cross).[124]

ANSYS is an industry standard 2D/3D finite element analysis system used on micros, minis, and mainframe computers. It utilizes an in-core wave front (or frontal) solution procedure for the system of simultaneous linear equations developed from the assembled finite elements.[127] The wave front is the number of equations which are active after any element has been processed during the solution procedure. The ordering of elements is crucial to minimize the size of the wave front. The computer time required for the solution procedure is proportional to the square of the mean wave front size. ANSYS is divided into three phases: a preprocessing phase, a solution phase, and a postprocessing phase. In the preprocessing phase, nodes, node connectivity and element definition, material properties, loading conditions, and boundary conditions are declared. This file is then passed to the solution phase, where the system of simultaneous linear equations are solved. The solution file is then passed to the postprocessing phase where the results can be displayed in table or graphic form. ANSYS is written in compiled FORTRAN and occupies approximately 8 megabytes of hard disk storage for all modules.

IFECS, written by Lewis and Cross,[124] is a two dimensional FE software package originally written in BASIC for the DEC PDP 11/45 (Digital Equipment Corporation) under the RSTS/E operating system. It was later ported to the Masscomp MC500 supermicrocomputer (Massachusetts Computer Corporation, Westford, MA) using SVS/Basic Plus (Unipress Software, NJ) under a UNIX operating system. P. Chow ported the Masscomp version to the PC/AT with many enhancements using compiled BASIC (TurboBasic, Borland International, Scotts Valley, CA) operating under MS-DOS.

IFECS was developed to provide an interactive computing environment for the FEM application. This includes a mesh generation program, input data verification and an option to selectively review the results. Three ASCII files are generated by the user: (1) XYD file-a listing of nodal coordinates, temperature coefficients as applicable, and external boundary, (2) EMT file-consisting of internal boundaries, material types and properties (Young's modulus and Poisson's ratio), and (3) INP file-consisting of loading and boundary conditions. These three files are presented to the automatic mesh generator and equation solver. An optimal triangular mesh is generated using the prescribed nodes as vertices and sorting out the relevant material properties for each element. Any errors incurred in defining the boundary are determined by the mesh generation procedure. The FEM solution routine is executed using the data files created by the automatic mesh generation routine. The nodes of the model are renumbered to minimize the profile of the stiffness matrix. A variable bandwidth method for storage of the stiffness matrix is used which allows only non-zero diagonal matrix values to be stored. These subvectors are kept consecutively in a one-dimensional array along with an integer array of pointers defining the position of each diagonal term. The solution to the linear set of equations is by Choleskii decomposition. The binary solution file can be interrogated to produce an ASCII listing of the results for the desired nodes and elements.

6.4.3 Enhancements contributed to IFECS

A batch processor was developed to provide repeated execution of the same model under load step conditions. Thus, new load steps could be run without constant operator attention. A graphics package was written using HALO (Media Cybernetics, MD) graphics in Pascal for the MS-DOS operating system. This provided graphic display of the defined nodes, boundary conditions, internal and external boundaries, material types, loads, triangulation mesh, material properties, and stress or strain contours. The system also incorporates an interactive node entry system using a Summasketch MM1201 digitizing tablet (Summagraphics, CA). Screen dumps to hardcopy output devices in black and white or color are possible. This graphics system allows a visual confirmation of the three ASCII files in graphics form prior to submitting the job to the equation solver. Files can be downloaded from any computer system running IFECS for verification. The graphics software has been subsequently optimized by P. Chow at Thames Polytechnic (London, England, UK) and S. Kemp at the University of Minnesota (Minneapolis, MN, USA).

The benefits of IFECS over ANSYS were in its ease of use, particularly for automatic mesh generation, which was not available in ANSYS, and direct strain solution. ANSYS had benefits over IFECS in graphics output and interactive capabilities in modification of the node definition. Nodal points were defined and modified in the ANSYS system, mesh generation performed in IFECS, then ported back to ANSYS for solution. A program was written by the author to translate the files from one system to the other. The port of IFECS to the PC/AT was in the process of completion at the time of this project, therefore the ANSYS solution served as a benchmark for the IFECS system.

Table 6-2. Material properties for restoaration model

material	Poisson's ratio	Mod. of elast (N/m2)
dentin	0.25	1.54 E10
enamel	0.30	4.69 E10
core composite	0.25	2.21 E10
"enamel" veneer	0.25	7.95 E9
feldspathic porcelain	0.30	8.3 E10
ceramometal alloy	0.30	8.6 E10
full crown cast gold	0.30	9.9 E10

A model was constructed from the mean dimensions taken from a large population of natural teeth[125] and therefore represented an "average" maxillary first premolar. The model consisted of 199 nodes and 362 elements with the 4 nodes apical to the cemento-enamel junction fixed in the X and Y direction (Fig. 6-4). All the other nodes were given two degrees of freedom (X and Y). The material types and properties of the teeth are listed in Table 6-1 as described by Morin.[120,120a,120b] Occlusal loads (5, 8, 10 pounds) were applied at discrete lateral excursive positions (6 lingual, 6 buccal and centric occlusion) to simulate the occlusal bruxing in the experimental configuration (Fig. 6-5). The mean principal strain from four contiguous elements on the buccal and lingual heights of contour approximating the location of the strain gages were taken to represent the strain measured by the strain gages.

Assumptions of the model:

1. Plane strain representation
2. Absolute bonding between enamel and dentin
3. Pulp chamber has negligible effect on the performance of the model
4. Enamel and dentin behave as isotropic, homogeneous materials.

A crown restoration model was adapted for incorporation of the restorative material layers. The crown preparation was designed with flat, butt shoulders and uniform reduction of the enamel into the dentin. Layers of the "enamel" composite was placed over the "body" composite material (Fig. 6-6). Appropriate materials constants were used as listed in Table 6-2. Nodes and elements were added to accommodate the additional layers of material. The model consisted of 343 nodes and 586 elements. The external boundary demarcated the junction between dentin and pulp chamber, and the model was fixed in the X and Y direction apical to the cementoenamel junction. The remainder of the nodes were given two degrees of freedom. A plane strain configuration was used.

Assumptions of the model:

1. Absolute bonding between composite layers and between the crown restoration and dentin
2. Pulp tissue has negligible effect on the performance of the model
3. Material properties represented by conventional materials in the same class.
4. Composite and dentin behave as an isotropic, homogeneous material.

Physiologic occlusal loads were placed in a several directions to simulate occlusal loading patterns. Loads were placed on the lingual incline of the buccal cusp between the cusp tip and central groove. The loading configuration is shown in Fig. 6-6. The location of occlusal loading estimated that which could be achieved clinically. A vertically oriented 3 pound load was placed on single nodes. This same load was applied to a single node normal to a tangent to the surface. For comparison, identical loading conditions were applied on a porcelain fused to metal (PFM) crown, gold crown, and a natural tooth.

The results from the experimental portion of the study are listed in Table 6-3. These results are graphed in Figures 6-7 and 6-8. The results are reported in microstrain for each of the buccal and lingual strain gages. Table 6-4 lists the results from the finite element computations. These results are graphed in Figures 6-9 and 6-10.

Table 6-3. Experimental strain gage results reported in microstrain

sample	load	location	30L	25L	20L	15L	10L	5L	CO	5B	10B	15B	20B	25B	30B
1	5	li	0	-38	-41	-47	-50	-26	-17	-11	-9	-8	-9	-12	-12
3	5		-74	-80	-82	-89	-71	-75	-18	26	47	54	62	52	0
4	5		-37	-46	-61	-79	-45	-31	-16	0	0	0	0	0	0
mean			-37	-54	-61	-72	-55	-44	-17	5	12	15	18	13	-4
1	8		0	-44	-50	-56	-56	-20	-9	-2	3	4	4	-1	-5
2	8		-123	-128	-136	-139	-113	-123	-31	30	56	70	90	82	0
4	8		-60	-73	-93	-113	-69	-49	-26	0	0	0	0	0	0
mean			-61	-82	-93	-103	-79	-64	-22	9	19	25	31	27	-2
1	10		0	-64	-72	-82	-75	-29	-17	-9	-5	-6	-6	-7	-7
2	10		-148	-158	-169	-170	-138	-149	-40	16	48	85	104	106	0
4	10		-74	-91	-113	-128	-88	-63	-39	-9	0	0	0	0	0
mean			-74	-104	-118	-127	-100	-80	-32	-1	14	26	33	33	-2
1	5	bu	0	17	17	20	21	17	2	-8	-20	-54	-70	-54	-48
2	5		0	0	0	0	0	0	-1	-14	-32	-41	-34	-32	-27
4	5		0	24	26	27	28	28	15	-0	-34	-41	-50	-55	-35
mean			0	14	15	15	16	15	5	-7	-29	-45	-51	-47	-36
1	8		0	13	16	19	19	8	-3	-23	-36	-72	-120	-102	-88
2	8		0	0	0	0	0	0	-2	-20	-47	-62	-57	-50	-43
4	8		0	28	27	26	29	32	2	-17	-49	-57	-80	-75	-58
mean			0	13	14	15	16	13	-1	-20	-44	-64	-86	-75	-63
1	10		0	15	20	29	26	16	8	-17	-37	-71	-138	-101	-117
2	10		0	0	0	0	0	0	-2	-23	-48	-74	-72	-60	-54
4	10		0	32	32	33	36	41	-41	-15	-38	-46	-61	-80	-47
mean			0	16	17	21	21	19	-12	-19	-41	-64	-90	-80	-73

Table 6-4. Finite element model results reported in microstrain

load	location	30L	25L	20L	15L	10L	5L	CO	5B	10B	15B	20B	25B	30B
5	bu					30	2	-118	-53	-65	-90	-116	-140	
	li					-115	-74	-152	142	143	145	144	144	

An interesting result from this study, demonstrated by both the strain gage and finite element methods, was the relative insensitivity of the unloaded cusp to the compression experienced by the loaded cusp. As the one cusp was loaded, strains measured at the opposite cusp were low, indicating little deflection of the unloaded cusp. It was expected that the two cusps would function as an integrated unit, i.e., as the height of contour of the loaded cusp experienced compression, the unloaded cusp should experience tension. Microscopic evaluation of the nature of the central fissure did not provide consistent evidence for the explanation of the independent movement of the cusps. The distribution of stresses within the natural tooth due to the material properties, lamination, and geometry contribute to this phenomenon. The ability of the resilient dentin layer to disperse the stresses protects the supporting structure of the tooth.

The finite element produced good correlation with the results from the experimental phase of the study. The finite element model demonstrated maximum compressive strains directly under the occlusal loads corresponding to the findings of Selna et al.[126] A plane strain finite element model was implemented because of the assumption of uniform loading and material properties in the mesial and distal dimension of the tooth. The strain normal to the x-y plane ε_z and the shear strains γ_{xz} and γ_{yz} are assumed to be zero. The assumption of plane strain is realistic for bodies with constant cross-sectional area along the z axis subjected to loads that act only in the x and/or y directions and do not vary in the z direction. Only a unit thickness of the structure is considered because each unit thickness behaves identically (except near the ends).

The finite element model used in this study is a 2 dimensional representation and is subject to criticism as such. However accurate representation of the morphology and careful definition of boundary and loading conditions has produced good correspondence to the experimental result. Increase of the number of elements as a convergence test did not produce significant changes in the results. The finite element model can be used to simulate other restorative system with confidence because of the validation by the experimental results.

Table 6-5. Finite element model results for restorations

LOAD pounds	NODE ORIENTATION	ELEM	sigma 1 stresses (N/m2)	critical initial flaw size (mm)
10	342 Y compressive	586	5.21E+06	1.87E+01
		584	1.93E+06	1.37E+02
3	342 Y compressive	586	1.56E+06	2.08E+02
		584	5.78E+05	1.52E+03
5	342 Y compressive	586	2.60E+06	7.49E+01
		584	9.63E+05	5.47E+02
8	342 Y compressive	586	4.17E+06	2.93E+01
		584	1.54E+06	2.14E+02
5	342 normal to surface	389	2.08E+06	1.18E+02
		374	2.02E+06	1.25E+02
		383	1.86E+06	1.47E+02
		379	1.85E+06	1.49E+02
		412	3.52E+06	4.11E+01
		446	3.41E+06	4.36E+01
		465	2.63E+06	7.32E+01
5	57 normal to surface	526	1.50E+06	2.26E+02
		465	1.36E+06	2.74E+02
		420	1.23E+06	3.37E+02
		564	1.12E+06	4.06E+02
5	59 normal to surface	412	1.32E+06	2.91E+02
		425	1.01E+06	5.01E+02
		401	9.96E+05	5.11E+02
3	342 normal to surface	412	2.11E+06	1.14E+02
		446	2.05E+06	1.21E+02
		465	1.58E+06	2.03E+02
		503	1.38E+06	2.68E+02
		435	1.33E+06	2.89E+02
		425	1.26E+06	3.22E+02
3	57 normal to surface	412	1.43E+06	2.47E+02
		446	1.26E+06	3.18E+02
		435	9.14E+05	6.08E+02
3	59 normal to surface	412	7.92E+05	8.08E+02
		425	6.04E+05	1.39E+03
5	342 PFM, Y compressive	586	2.01E+06	401000
5	342 NATURAL TOOTH, Y compressiv	586	1.78E+06	356100

Displacements for the loaded nodes and stresses generated in the immediate area of the load for the restored tooth is listed in Table 6-5. Stress contours displaying the σ_1 and σ_3 stresses (highest compressive and highest tensile stresses) are shown in Fig. 6-11. Isocolor areas represent isostress areas within the limits shown in the legends. Tension is represented by positive stresses, compression by negative.

Microfil composites are prone to microcrack generation and chipping and fracturing, as described earlier. Crack growth in glassy polymers proceeds through distinct stages of initiation and propagation, as in all brittle materials. Macroscopic defects will develop from a single flaw and traverse the specimen resulting in failure.[130] Composites are particularly sensitive to microdefects that can be produced by air inclusion, dust and other contaminants. These inherent flaws potentially act as sites for stress concentration. If a stress intensity at one of the flaw tips is produced which is greater than the material can withstand the flaws begins to grow in size. At some critical condition the crack front becomes unstable and propagates catastrophically through the remaining cross-section of material. Fillers acting as stress concentrators significantly multiply the number of sites for potential crack growth. When debonding of the polymer from the filler occurs, a crack of substantial dimensions can result. In a brittle particle reinforced composite, cracks can be impeded by obstacles in the form of second phase dispersions (fillers). Primary cracks tend to bow out between the fillers forming secondary cracks.[128]

Small surface defects or flaws can propagate when subjected to sufficient stress resulting in a surface crack. Using a linear elastic fracture mechanics (LEFM) approach for a surface crack in a semi-infinite body:[129]

$$K_I = \sigma\sqrt{\pi a} \qquad (6.8)$$

where K_I is the stress intensity factor for opening mode (Mode I) crack propagation, σ is the maximum allowable design stress, and a is the allowable crack size. Crack propagation and brittle fracture can be prevented by altering the (1) structure shape, (2) stresses incurred by the material, (3) initial flaw size, or (4) material property, K_{Ic}, the fracture toughness. Generally, the structure shape, stresses, and flaw size are not easily controlled, therefore, a material with adequate K_{Ic} needs to be chosen carefully to minimize fracture. It is only when K_I reaches the critical value of the material property K_{Ic} that the crack will propagate.

The maximum size surface crack, a, that can be tolerated before crack propagation occurs at a given stress, σ, is given by

$$a = 1/\pi \, (K_{Ic}/\sigma)^2 \qquad (6.9)$$

For a cyclic loaded structure, Forman, et al.,[129a] proposed that the crack growth rate could be determined from the relationship

$$da/dN = [A\,\Delta K^p]/[(1-R_1)K_c - \Delta K] \qquad (6.10)$$

$$= A\,[(\sigma\sqrt{\pi a})^p]/[K_c - (\sigma\sqrt{\pi a})] \qquad (6.11)$$

where A and p are material constants, ΔK, the range of the stress intensity factor equals K_{max}-K_{min} which also equals $1.14\Delta\sigma\sqrt{\pi a}$, K_c is the fracture toughness, and $R_1 = K_{min}/K_{max}$. As R_1 increases with higher load ratios and/or the fracture toughness, K_c decreases, the crack growth rate, da/dN, for a given ΔK increases.

Given the restoration design and materials presented above, the crack propagation rate initiated by a small surface flaw of 1 micrometer can be determined. Using the following material constants,

$A = 5.00 \times 10^{-14}$

$p = 3.00$

$K_{max} = 1.00 \times 10^6\ N/m^{3/2}$ for filled composites

$R_1 = 0$ when cycling from $\sigma_{min} = 0$ to σ_{max}

$a = 5.00 \times 10^{-7}$ meter where 2a, the initial flaw size = 1 micrometer

$\sigma = 1.56 \times 10^6\ N/m^2$ which is the maximum stress for the restoration design as a result of a 3 pound load at the buccal cusp tip

$$\Delta K = \sigma \sqrt{\pi a} = 2189.8\ N/m^{3/2}$$

$$da/dN = 5.26 \times 10^{-10} \text{ meters/cycle} = 5.26 \times 10^{-4} \text{ microns/cycle}$$

given one year = 250,000 cycles, the crack propagation rate is 131.5 microns/year. Although this is a worst case estimate because it assumes that each contact is at the same location and has the same magnitude, the location of the loads and magnitudes are well within physiologic limits. The propagation rate suggests that a small defect on the order of a micron can initiate a fatigue fracture within the restoration under physiologic loads.

For comparison, the stresses for a conventional porcelain fused to metal crown (PFM) and natural tooth are listed in Table 6-5 and shown in Figure 6-12 and 6-13. Using the resultant stresses from a 3 pound load applied at the same location as in the composite, the crack in the PFM propagated at a rate of 60.3 micrometers/250K cycles and the natural tooth at a rate of 42.4 micrometers/250K cycles. These values are less than half the rates found in the composite crown design.

It has been proposed that microfil composites fracture and wear through a subsurface damage mechanism. Small defects initiate cracks which propagate when stressed (occlusally loaded). Failure from fatigue is promoted by microdefects generated during wear.[6] Bulk fracture results in areas of high stress concentration.[58]

If the wear rate of composite, porcelain, and natural enamel is considered, the wear rate of composite (49 micrometers/250K cycles) is approximately one-half that of porcelain (105 micrometers/250K cycles) and slightly lower than that of enamel (92 ± 51 micrometers/250K cycles). The influence of microcracking, based on the analysis presented representing composite as a homogeneous material, does not appear to contribute to the overall wear rate as much as was expected. The observed wear rate can be attributed to pinning of the crack with the filler particles and the possible arrest of the crack before catastrophic failure.[130] The crack only moves within the matrix phase. However, microcrack and microchip generation play a role in the wear process of composites by abrasion and fatigue. Natural enamel, which is also a composite material, does not generally experience bulk fracture because of the rod structure of the enamel and the resilient, supportive dentin. Stresses in natural enamel are dispersed into the dentin rather than localized at the area of load application. It should also be noted that wear may be beneficial in situations where the occlusion is incorrect, i.e., where an elevated contact exists. If the high occlusal contact is not worn, excessive contact stresses are generated which could result in bulk fracture.

Early clinical evidence shows that cracks are propagated adjacent to areas of contact stress (Fig. 6-14). Although bulk fracture has not been observed to date, it appears that cracks initiated by flaws in the fabrication of the restoration tend to propagate within the outer veneer of the crown. This problem can be remedied through minimizing defects in fabrication and careful occlusal adjustment. The material properties of the composite may also need further enhancement.

Figure 6-1. Craze lines in aged natural enamel.

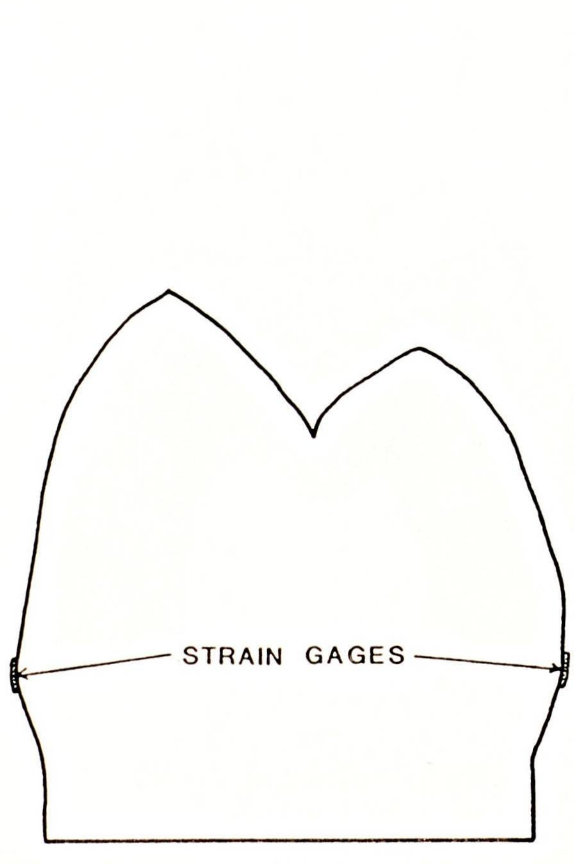

Figure 6-2. A physical model of a natural premolar tooth

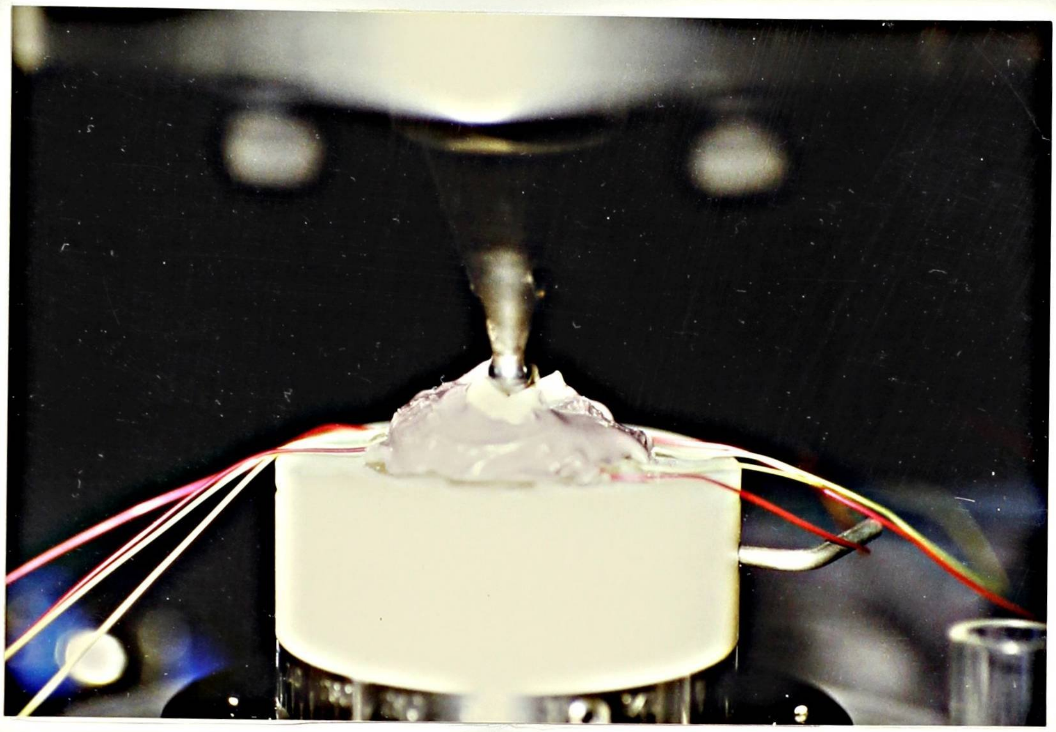

Fig. 6-3. Spherical loading element placed on cuspal inclines

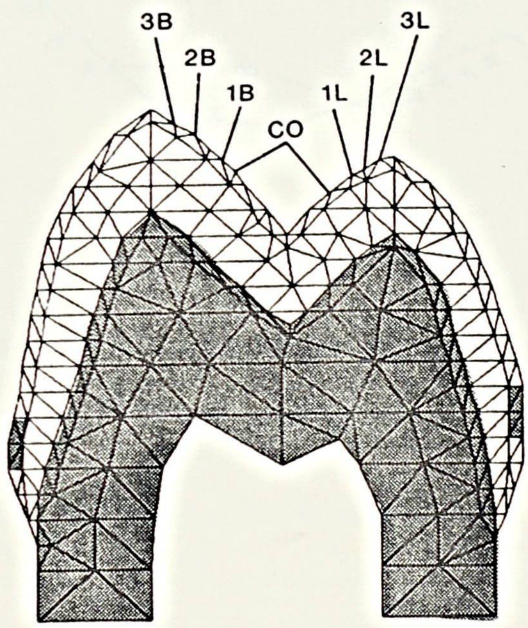

FINITE ELEMENT MODEL

Fig. 6-4. Finite element model for natural premolar. Shaded region indicates dentin with lighter shaded enamel layer overlying. Occlusal loading areas designated by distance from centric occlusion (CO) followed by (b)uccal or (l)ingual.

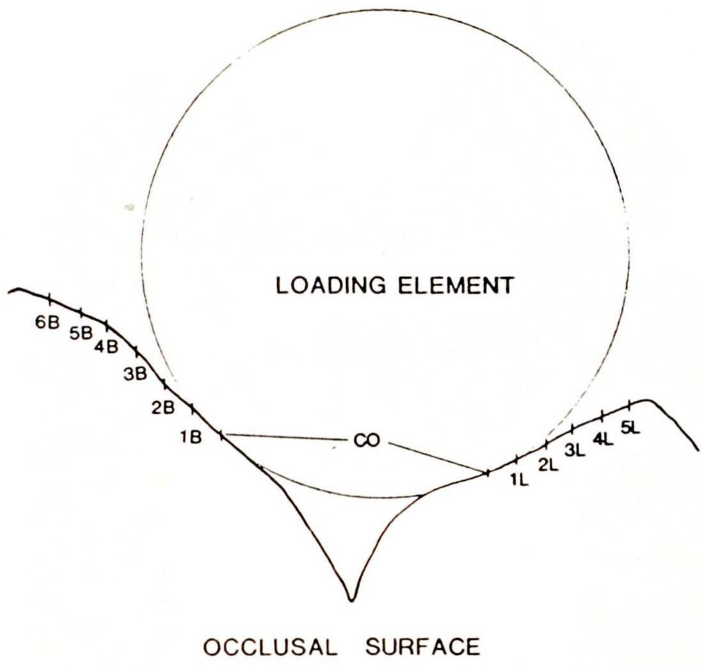

Fig. 6-5. Loading positions on natural tooth to correspond to those on the FE model

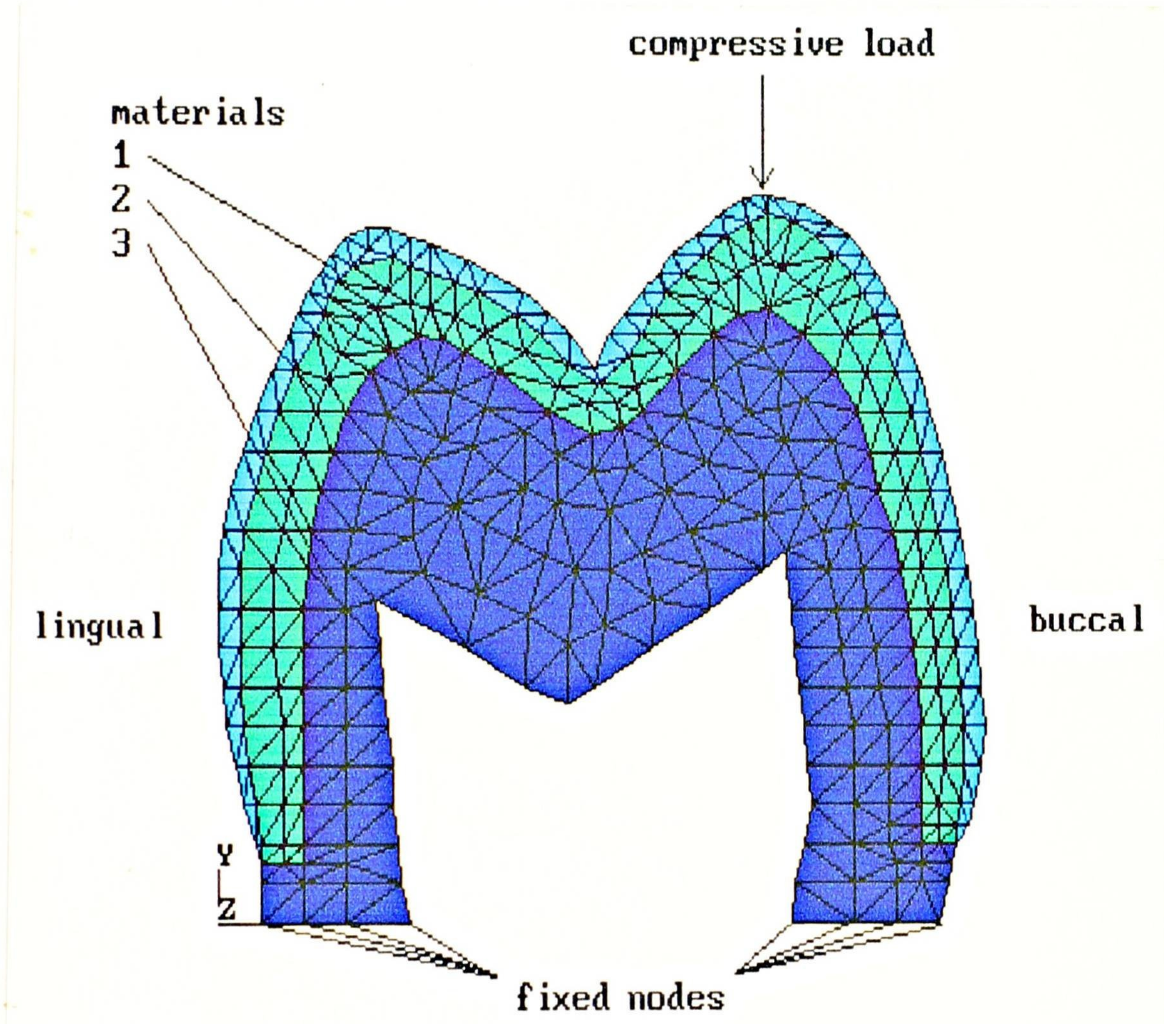

Fig. 6-6. Loading and boundary conditions for restoration model

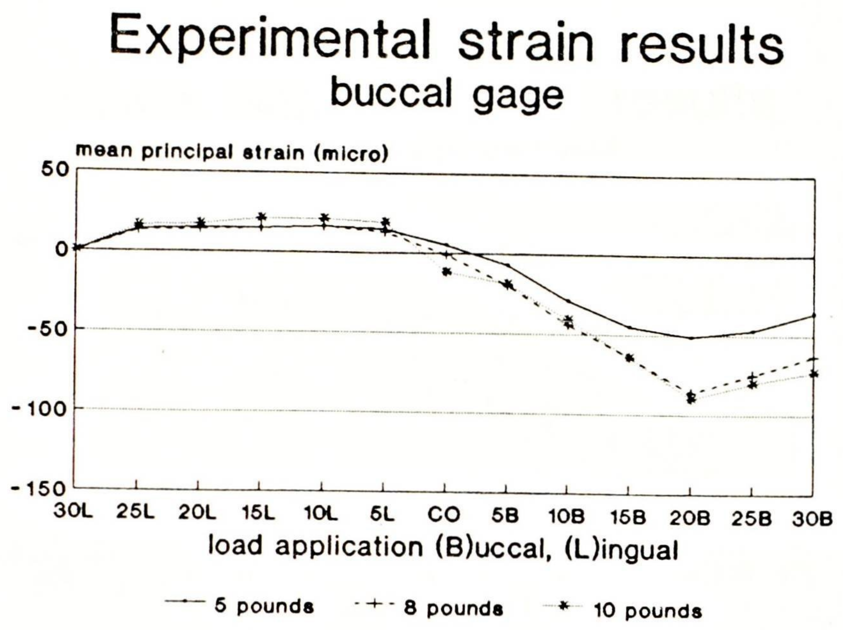

Fig. 6-7. Experimental strain results for buccal gage

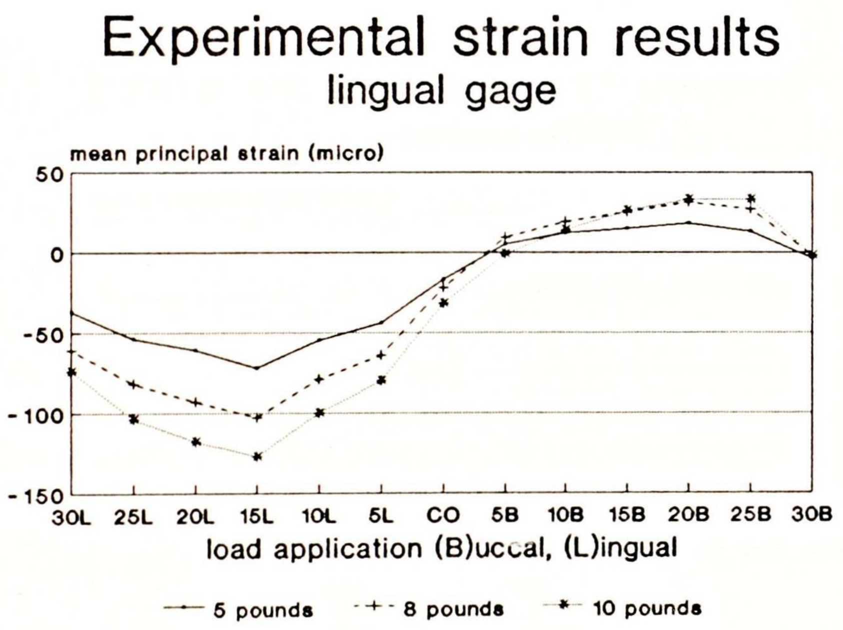

Fig. 6-8. Experimental strain results for lingual gage

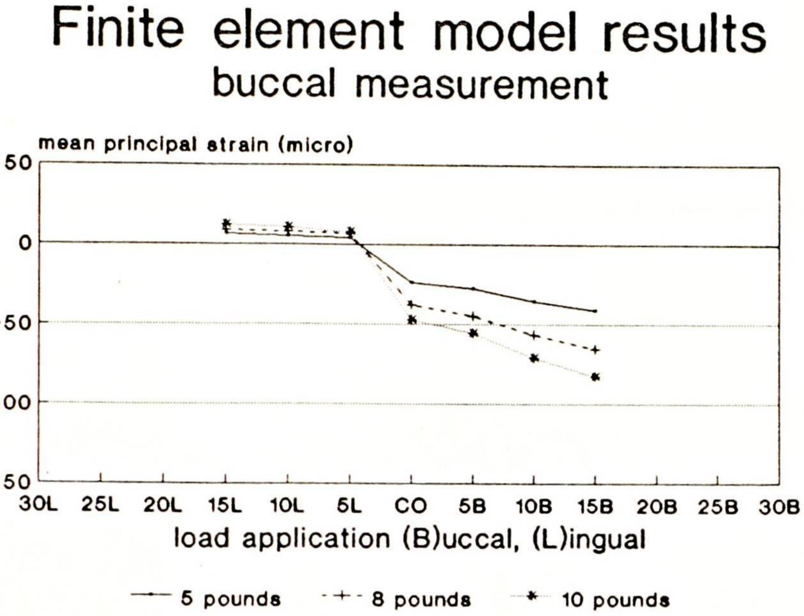

Fig. 6-9. Finite element model results for buccal measurement

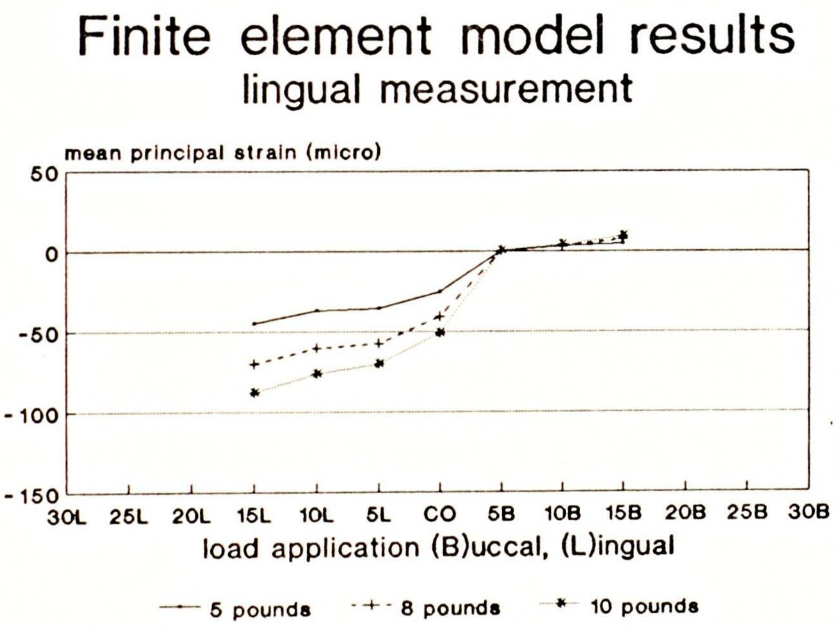

Fig. 6-10. Finite element results for lingual measurement

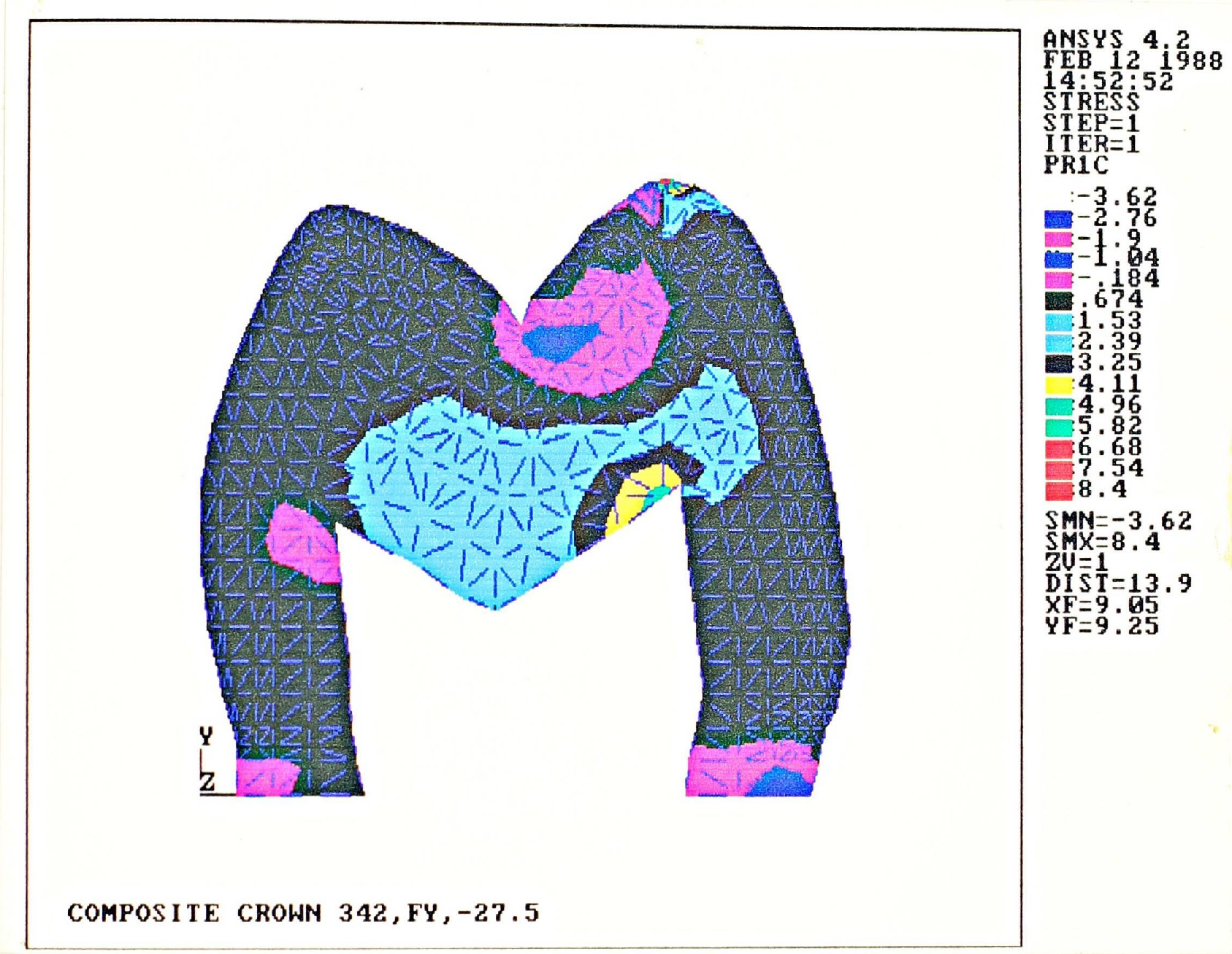

Fig. 6-11. Stress distribution in layered composite crown design. Negative stresses represent compressive, positive represents tensile

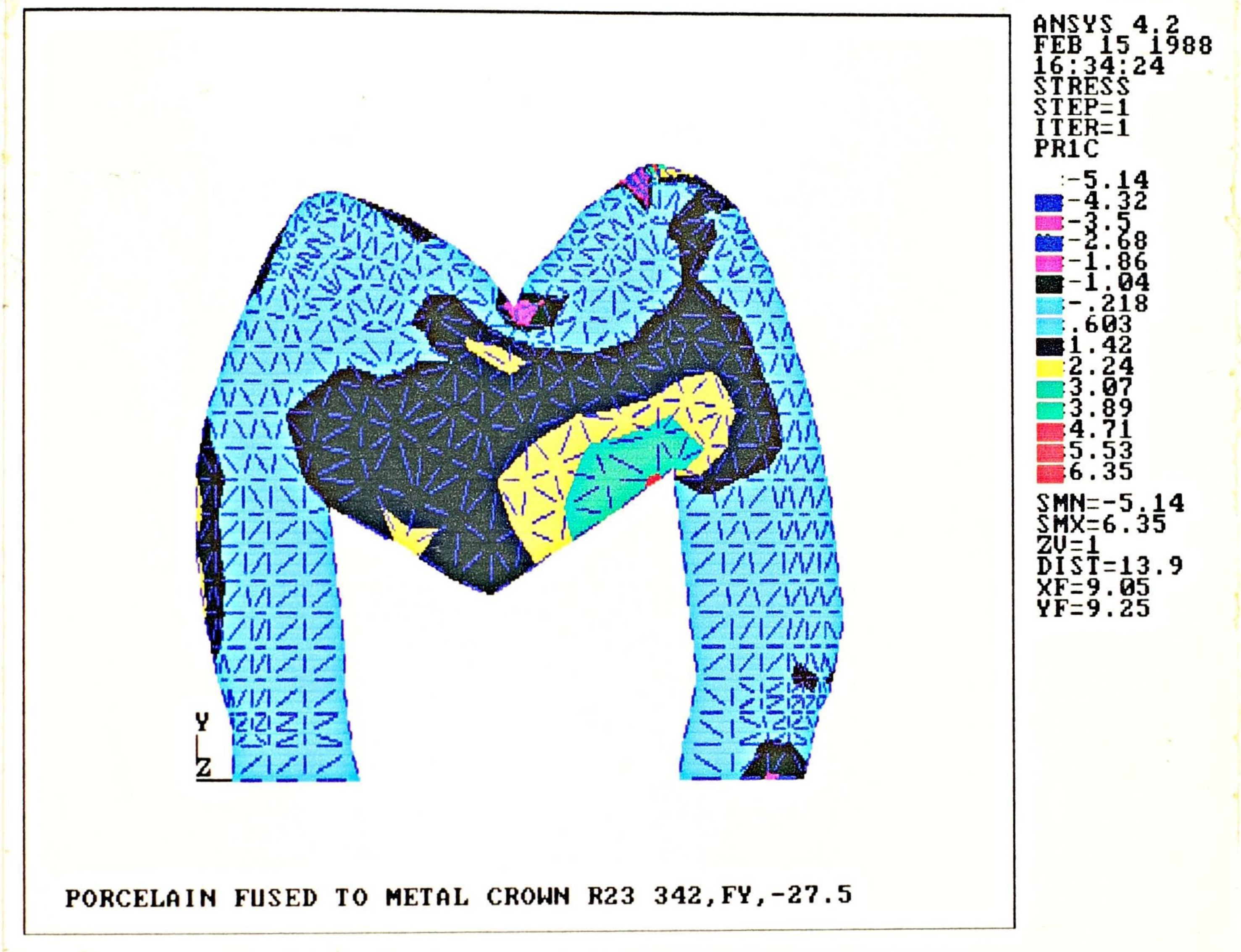

Fig. 6-12. Stress distribution within porcelain fused to metal crown

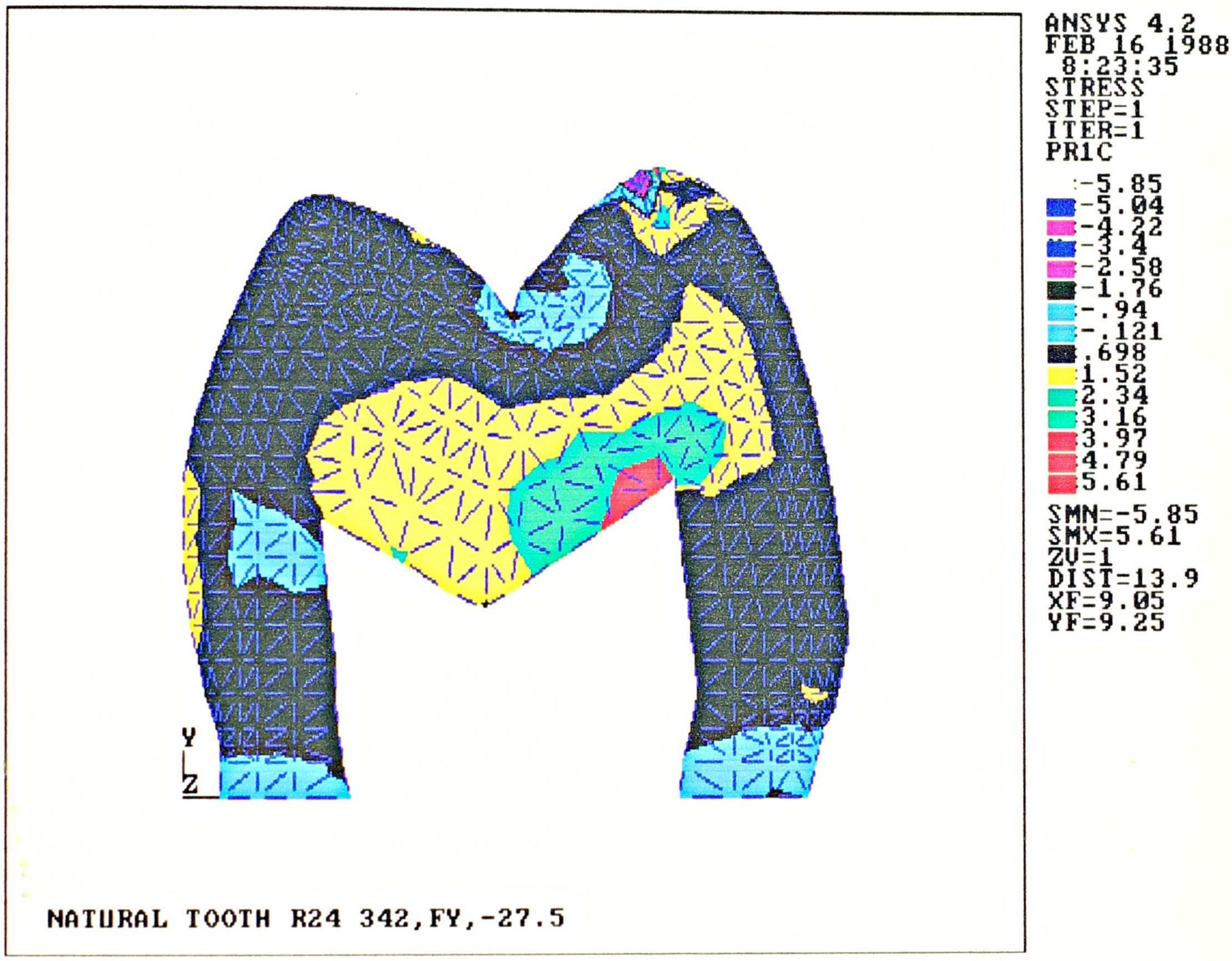

Fig. 6-13. Stress distribution within natural tooth

Fig. 6-14. Clinical evidence of crack adjacent to occlusal stress area in composite crown restoration. Horizontal cracks are evident on the lingual surfaces of the maxillary canine teeth as noted by arrows.

7 General Discussion and Conclusions

Understanding of the wear mechanisms and wear potential of dental materials allows the clinician to design restorative treatment which preserves the natural dentition. It does not appear that any prosthetic dental material performs as well as natural enamel, in terms of aesthetics, wear and fracture resistance. The oldest of the materials studied, dental amalgam, demonstrates the lowest wear potential. Unfortunately, it is not an aesthetic restorative material. Porcelain abrades the opposing dentition and composites have fair wear properties, but tend to fracture.

The artificial mouth has been demonstrated to have the ability of reproducing clinically simulated wear both in magnitude and mechanism. Reiterating the benefits of the artificial mouth for laboratory testing of dental materials: decreased variation of data compared to clinical methods, more precise control of physiologic parameters, accelerated testing, reproduction of the parameters of mastication with an oral environment, flexibility to evaluate other parameters such as friction, and relative ease of operation through standardized procedures. The artificial mouth studies have shown good correlation with the clinical studies of Lambrechts[61] and Braem[62] which instills confidence in predicting wear. The profiling system is a crucial component of the simulation system and can also be used successfully in assessing clinical wear through the use of carefully prepared replicas. It is one of the few profiling systems which has addressed the problem of fitting two images ("before" and "after" wear) together.

A few weaknesses are associated with the versatility of the artificial mouth. A steep learning curve and high cost limit the use of the instrument for routine quality control and screening tests in manufacturing of dental materials. However, the development of a centralized testing center using the artificial mouth as a standard testing tool should be attractive to dental materials manufacturers. Load control is achieved with a minimum peak load of approximately 1.5 to 2 pounds which is believed to be lower than the range of physiologic loads desired for testing, however, low loads are desirable for friction measurements. This was addressed in the design of the Bionix testing instrument.

Amalgam demonstrated the lowest wear potential of the materials tested. The wear of the opposing enamel was not measurable. Amalgam wears by an adhesive wear mechanism which was indicated by the low coefficient of wear and confirmed by the transfer of amalgam onto the opposing cusp shown by SEM analysis.

Porcelain produced the highest wear of the opposing enamel cusp and demonstrated considerable wear itself. The wear progresses by an abrasive mechanism which corresponded to a high coefficient of abrasion and wear tracks through the sample.

Composite wear was intermediate and could not be explained on the basis of abrasion alone. Wear tracks were evident on the sample as well as microcracks spread laterally from the wear tracks. This suggested a fatigue mechanism was operating together with the abrasive mechanism which was explored with mathematical modelling techniques.

In general, all of the materials demonstrated a linear volumetric wear curve as predicted by the general wear equation and a parabolic wear curve for the maximum depth of the wear facet. This was confirmed by evaluating shape factors of the wear facet and establishing the parabolic relationship between volume loss and depth of loss.

The study of the wear of enamel revealed that the anisotropic nature of enamel makes the study difficult, demonstrated by the high variability when enamel opposed enamel. It is evident that studies of natural enamel to enamel wear require matched pairs of teeth from the same opposing segments of the arch from the same patient in the correct occlusal scheme. This would be possible if impressions of both arches and an occlusal registration are made prior to extraction, fitting the extracted teeth into the impressions, pouring the model, then aligning the casts with the occlusal registration. However, the possibility of obtaining virgin opposing teeth is limited to extractions for orthodontic purposes, and generally these teeth have not been in occlusion. Measurements of friction for various orientations of enamel indicated that the physiologic orientation of enamel to enamel contact produced the lowest friction.

The friction of enamel to enamel was shown to be insensitive to the fluid used. Only lubricants containing surfactants providing boundary lubrication and high viscosity lubricants were capable of reducing interfacial friction. The friction was most influenced by surface texture as was demonstrated by the twofold increase in friction after roughening the enamel surface. The fluid film was penetrated at the speeds and occlusal loads tested resulting in true enamel to enamel contact. Friction between enamel and glass was elevated with water and saliva and diminished with glycerol. This indicated that the water and saliva permitted more intimate contact between the opposing materials. There was evidence that saliva provided lubrication between enamel couples and it is probable that the effect of saliva and the natural oral environment is to promote adhesion of a pellicle onto the enamel surface which serves to reduce interfacial friction and wear.

The finite element method produced the same trends as were measured by the experimental strain gage configuration. The validated mathematical model demonstrated a difference in the distribution of occlusal stresses by a natural tooth and composite crown. The localized stresses were adequate to propagate a microcrack which could be initiated through defects in the composite. The crack propagation rate determined by cycling confirmed a fatigue mechanism operating in conjunction with the abrasive wear mechanism observed earlier.

7.1 Clinical recommendations

1. Natural dentition should not be opposed by a porcelain surface unless the lateral sliding contacts are eliminated by establishing a canine guided occlusion. If a porcelain fused to metal crown is required for aesthetic purposes, the occlusal contacts should be made in metal if at all possible.

2. From the standpoint of wear, amalgam is a very satisfactory restoration to oppose natural dentition. They should not be routinely replaced by posterior composite restorations.

3. Posterior composites should be placed conservatively because of their potential for wear and fracture. Large composite restorations encompassing a large portion of the occlusal table and cusps should be avoided.

Fig. 7-1. Severe wear of maxillary anterior teeth produced by porcelain fused to metal bridge on mandibular anterior segment

References

1. Suit SR, Gibbs CH, Benz ST. Study of gliding tooth contacts during mastication. J Periodontol 1975; 47:331-334.

2. Jent T, Karlsson S, Hedegard B. Mandibular movements of young adults recorded by intraorally placed light-emitting diodes. J Prosthet Dent 1979; 42(6):669-673.

3. Whitman DJ, McKinney JE, Hinman RW, Hesby RA, Pelleu GB Jr. In vitro wear rates of three types of commercial denture tooth materials. J Prosth Dent 1987; 57(2):243-246.

4. Mueller HJ, Mahendra SB, Knoeppel R. Human enamel-dental amalgam pin on disc wear. Dent Mater 1985; 1:31-35.

5. Harrison A, Lewis TT. The development of an abrasion testing machine for dental materials. J Biomed Mater Res 1975; 9:341-353.

6. McKinney JE, Wu W. Chemical softening and wear of dental composites. J Dent Res 1985; 64(11):1326-1331.

7. Rootare HM, Powers JM, Craig RG. Wear of composites by abrasives of varying hardness. J Dent Res 1979; 58(3): 1097-1100.

8. Harrison A, Draughn RA. Abrasive wear, tensile strength, and hardness of dental composite resins - is there a relationship? J Prosthet Dent 1976; 36:395-398.

9. Powers JM, Allen LJ, Craig RG. Two body abrasion of commercial and experimental restorative and coating resins and an amalgam. JADA; 89:1118-1122.

10. Smith BH, McCabe JF. Three laboratory methods for evaluating wear of restorative materials. J Dent Res 1981; 60A:478.

11. Ehrnford L, Derand T, Larsson LA, Svensson A. An abrasion test for composite resins. J Dent Res 1980; 59:716-720.

12. Derand T, Ehrnford L. A long-term evaluation of abrasion of dental composite resins. J Dent Res 1980; 59-721-723.

13. Powell JM, Phillips RW, Norman RD. In vitro wear of composite resin, amalgam and enamel. J Dent Res 1975; 54:1183-1195.

14. Phillips RW, Avery DR, Mehra R, Swartz ML, McCune RJ. Observations on a composite resin for Class II restorations: three year report. J Prosthet Dent 1973; 30:891-897.

15. Jaworzyn JF, Arundel PA, Cantwell JB. Posterior composite restorations: simultaneous hydrothermal cycling and wear studies in vitro. J Dent Res 1978; 57:708.

16. Powers JM, Roberts JC, Craig RG. Wear of filled and unfilled restorative resins. Wear 1976; 39:117-122.

17. Roberts JC, Powers JM, Craig RG. Wear of dental amalgam. J Biomed Mater Res 1977; 11:513-523.

18. Harrison A. Effect of packing pressure on abrasion resistance of dental amalgams. J Dent Res 1977; 56:613-615.

19. Harrison A and Moores GE. Influence of abrasive particle size and contact stress on the wear rate of dental restorative materials. Dent Mater 1985; 1(1):14-18.

20. DeGee AJ, Pallav P, Davidson CL. Effect of abrasion medium on wear of stress-bearing composites and amalgam in vitro. J Dent Res 1986; 65(5):654-658.

21. Pallav P, Davidson CL, DeGee AJ. Wear rates of composites, an amalgam, and enamel under stress bearing conditions. J Prosth Dent 1988; 59(4):426-429.

22. Heath JR, Wilson HJ. Abrasion of restorative materials by toothpaste. J Oral Rehabil 1976; 3:121-138.

23. Shell JS, Hollenback GM, Villanyi AA. Comparative abrasion rates of restorative materials. J Calif Dent Assoc 1966; 42:521-524.

24. Harrington E, Jones PA, Fisher SE, Wilson HJ. Toothbrush-dentifrice abrasion. Br Dent J 1982; 153:135-138.

25. Jones DW, Jones PA, Wilson HJ. A simple abrasion test for composites. J Dent 1972; 1:28-34.

26. Pilliar RM, Smith DC, Maric B. Oscillatory wear tests of dental composites. J Dent Res 1984; 63:1166-1172.

27. McCabe JF, Smith BH. A method for measuring the wear of restorative materials in vitro. Br Dent J 1981; 151:123-126.

28. DeLong R, Douglas WH. Development of an artificial oral environment for the testing of dental restoratives: bi-axial force and movement control. J Dent Res 1983; 62:32-36.

29. Lambrechts P, Ameye C, Vanherle G. Conventional and microfilled composite resins. Part II: chip fractures. J Prosthet Dent 1982; 48(5): 527-538.

30. Boksman L, Jordan RE, Suzuki M, Charles CH. A visible light-cured posterior composite resin: results of a 3 year clinical evaluation. JADA 1986; 112:627-631.

32. Swift EJ. Research report: Wear of composite resins. JADA 1987; 115:585-588.

33. Council on Dental Materials, Instruments, and Equipment. Expansion of the acceptance program for dental materials, instruments, and equipment: composite resin materials for occlusal Class I and Class II restorations. JADA 1981; 102(3):349-350.

34. Eick JD. In vivo wear measurement of composite resins. In: Vanherle G, Smith DC eds. Intl symp on posterior composite resin dental restorative materials. The Netherlands: Peter Szulc Publ Company, 1986:351-364.

35. Phillips RW, Avery DR, Mehra R, Swartz ML, McCune RJ. Observations on a composite resin for Class II restorations: Two year report. J Prosthet Dent 1972; 28:164-169.

36. Leinfelder KF, Sluder TB, Sockwell CL, Strickland WE, Wall JT. Clinical evaluation of composite resins as anterior and posterior restorative materials. J Prosthet Dent 1975; 33(4):407-416.

37. Leinfelder KF, Sluder TB, Santos JFF, Wall JT. Five-year clinical evaluation of anterior and posterior restorations of composite resin. Operative Dent 1980; 5:57.

38. Cvar JF, Ryge G. Criterion for the clinical evaluation of dental restorative materials. USPHS Publication no. 790-244, San Francisco, US Gov Printing Office, 1971.

39. Ryge G. Clinical criteria. Int Dent J 1980; 30:347-358.

40. Ryge G, Jendresen MD, Glantz PO, Mjor J. Standardization of clinical investigators for studies of restorative materials. Swed Dent J 1981; 5:235-239.

41. Ryge G, DeVincenzi RG. Assessment of the clinical quality of health care-search for a reliable method. Evaluation and the Health Professions 1983; 6:311-326.

42. Glantz PO. Ryge G, Jendresen MD, Nilner K. Quality of extensive fixed prosthodontics after five years. J Prosthet Dent 1984; 52:457-459.

43. Jorgensen KD, Asmussen E. Occlusal abrasion of a composite restorative resin with ultrafine filler - an initial study. Quintessence Int 1978; 6:73-78.

44. Dennison JB, Powers JM, Charbeneau GT. In vivo evaluation of posterior composite and amalgam restorations. J Dent Res 1980; 59: abst 202.

45. Mitchem JC, Gronas DG. In vivo evaluation of the wear of restorative resin. JADA 1982; 104:333-335.

46. Mitchem JC, Gronas DG. The continued in vivo evaluation of the wear of restorative resins. J Dent Res 1984; 63:abst 1498.

47. de Rijk WG, Conner ML, Jennings KA, Wu WL. The vivo resistance of dental composites with enhanced polymerization. J Dent Res 1984; 63:abst 951.

48. Mitchem JC, Gronas DG. The continued in vivo evaluation of the wear of restorative resins. JADA 1985; 111:961-964.

49. Wilder AD, May KN, Leinfelder KF. Five-year clinical study of UV-polymerized composites in posterior teeth. J Dent Res 1984; 63:abst 1497.

50. Goldberg AJ, Rydinge E, Lambert K, Sanchez L, Santucci E. Clinical evaluation methods for posterior composite restorations. J Dent Res 1981; 60:abst 1089.

51. Leinfelder KF, Barkmeier WW, Goldberg AJ. Quantitative wear measurement of posterior resins. J Dent Res 1983; 62:abst 194.

52. Leinfelder KF, Wilder AD Jr, Teixeira LC. Wear rates of posterior composite resins. JADA 1986; 112:829-833.

53. Heymann HO, Wilder AD, May KN, Leinfelder KF. Two clinical studies of composites in posterior teeth. J Dent Res 1984; 63:abst 952.

54. Eick JD, McGarrah HE, Lamb RD. Application of stereo-photogrammetry to measure wear of posterior composites. J Dent Res 1984; 63:abst 1482.

55. Hengchang X, Tong W, Shiqing S. Wear patterns of composite restorative resins in vivo; observations by scanning electron microscopy. J Oral Rehab 1985; 12:389-400.

56. Roulet JF. In vivo wear measurement of composite resins. In: Vanherle G, Smith DC, eds. Intl symp on posterior composite resin dental restorative materials. The Netherlands: Peter Szulc Publ Company, 1985:365-372.

57. Hirt TM, Lutz F, Roulet JF. In vivo evaluation of occlusal wear of two experimental composites versus amalgam. J Oral Rehab 1984; 11:511-520.

58. Lutz F, et al. Potential posterior composites. An in vivo-in vitro comparison for wear. J Dent Res 1984; 63:914-920.

59. Lutz F. Beitrage zur entwicklung von seitenzahnkomposits. KAR PAR PAM, Zurich 1980.

60. Lutz F, Imfeld T, Phillips RW. P10-its potential as a posterior composite. Dent Mater 1985: 1: 61-65.

61. Lambrechts P, Vanherle G, Vuylsteke M, Davidson CL. Quantitative evaluation of the wear resistance of posterior dental restorations: a new three-dimensional measuring technique. J Dent 1984; 3:252-267.

62. Braem M, Haspeslagh L, Lambrechts P, Vanherle G. Four posterior composites: a one year report. J Dent Res 1985; 64(4):713 abst 88.

63. Lambrechts P, Vuylsteke M, Vanherle G, Davidson CL. Quantitative in vivo wear of posterior dental restorations: four-year results. J Dent Res 1985: 62(spec issue):abst.1759, 370.

64. Powell JM, Phillips RW, Norman RD. In vitro wear of composite resin, amalgam and enamel. J Dent Res 1975: 54: 1183-1195.

65. Bailey WF, Rice SL. Comparative sliding-wear behavior of a dental amalgam and a composite restorative as a function of contact stress. J Dent Res 1981: 60: 731-732.

66. Rice SL, Wayne SF, Bailey WF. Influence of variation in contact stress on the sliding-wear behavior of a dental amalgam. Biomater 1981; 2:46-48.

67. Mahalick JA, Knap FJ, Weiter EJ. Occlusal wear in prosthodontics. JADA 1971; 82:154-159.

68. Monasky GE, Taylor DF. Studies on the wear of porcelain, enamel and gold. J Pros Dent 1971; 25:299-306.

69. Miller GR, Powers JM, Ludema KC. Frictional behavior and surface failure of dental feldspathic porcelain. Wear 1975; 31:307-316.

70. Leinfelder KF. Wear patterns and rates of posterior composite resins. Inter Dent J 1987; 37:152-157.

71. Braem M, Haspeslagh L, Lambrechts P, Vanherle G. Four posterior composites: a one year report. J Dent Res 1985: 64(4): 713 (abst 88).

72. Leinfelder KF. Evaluation of clinical wear of posterior composite resins. In: Vanherle G, Smith DC. Posterior composite resin dental restorative materials. The Netherlands: Peter Szulc Publ Company, 1985: 501-510.

73. Vrijhoef MMA, Hendriks, FHJ, Letzel H. Loss of substance of dental composite restorations. Dent Mater 1985: 1: 101-105.

74. Abeil AK, Leinfelder KL, Turner DT. Microscopic observations of the wear of a tooth restorative composite in vivo. J Biomed Mat Res 1983; 17: 501-507.

75. Dickson G. Physical and chemical properties and wear. J Dent Res 1979; 58(5):1535-1543.

76. Lutz F, Imfeld T, Meier CH. Composites versus amalgam. Comparative measurements of in vivo wear resistance: 1-year report. Quint Int 1979; 10:77.

77. Pugh B. Friction and wear, a tribology text for students. London: Newnes-Butterworths, 1973.

78. Halling J. Principles of tribology. London: The Macmillan Press Ltd, 1975

79. Kruschov MM. Resistance of metals to wear by abrasion, related to hardness. Inst mech engrs conf lubrication and wear, London, 1957; 655-659.

80. Richardson RCD. The wear of metals by relatively soft abrasives. Wear 1968; 11:245-275.

81. Rabinowicz E. In: Sakurai T, ed. Proc of the JSLE-ASLE Intl Lubr Conf, Tokyo, Japan. Amsterdam: Elsevier, 1975:76-80.

82. Oberle TL. Properties influencing wear of metals. J Metals 1951; 3:438-439.

83. Spurr RT, Newcombe TP. The friction and wear of various materials sliding against unlubricated surfaces of different types and degrees of roughness. Instn mech engr conf lubrication and wear, London. 1981:269.

84. Amontons G. De la resistance causee dans les machines. Acad Roy des Sci, Memoires de mathematique et de physique, 1699, 259-286.

85. Sarkar AD. Friction and wear. London: Academic Press, Inc Ltd, 1980.

86. Bowden FP, Tabor D. The friction and lubrication of solids. London: Oxford Univ Press, 1964.

87. Greenwood JA, Williamson JB. Contact of nominally flat surfaces. Proc Royal Soc (London) 1966; A295:300.

88. Norton AE. Lubrication. New York: The McGraw-Hill Book Company, Inc, 1942.

89. Levine M. Private communication, 1988.

90. DeLong R, Douglas WH. Development of an artificial oral environment for the testing of dental restoratives: bi-axial force and movement control. J Dent Res 1983; 62(1):32-36.

91. DeLong R, Pintado MR, Douglas WH. The measurement of change in contour by computer graphics. Dent Mater 1985; 1:27-30.

92. Tillitson EW, Craig RG, Peyton FA. Friction and wear of restorative dental materials. Dent Res 1971; 59(1):149-154.

93. Koran A, Craig RG, Tillitson EW. Coefficient of friction of prosthetic tooth materials. J Prosthetet Dent 1972; 27(3):269-274.

94. Craig RG, Powers JM. Wear of dental tissues and materials. Int Dent J 1976; 26(2):121-133.

95. Szeri AZ. Tribology-friction, lubrication, and wear. Washington D.C.: Hemisphere Publishing Corp, 1980.

96. Raptis CN, Powers JM, Fan PL. Frictional behavior and surface failure of acrylic denture teeth. J Dent Res 1981; 60(5):908-913.

97. Nordbo H, Darwish S, Bhatnagar RS. Rate of viscosity changes in five salivary protein fractions following pH changes. Scand J Dent Res 1984; 92(4):302-305.

98. Nordbo H, Darwish S, Bhatnagar RS. Salivary viscosity and lubrication: influence of pH and calcium. Scand J Dent Res 1984; 92(4):306-314.

99. Nordbo H, Darwish B, Dymbe and Dahl B. J Dent Res 1985; 64:8732, abst 55.

100. Coffey JP, Goodkind RJ, DeLong R, Douglas WH. In vitro study of the wear characteristics of natural and artificial teeth. J Prosthet Dent 1985; 54:273-280.

101. Ogle RE, David LJ, Ortman HR. Clinical wear study of a new tooth material: Part II. J Prosthet Dent 1985; 54:67-75.

102. Quinn TFJ. The application of modern physical techniques to tribology. London: Newnes-Butterworths, 1971.

103. Kusy RP, Leinfelder KF. Pattern of wear in posterior composite resotrations. J Dent Res 1977; 56(5):544.

104. Wu W, Toth EE, Moffa JF, Ellison JA. Subsurface damage layer of in vivo worn dental composite restorations. J Dent Res 1984; 63(5):675-680.

105. Powers JM, Fan PL. Erosion of composite resins. J Dent Res 1980; 59(5):815-819.

106. Draughn RA. Effects of microstructure on compressive fatigue of composite restorative materials. In: Gebelein CG and Koblitz FF (eds) Biomedical and dental applications of polymers. New York: Plenum Press, 1981.

107. Draughn RA. Compressive fatigue limits of composite restorative materials. J Dent Res 1979; 60:1093-1096.

108. Draughn RA. Influence of fillers on performance in posterior composites, Proceedings of International Symposium on Posterior Composite Resins, Taylor DF (ed). Chapel Hill: Univ. of NC Press, 1984.

109. Phillips RW. Current status and future developments of posterior resin compounds. In: Leinfelder KL, Taylor DF (eds) Posterior Composites. Chapel, North Carolina, 1982: 1-5.

110. Christianson GJ. The use of porcelain-fused-to-metal restorations in current dental practice: a survey. J Prosthet Dent 1986; 56(1)1-3.

111. Mulhearn TO and Samuels LE. The abrasion of metals: a model of the process. Wear 1972; 5:478-498.

111a. Andreasen JO. Traumatic injuries of the teeth. Copenhagen: Munksgaard, 1972.

112. Embong A, Glyn Jones J, Harrison A. The wear effects of selected composites on restorative materials and enamel. Dent Mater 1987; 3(5):236-240.

113. Norman RL. Frictional resistance and dental prosthetics. J Pros Dent 1964; 14(1);45-51.

114. Noonan MA. The use of photoelasticity in a study of cavity preparations. J Dent Child 1949; 16:24-28.

115. Tanner AN. Factors affecting the design of photoelastic models for two-dimensional analysis. J Prosthet Dent 1972; 27:48-61.

116. Fisher JW, Godfrey K, Stephens RI. Experimental strain analysis of infant, adolescent, and adult miniature swine subjected to simulated mastication forces. J Biomech 1976; 9:333-338.

117. Hood JA, Farah JW, Craig RG. Modification of stresses in alveolar bone induced by a tilted molar. J Fixed Prosth 1975; 34:415-421.

118. Farah JW, Craig RG, Sikarski DL. Photoelastic and finite element stress analysis of a restored axi-symmetric first molar. J Biomech 1973; 6:551-520.

119. Kitoh M, Suetsugu T, Murakami Y. Mechanical behavior of tooth, periodontal membrane and mandibular bone by the finite element method. Bull Tokyo Med Dent Univ 1977; 24:81-87.

120. Morin DL. Relationship between cavity form, restorative technology and strength of restored teeth. Master of Philosophy thesis, Thames Polytechnic, London, England, 1985.

120a. Morin DL, Douglas WH, Cross M, DeLong R. Biohysical stress analysis of restored teeth: experimental strain measurement. Dent Mater 1988; 4:41-48.

120b. Morin DL, Cross M, Voller VR, Douglas WH, DeLong R. Biophysical stress analysis of restored teeth: modelling and analysis. Dent Mater 1988; 4:77-84.

121. Fisher DW, Caputo AA, Shillingburg H, Duncanson J. Photoelastic analysis of inlay and onlay preparations. J Prosthet Dent 1975; 33:47-53.

122. Buckland-Wright JC. Body structure and pattern of force transmission in the cat skull. J Morphology 1978; 155:35-62.

123. Hylander WL. Mandibular function in Galago Crassicaudatus and Macaca Fascicularis: an in vivo approach to stress analysis of the mandible. J Morphology 1979; 159:253-296.

124. Lewis BA, Cross M. IFECS-an interactive finite element computing system. Appl Math Modeling 1978; 2:165-176.

125. Langsjoen OM, Noble FW. Descriptive Dental Anatomy. Minneapolis: University of Minnesota, 1982.

126. Selna LG, Shillingburg HJ, Kerr PA. Finite element analysis of dental structures-axisymmetric and plane stress idealizations. J Biomed Mater Res 1975; 9:237-252.

127. Swanson Analysis System Inc. ANSYS Engineering Analysis System User's Manual, 1987.

128. Spanoudakis J, and Young RJ. Crack propagation in a glass particle-filled epoxy resin, part I. J Mater Sci 1984; 19:473-486.

129. Caddell RM. Deformation and fracture of solids. New Jersey: Prentice-Hall, Inc. 1980.

129a. Forman RG, Kearney VE, Engle RM. Numerical analysis of crack propagation in cyclic-loaded structures. Trans ASME, Jour Bas Engr 1967; 89:459-464.

130. DiBenedetto AT. Crack propagation in amorphous polymers and their composites. J Macromol Sci-Phys 1973; B7(4):657-678.

131. Ross CTF. Applied stress analysis. Chicester: Ellis Horwood Limited, 1987.

132. Logan DL. A first course in the finite element method. Boston: PWS Engineering, 1986.

Appendix A

Publications based on work presented

Douglas WH, Sakaguchi RL, DeLong R. Frictional effects between natural teeth in an artificial mouth. Dent Mater 1985; 1:115-119.

DeLong R, Sakaguchi RL, Douglas WH, Pintado MR. The wear of dental amalgam in an artificial mouth: a clinical correlation. Dent Mater 1985; 1:238-242.

Sakaguchi RL, Douglas WH, DeLong R, Pintado MR. The wear of a posterior composite in an artificial mouth: a clinical correlation. Dent Mater 1986; 2:235-240.

DeLong R, Douglas WH, Sakaguchi RL, Pintado MR. The wear of dental porcelain in an artificial mouth. Dent Mater 1986; 2:214-219.

Abstracts

Sakaguchi RL, Douglas WH, DeLong R. The friction and lubrication of enamel-to-enamel contact. J Dent Res 1988; 67:253.

DeLong R, Douglas WH, Pintado MR, Sakaguchi RL. Accuracy of 3-D digitalization of posterior composite wear. J Dent Res 1988; 67:362.

Brust E and Sakaguchi RL. Biomechanics of natural and restored teeth during bruxing in an artificial mouth. J Dent Res 1988; 67:380.

Brust E, Sakaguchi RL, Douglas WH, DeLong R, Pintado MR. Finite element analysis of the biomechanics of natural teeth. J Dent Res 1987; 66:204.

Olin PS, Lehner CR, DeLong R, Douglas WH, Sakaguchi RL. Surface friction and porcelain wear in an artificial mouth. J Dent Res 1987; 66:66.

Sakaguchi RL, Douglas WH, DeLong R, Pintado MR. Occlusal wear of natural enamel in an artificial mouth. J Dent Res 1986; 65:749.

DeLong R, Sakaguchi RL, Douglas WH, Pintado MR. Remote-site clinical measurement of occlusal wear. J Dent Res 1986; 65:749.

Douglas WH, Sakaguchi RL, DeLong R, Pintado MR. Posterior composite wear in an artificial mouth: a clinical correlation. J Dent Res 1986; 65:797.

Douglas WH, DeLong R, Sakaguchi RL. Surface frictional changes in posterior materials during wear experiments in an artificial mouth. J Dent Res 1985; 64:371.

DeLong R, Sakaguchi RL, Douglas WH. Occlusal wear of posterior materials in an artificial mouth-a comparative study. J Dent Res 1985; 64:371.

Sakaguchi RL, DeLong R, Douglas WH. Friction and wear of posterior enamel in an artificial mouth. J Dent Res 1985; 64:370.

Frictional effects between natural teeth in an artificial mouth

W. H. Douglas, R. L. Sakaguchi, R. DeLong

School of Dentistry, University of Minnesota, Minneapolis, USA

Douglas WH, Sakaguchi RL, DeLong R. Frictional effects between natural teeth in an artificial mouth. Dent Mater 1985: 1: 115–119.

Abstract. – A method for measuring frictional forces on enamel of natural teeth and restorative materials was developed using the Artificial Oral Environment. Enamel/enamel systems were tested using different oral fluids in a mini-environmental chamber capable of introducing biologic fluids between the occluding surfaces. Matched, extracted opposing human premolars mounted in physiologic occlusion under an occlusal load of 3 pounds were bruxed at approximate masticatory velocities. A load cell measured the resulting horizontal forces and an X-Y record was attained. 31 independent measurements of friction in both buccal and lingual directions were performed with the teeth dry, and with human saliva, Xerolube, and distilled water intervening. It was found that typical values for enamel/enamel coefficients of friction, μ, were in the range of 0.1–0.42. μ was independent of different fluids within any one enamel/enamel couple (coefficient of variation was typically 10%). However, the coefficient of friction of the enamel pair was highly dependent on surface texture. Roughening virgin enamel led to a 3 fold increase in μ. Conversely surfactants present in mineral oil reduced the friction of roughened enamel by 3 fold. Where the wear process is by abrasion it is likely that the reduction of the tangential forces due to friction could lead to reduced loss of contour. It is likely that finishing procedures in dentistry are important in this process. Finally, the production of low friction restorative materials are clearly indicated as a future development.

Key words: artificial oral environment, coefficient of friction, enamel, friction, saliva, wear.

Ronald L. Sakaguchi, D.D.S., Biomaterials Program, 16-212 Moos Tower, School of Dentistry, University of Minnesota, 515 Delaware Street SE, Minneapolis, Minnesota 55455, USA

Accepted for publication January 23, 1985

The frictional effect generated by tooth to tooth contact is of considerable significance in dentistry. Friction between teeth develops a force which has a component in the horizontal plane, and thus, contributes to the lateral thrust on the periodontal membrane. It may also contribute to the abrasive wear of dental enamel or restorative materials on occlusal surfaces. It is this latter point, coupled with the current interest in the wear performance of new restorative materials, which has caused the consideration of friction to gain importance.

Norman (1) used saliva between a 1 mm rounded tip and flat disc of material to examine the frictional forces. The highest frictional resistance found was the combination of porcelain against porcelain and the lowest was between chrome-cobalt alloy pairs. The friction between enamel pairs was intermediate. Several references (2, 3, 4, 5) indicate that friction between dental materials may be higher in the presence of a liquid than under dry conditions. This increased friction has been suggested to be due to the polarity of the fluid and the material being tested influencing the friction.

Mahalick (6), using half-elliptical against hemispherical samples in a rotating abrading apparatus, found gold-gold, acrylic-gold, enamel-gold and porcelain-gold couples to have the lowest wear values. Enamel-porcelain, enamel-enamel, and porcelain-porcelain demonstrated the highest wear rates. Acrylic-acrylic, porcelain-acrylic, and enamel-acrylic showed intermediate wear rates. Monasky (7) reported on the relationship between wear rate and surface texture of the porcelain specimens tested using a reciprocating carriage capable of producing intermittent sliding contacts. He found rapid wear rates in samples opposing rough porcelain surfaces. Natural tooth structure tended to polish the porcelain surfaces diminishing the wear rate, while gold did not alter the surface texture of the porcelain appreciably.

If frictional trends are compared with abrasive wear a correlation between friction and abrasive wear may be indicated. However, it appears that there is a gap in the literature regarding basic information on the coefficient of friction of dental materials functioning physiologically under a variety of environmental conditions and under functional conditions. The present report is an attempt to supply some of this data by measuring the coefficient of friction in simulated conditions in an artificial mouth (8) using opposing natural premolars. The long-term goal of this work is to determine the influence of tooth to tooth friction on the wear of enamel and posterior materials.

Material and methods

The artificial mouth used in this expe-

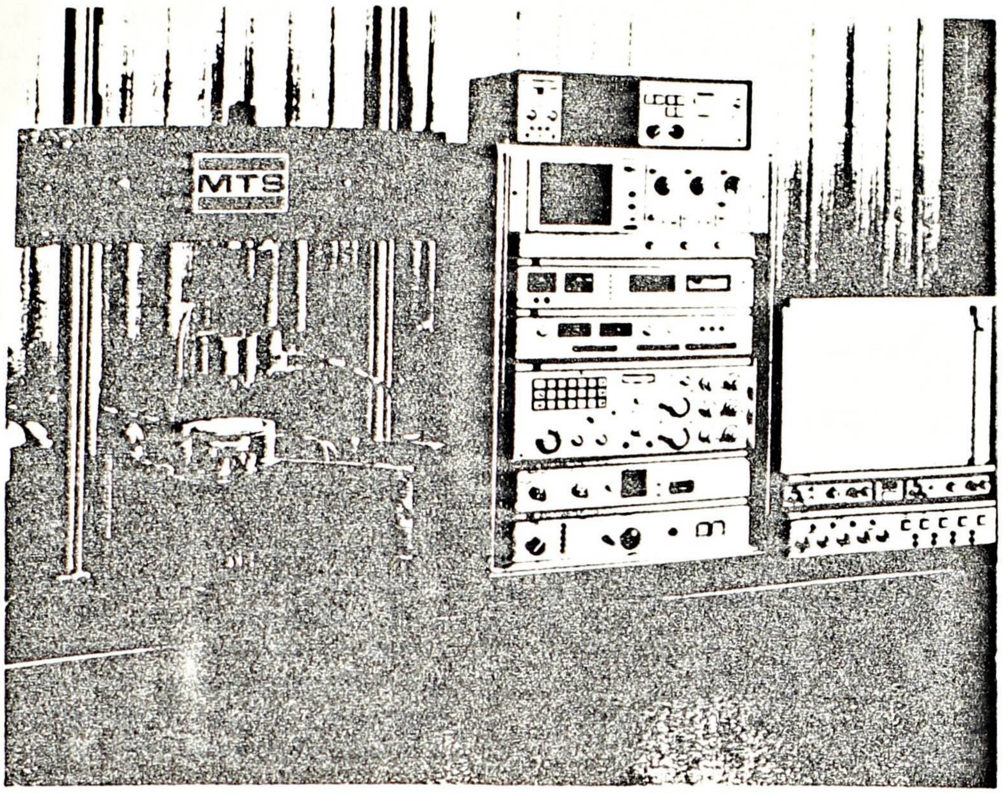

Fig. 1. The artificial mouth.

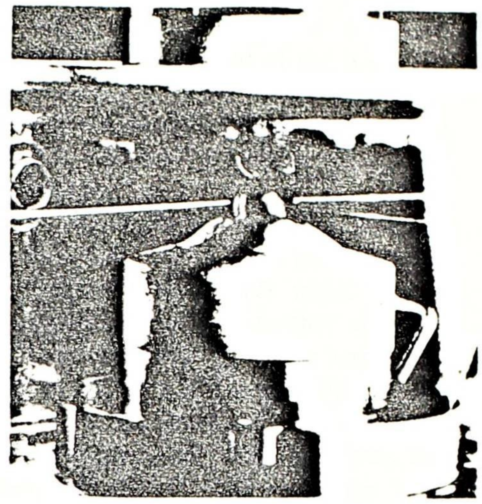

Fig. 3. Premolars in artificial oral environment.

riment was a servohydraulic model capable of reproducing the main parameters of the human masticatory cycle (Fig. 1) (8). A load cell was included in the path of the lateral excursion so that the side thrust or the resultant horizontal force on the mandibular tooth could be accurately monitored.

The coefficient of kinetic friction μ is defined by the equation

$$F = \mu N$$

where F is the frictional force and N is the force normal to the surface at the point of contact. The artificial oral environment can measure the horizontal and the vertical forces, thus, if it is assumed that the only force in the horizontal direction is the frictional force then the coefficient of friction can be calculated from

$$\mu = \frac{ST}{OF}$$

where OF is the occlusal force measured by the vertical load cell and ST is the frictional force (side thrust) measured by the horizontal load cell. This equation is true only for motion in the horizontal plane. Unfortunately, this generally is not the case for teeth since the path of motion is usually along an incline on a cuspal surface. For these cases, the normal force is no longer equal the occlusal force. However, the magnitude of the normal force at any point on the surface can be calculated from

$$N = OF \operatorname{Cos} \theta \operatorname{Cos} \Phi$$

where θ is the angle of inclination of the tangent to the surface parallel to the path of motion at the point of contact (Fig. 2). Φ is defined similarly, except it is perpendicular to the path of motion. During bruxing or chewing it is possible to find a path of motion where Φ is approximately zero (e.g., along a triangular crest) then $\operatorname{Cos} \Phi = 1$ and

$$N = OF \operatorname{Cos} \theta$$

If θ does not equal zero then ST does not equal F, however, from the geometry depicted in Fig. 2 it can be shown that

$$\mu = (ST \operatorname{Cos} \theta + OF \operatorname{Sin} \theta)/(ST \operatorname{Sin} \theta - OF \operatorname{Cos} \theta)$$

where ST, OF, and θ are measurable parameters.

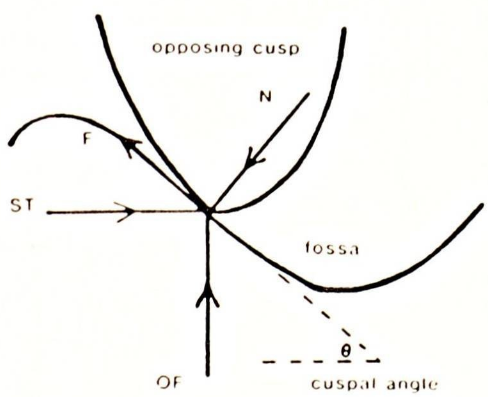

Fig. 2. Geometry for determination of coefficient of friction θ = cuspal angle; OF = occlusal force; ST = side thrust; F = friction; N = normal force.

Opposing pairs of human premolars from the same patient were stored in deionized water at 4°C. The teeth were mounted in nylon rings using a laboratory-prepared, chemically cured composite of 50/50 (W/W) by weight of ground quartz*. This mounting medium was more resistant to degradation by fluids than improved stone. The physiologic relationship between the maxillary and mandibular premolars was established with the mandibular buccal cusp in contact with the lingual incline of the maxillary buccal cusp (Fig. 3). In this manner, 4 pairs of human premolars were established successively in the artificial mouth.

The artificial mouth was programmed to perform a bruxing motion with a lateral excursion of 1 mm through centric occlusion and an occlusal force of 13.35 N (3 pounds) on the single tooth pair. The velocity of the lateral excursion was 2 mm/sec. A physiologic oral environment was simulated by circulating fluids maintained at 37°C onto the occluding surfaces.

Using the formula indicated earlier the coefficient of friction μ was derived for both the buccal and lingual excursions. The terms buccal and lingual excursions refer to the movement of the lower tooth. Thus, in a buccal excursion the maxillary cusp slides down the lower cuspal incline (Fig. 2). In a lin-

* 3M Co., St. Paul, MN 55144.

gual excursion the reverse in the case. The environmental conditions were changed by altering the circulating fluids. The following procedure for changing the environmental fluids was adopted. Occlusal surfaces were cleaned with ethanol and acetone and were dried with oil-free compressed air. The surface was wetted with the new fluid and bruxing was continued until equilibrium was achieved.

The list of different fluids and enamel conditions are shown in Table 1. The sequencing of the liquids used was randomized and is indicated in Table 1. In addition to circulating relatively low viscosity fluids, white petrolatum gel* and a lubricating oil** were applied to an occlusal surface roughened by a green abrasive stone'. Under these 2 last conditions no circulating fluid was applied during bruxing but the ambient temperature was maintained at 37°C in the environmental chamber.

Results

A typical X-Y record of the side thrust measured by the horizontally positioned load cell is shown in Fig. 4. The tracing generated during bruxing motion shows the zero side thrust line through the middle of the record. The distance of the tracing from the zero

* Petrolatum, White, U.S.P.
** Titan handpiece oil, Star Dental, Valley Forge, PA 19482.
' Shofu Dental Corp., Menlo Park, CA 94025.

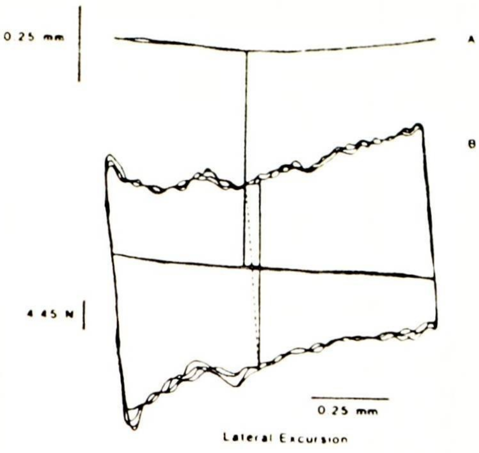

Fig. 4. Typical X-Y record of side thrust.
A – profile of the contact area, showing the shape of the bruxing motion.
B – record of the side thrust. The dashed line coordinates identical points on plot A and plot B.

horizontal load component is determined by the direction of the frictional forces and the angle of the cuspal incline. Thus, the coefficient of friction μ can be determined under functional conditions.

The results for tooth pairs 1, 2, and 3 are shown in Fig. 5, with the sequence of environmental fluids used. Fig. 6 shows the results for 2 further matched pairs of teeth. One of these was a second run on matched pair 3. The results in Fig. 6 are grouped because they show an essential difference from the results in Fig. 5. The influence of a number of surface effects are shown on a second run of tooth pair 2 in Fig. 7. The arrows and dotted lines in these figures indicate the direction in which

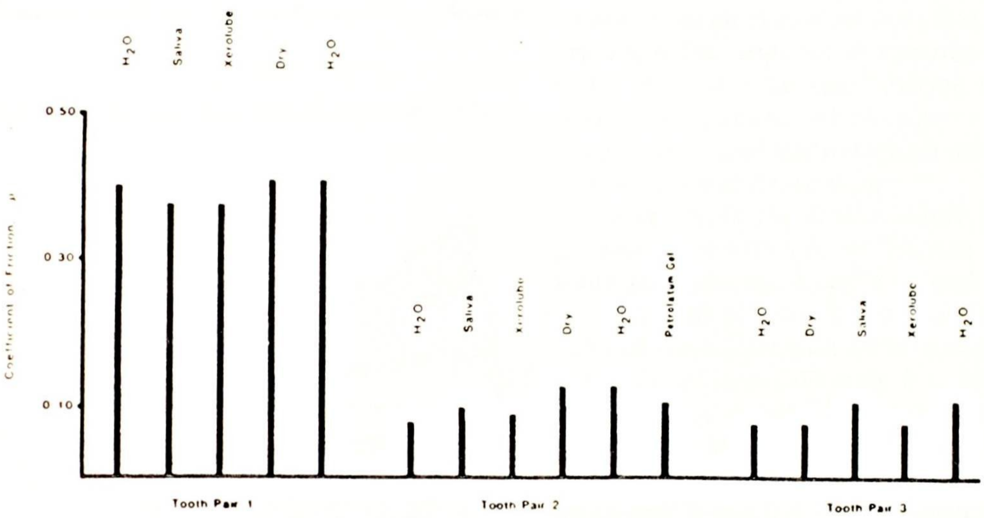

Fig. 5. The coefficients of friction for 3 different premolar pairs with different intervening liquids. The dark bars represent the coefficient of friction measured in the buccal excursion; lighter bars measured in the lingual excursion.

Table 1. Study design. The numbers indicate the sequence of environmental fluids used. All tooth pairs were natural premolars opposing natural premolars. All fluids were circulated at 37°C.

Intervening environmental fluid	Tooth pair no.				
	1	2	3		4
			Run 1	Run 2	
H_2O	1	1	1	1	1
Saliva, centrifuged	2	2	3	2*	4
Xerolube	3	4	4	3	2
Dry	4	3	2	4	3
H_2O	5	5	5	5	5
Petrolatum gel		6			
Other environmental conditions					
H_2O		7			
H_2O on roughened enamel		8			
Petrolatum gel		9			
Cleaned, H_2O		10			
H_2O on roughened enamel		11			
Lubricant, oil		12			
Cleaned, H_2O		13			

* not centrifuged, whole.

the magnitude of the coefficient of friction is moving and the initial and stabilized coefficient magnitudes.

The calculated coefficients of friction averaged over all conditions are shown in Table 2 for all sample pairs. This table includes the coefficients of variation and the number of measurements performed. Each measurement in Ta-

Table 2. Coefficients of friction, μ, averaged over all conditions for tooth pair.

Mean coefficient of friction, μ	(coeff. of variation)	Tooth pair	No. of measurements
0.418	(7%)	1	20
0.097	(18%)	2 (run #1)	24
0.1	(15%)	3 (run #1)	20
0.20	(55%)	3 (run #2)	20
0.313	(58%)	4	20

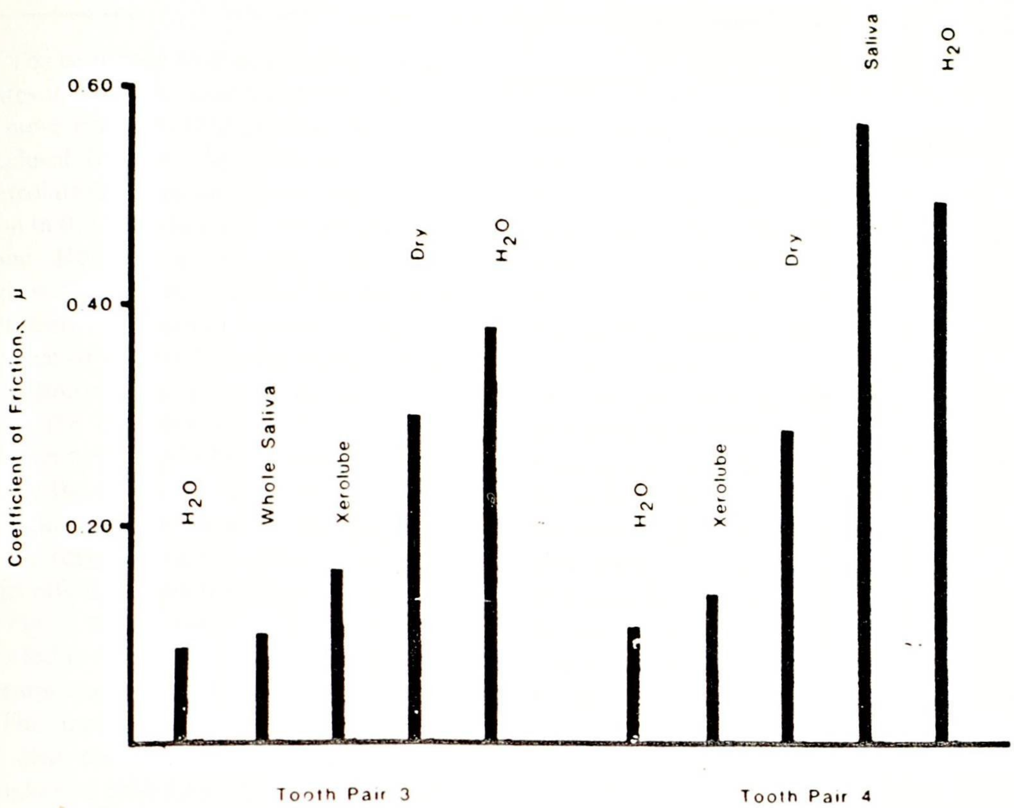

Fig. 6. The coefficients of friction for 2 different premolar pairs with different enamel surface conditions.

ble 2 represents an equilibrium value achieved after 20 lateral excursions.

Discussion

The premolar pairs of teeth were from the same patient. Even though the enamel was genetically matched it was not possible to verify the environmental history of the teeth before they were collected. Observations under low stereomicroscopy (50×) did not reveal significant differences in the surface enamel.

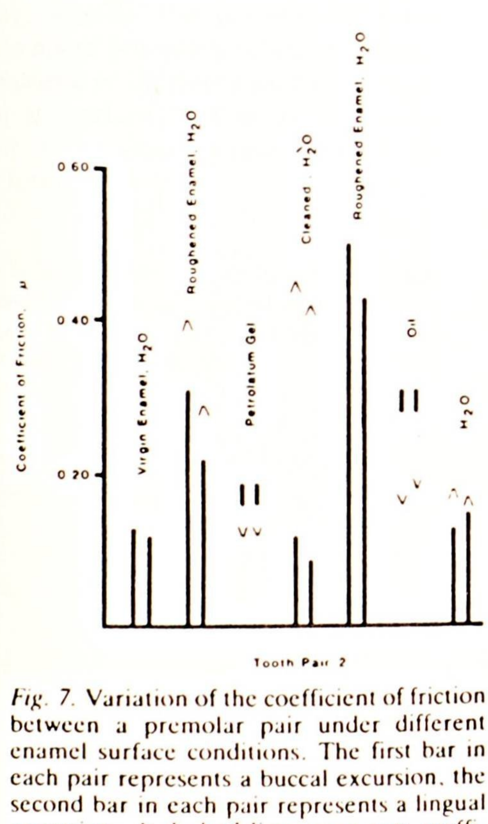

Fig. 7. Variation of the coefficient of friction between a premolar pair under different enamel surface conditions. The first bar in each pair represents a buccal excursion, the second bar in each pair represents a lingual excursion. A dashed line represents coefficient of friction changing during the coursé of an experiment. The arrow position represents the final equilibrium position of the coefficient of friction.

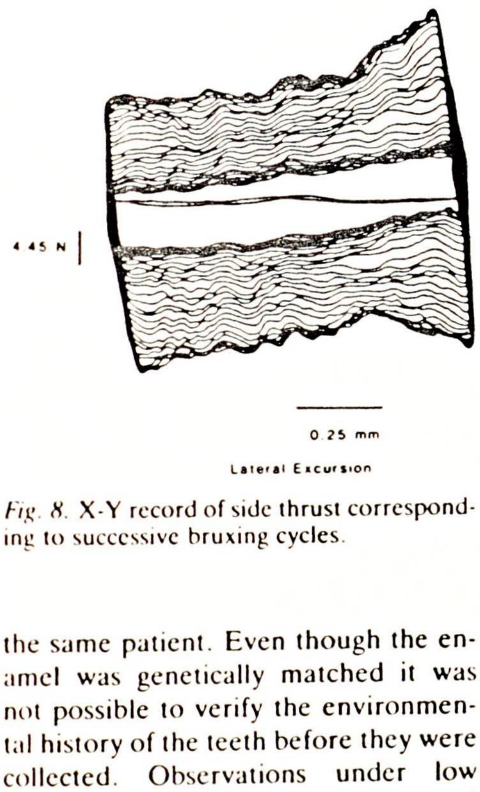

Fig. 8. X-Y record of side thrust corresponding to successive bruxing cycles.

Fig. 5 shows that there is a substantial difference in the coefficient of friction between different pairs of teeth. The means shown in Table 2 indicate that typically the coefficient of friction for tooth pair 1 is 4 times that of either 2 or 3 over all conditions. These differences could not be related to any gross variations in enamel, and thus, probably reflect surface textural changes at the histological level.

A further observation in Fig. 5 is that from one environmental fluid to another the coefficient of friction μ does not exhibit a great variation. This is again reflected in Table 2 where the coefficient of variation over all environmental conditions is typically in the range of 7–18%. This effect is independent of the sequence in which the fluids are used. At the bruxing velocities and occlusal forces used in this experiment the occluding cusp may be capable of penetrating the intervening fluids to give enamel to enamel contact, i.e., the intervening fluids may be expressed from the interface resulting in point to point contact.

Bruxing is associated with excessive clinical wear of enamel (9). It is assumed that this is due to the prolonged enamel to enamel contact time that the bruxing habit produces. A contributing factor may also be that bruxing is a movement pattern which maximizes enamel to enamel friction which may in turn increase abrasive wear.

The results in Fig. 6 show a different pattern of coefficient of friction for tooth pair number 4 and a second run of tooth pair number 3. Both of these pairs of teeth start with a coefficient of friction μ of approximately 0.1. However, as the experiments proceeded, the friction steadily increased until a stable value for μ of about 0.50 for tooth pair 4 and 0.4 for the tooth pair number 3 (run #2) was reached. This was in marked contrast to a rather constant μ previously measured. Quantitatively this is shown in the coefficients which are 58% and 55% for tooth pairs 4 and 3 (run #2) respectively. Further, the increases in μ at the end of each experiment compared to the beginning were a factor of 4 for tooth pair 3 (run #) and a factor of 5 for tooth pair 4. These differences again could not be accounted for by the differences in environmental fluids, which were sequenced differently in the two experiments. It appears that once the surface enamel is penetrated by the wear process the subsurface enamel may generate a higher coefficient of friction. If this is true then further studies should be conducted to determine the enamel depth at which these changes take place and how they are related to the hard tissue histology. In those systems where friction does increase with time, sustained bruxing may have more potential for devastating wear.

The sequence of events in Fig. 7 indicates that roughening the enamel led to a more than twofold increase in interocclusal friction. Applying a layer of petrolatum gel yielded a twofold reduction in the friction on the roughened incline. Removal of the petrolatum gel led to a steady recovery of the friction between the enamel surface. This sequence of results may be explained by the ability of the petrolatum gel to reduce the effective enamel to enamel contact by filling in the microspaces between the roughness asperities. The petrolatum gel may be removed resulting in the recovery of the original friction. This effect is shown in the X-Y record in Fig. 8 where successive bruxing cycles led to increasing friction until equilibrium was attained.

The application of a fine lubricating oil also reduced the friction on the roughened enamel surface as described above (Fig. 7). However, in contrast to petrolatum gel, attempts to remove the lubricating qualities failed. Lubricating oil, unlike petrolatum gel, contains surfactants which form a good retentive film on the enamel surface, even after the bulk of the oil has been removed. This retentive film, which is referred to as a boundary lubricant, appears to have a profound effect in reducing the surface friction. It is interesting to speculate, whether the presence of small amounts of boundary lubricants within composite resins might lead to a reduction in surface friction and abrasive wear. This is clearly a research topic for the future.

Acknowledgement – This study was supported by National Institute of Dental Research Grant No. 1 RO1-DE 06762-01, Bethesda, Maryland, 20205.

References

1. Norman RL. Frictional resistance and dental prosthetics. *J Pros Dent* 1964: *14*(1): 45–51.
2. Tillitson EW, Craig RG, Peyton FA. Friction and wear of restorative dental materials. *J Dent Res* 1971: *50*(1): 149–54.
3. Koran A, Craig RG, Tillitson EW. Coefficient of friction of prosthetic tooth materials. *J Pros Dent* 1972: *27*(3): 269–74.
4. Craig RG, Powers JM. Wear of dental tissues and materials. *Int Dent J* 1976: *26*(2): 121–33.
5. Miller GR, Powers JM, Ludema KC. Frictional behavior and surface failure of dental feldspathic porcelain. *Wear* 1975: *31*: 307–16.
6. Mahalick JA, Knap FJ, Weiter EJ. Occlusal wear in prosthodontics. *JADA* 1971: *82*: 154–59.
7. Monasky GE, Taylor DF. Studies on the wear of porcelain, enamel and gold. *J pros Dent* 1971: *25* (3): 299–306.
8. DeLong R, Douglas WH. Development of an artificial oral environment for the testing of dental restoratives: bi-axial force and movement control. *J Dent Res* 1983: *62*(1): 32–36.
9. Nadler SC. The effects of bruxism. *J Periodont* 1966: *37*: 311–319.

The wear of dental amalgam in an artificial mouth: a clinical correlation

R. DeLong, R. L. Sakaguchi, W. H. Douglas, M. R. Pintado
School of Dentistry, University of Minnesota, Minneapolis, USA

DeLong R, Sakaguchi RL, Douglas WH, Pintado MR. The wear of dental amalgam in an artificial mouth: a clinical correlation. Dent Mater 1985: 1: 238–242.

Abstract – The wear of dental amalgam by a smear mechanism and amalgam transfer onto the opposing cusp was confirmed by simulated studies in an artificial mouth. The coefficient of wear for dental amalgam was 4.89×10^{-5}. Calculation of the coefficient of friction for the enamel/amalgam couple indicated that friction was overcome by shallow slippage and shear within the amalgam. On the basis of these facts, the good wear performance of both the amalgam and the opposing enamel was rationalized. A retrospective clinical correlation of amalgam wear in an artificial mouth showed a correlation coefficient of 0.938 as far as the mean wear values were concerned. Further, the wear rates in both studies were linear except in a narrow region at time zero. The variances, however, in the 2 studies were very different. The desirability of *in vitro* studies to reproduce the same variance, as well as the same mean values, is a point for further discussion and experimentation.

Key words: amalgam, wear, artificial mouth, clinical correlation.

Dr. William H. Douglas, Biomaterials Program, 16-212 Moos Tower, University of MN School of Dentistry, 515 Delaware Street SE, Minneapolis, MN 55455, USA.

Received August 19, 1985; accepted September 9, 1985.

Dental amalgam is distinguished from many other direct restoratives by a resistance to occlusal wear. This property makes it one of the materials of choice for stress-bearing areas in the posterior segment of the dental arch. The wear of amalgam is a continuing topic of interest because it is taken as the standard by which newer direct restoratives are judged. Further, if the mechanisms of amalgam wear were more fully understood, it may provide a guide to the development of amalgam substitutes, which at present, occupies a large part of the modern research effort.

It is usual in clinical occlusal wear studies to report loss of contour in areas with no contact as well as in contact areas. Lambrechts' (1, 2) in quantitative clinical studies indicated that dental amalgam typically loses 200 μm in contact areas after 4 years in the mouth. Non-contact wear of amalgam is very small and in the same clinical study only 24 μm were lost. This pattern of clinical wear is in sharp contrast to that of conventional composites which show a dished-out effect over the entire occlusal surface as illustrated by Kusy and Leinfelder (3). The Lambrechts' study (1, 2) showed a conventional composite with non-contact wear amounting to over 40% of the total occlusal attrition.

In *in vitro* experiments in amalgam wear, the different methodologies in use, as well as different methods of reporting wear, often make comparisons between different laboratories difficult. Powell (4) tested amalgam, composites and composite resins under enamel pins with a total sliding distance of 28,750 cms and a force of 10 MPa (1 Kg/mm^2). These authors were able to rank amalgam and conventional composites according to clinical experience of occlusal wear. They found that enamel wear against amalgam was very small. They further noted considerable amalgam transfer onto enamel, but concluded that the dominant wear process was abrasion. Bailey & Rice (5) found that amalgam wear was essentially independent of contact stress. However, they concluded that stress was important in ranking comparisons involving amalgam and other materials which might be contact stress sensitive. Single-pass sliding experiments by Roberts (6) indicate smearing of amalgam phases by the diamond slider. Rice (7) also noted heavy amalgam transfer during wear experiments. This finding was confirmed by Mueller (8) in enamel/amalgam wear studies. Further, these workers could not identify Ca or P on the amalgam, and could offer no support for the 3-body abrasive model of wear of amalgam.

It appears, therefore, that amalgam smears against its antagonist during wear experiments, and loses surface contour by a process of transfer. Further, it appears that certain 2-body wear tests offer reasonable correlation with clinical experience, and facilitate insight into the wear process.

However, although there is considerable understanding of the amalgam process when opposed by enamel, there is no clear indication why the wear of this couple should be so small in clinical experience. Further, since progress has been made in correlation between clinical ranking of materials and in vitro tests, by careful use of correct contact stresses, it appears that the next step is to include additional major parameters of mastication in laboratory simulations. This may further improve the ability of laboratory simulation tests to correlate closely with clinical experience.

The following study using a servo-hydraulic-based artificial mouth was undertaken to throw light on these problems. Recently published clinical studies were used (1, 2) to test retrospectively the correlation between the mean wear of amalgam in the artificial mouth and clinical experience.

Material and methods

The servohydraulic apparatus used in this experiment comprised maxillary and mandibular elements, and has been described in the literature (9, 10, 11). Maxillary molars were stored in deionized water at 4°C until use. The mandibular element in each case was a dispersalloy* disk 12 mm in diameter by 3 mm in thickness. Three spills of alloy were amalgamated and condensed into split steel molds. The amalgam was carved, and after 24 h storage in water at 37°C, one face was finished and polished. The maxillary and mandibular elements were mounted in nylon rings using a laboratory-prepared chemical-cured composite 50/50 (w/w) ground quartz (11).

Before each masticatory test, the apparatus was configured to record occlusal anatomy of both the mandibular and maxillary elements as previously described in the literature (12). The occlusal surfaces were mapped and digitally recorded on 5¼" floppy disks using a microcomputer. This procedure was followed at the beginning and end of each masticatory test, enabling the change in occlusal contour to be determined quantitatively and visually in terms of computer graphics.

During each masticatory cycle, the following parameters were maintained: the lateral excursion at 0.82 mm; occlusal force at 13.35 N (3 lbs.) with a force profile in the form of a half sine wave; time of cuspal contact 0.23 s; and a chewing rate at 4 cycles/s. Deionized water was circulated at 37°C during mastication. The fluid was conveyed through ducts onto the occluding surfaces.

Three replications were carried out for each experiment. The total number of masticatory cycles for each enamel/amalgam couple was 500,000. Occlusal mapping of both maxillary and mandibular elements took place at 0; 30,000; 100,000; 200,000; and 500,000 cycles. At each point, occlusal change was recorded in terms of depth and volume. Finally, SEM photomicrographs were taken at the beginning and end of each experiment, and the energy dispersive attachment was used to identify chemical species on the on the surfaces.

* Johnson and Johnson, East Windsor, New Jersey

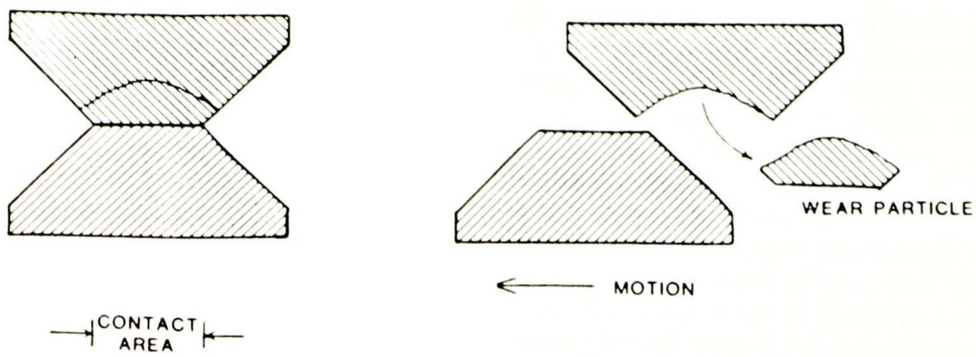

Fig. 1. Diagram of an adhesive junction between two asperity tips.

Mathematical methods and concepts. The dominant idea in modern contact theory is that under typical loads, surfaces contact each other only at the tips of the asperities (13). Greenwood and Williamson (14) demonstrated that the true contact area may be as little as 1/10,000 of the nominal contact area. Burton (13), therefore, concludes that "the asperity contacts are at the plastic yield point, and that the true contact area is determined by the hardness or flow pressure of the softer material".

If friction in the enamel/amalgam couple is mainly due to shear at the interface, then it can be shown that the coefficient of friction μ is approximately equal to the ratio of the shear strengths to the hardness pressure (13), (hardness expressed in MPa).

$$\mu = \frac{S}{P} \ldots\ldots \qquad (1)$$

Further, if it is assumed, as in Fig. 1, that the wear particles are spherical and that the wear is expressed as a volume change in occlusal contour, V divided by the total excursion L, then it can be shown that

$$\frac{V}{L} = K \frac{W}{3P} \ldots\ldots \qquad (2)$$

where W is the average occlusal force over the lateral excursion and P is the hardness pressure. This law was developed by J. F. Archard (15) and is useful in the analysis of sliding wear. The factor 3 in the divisor is a shape factor due to the assumption that the wear particles are hemispherical. K is a proportionality constant known as the coefficient of wear. It is dimensionless like the coefficient of friction. If K = 1, it indicates that each time a friction junction is formed at the interface, then lateral movement would result in a wear particle. By inserting the parameters of mastication and wear data into this equation, the coefficient of wear was determined.

Clinical correlation with the artificial mouth was tested at a conversion factor of 250,000 masticatory cycles equivalent to one year of clinical wear. This conversion factor was strongly suggested by preliminary experiments as discussed later in this report.

Table 1. Amalgam loss of contour by volume in an artificial mouth

Years (250,000 cycles = one year)	Masticatory cycles in thousands	Volume changes mm^3
.12	30	.00425±.0049
.4	100	.0136±.0048
.8	200	.021±.004
1.2	300	.0307±.0036
2	500	.052±.0063

Table 2. Amalgam loss of contour by depth in an artificial mouth

Years (250,000 cycles = one year)	Masticatory cycles in thousands	Maximum depth in microns (μm)
.12	30	20±11
.4	100	39±3.9
.8	200	57±1.7
1.2	300	72±1.7
2	500	94±2.5

Table 3. Regression constants for wear studies on amalgam against enamel

	Slope	Y intercept	Correlation coefficient
Clinical* study	44.71	21.43	.997
Artificial mouth study	38.31	21.77	.98

* Lambrechts et al. (1, 2)

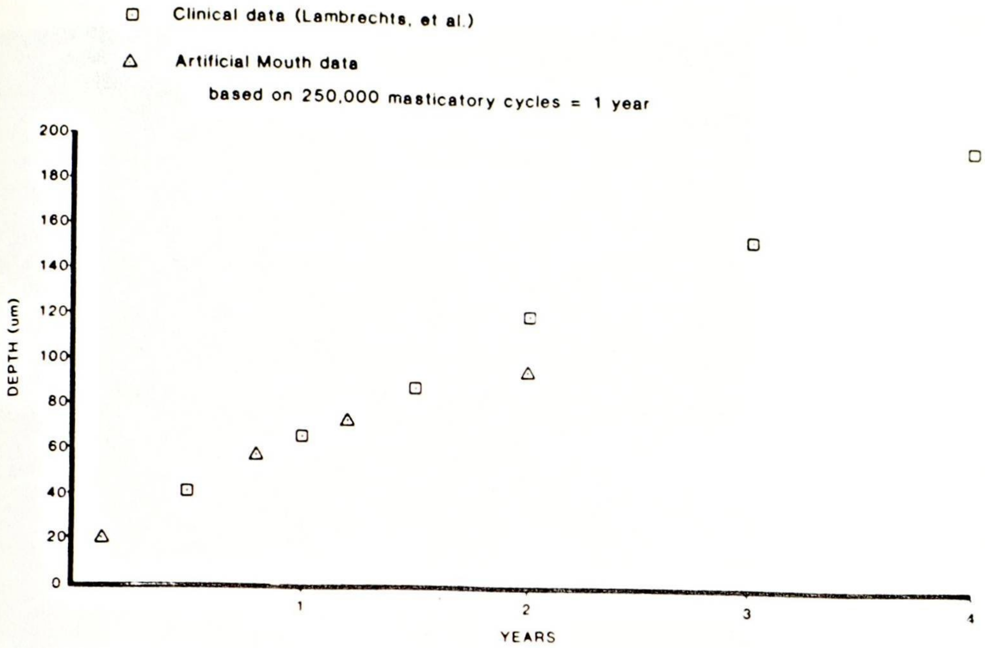

Fig. 2. Graph of the artificial mouth and clinical wear data.

Results

The loss of surface contour of amalgam due to wear is shown by volume in Table 1. In Table 2, amalgam wear is recorded by maximum depth of the wear facet. A plot of the raw data in Table 2 is shown in Fig. 2, with the clinical data of Lambrechts (1, 2) superimposed. The regression constants for these 2 sets of data are shown in Table 3. The clinical data has been recalculated using the clinical regression line as shown in Table 4.

A diagram of the occlusal force profile for one masticatory cycle is shown in Fig. 3. The maximum force is 13.35 N (3 lbs.) and the shape is approximately a half sine curve. The lateral excursion and the average occlusal force are obtained from this curve. By substituting in Equation 2, the coefficient of wear, K, can be derived. These results are shown in Table 5.

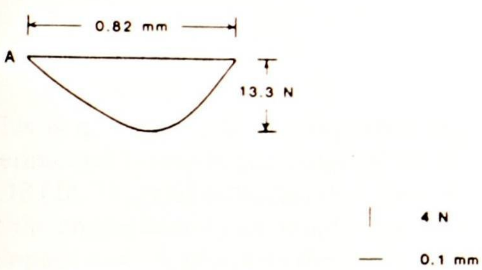

Fig. 3. Profile of a masticatory cycle showing lateral excursion against vertical occlusal force. "A" is the point of eccentric contact.

Discussion

In the scientific literature, there is no generally agreed method of reporting wear. Volume loss may be a more fundamental measurement than depth of loss because it is less dependent on the morphology of the opposing cusp. However, clinically, it is usually the depth of loss of the occlusal surface due to wear, that is assessed. Table 3 shows that the wear of amalgam in the artificial mouth gave a linear relationship in respect of the depth of loss. The fact that the Y intercept is not zero indicates that the wear depth is curvilinear near the zero (time of placement). However, a linear relationship is quickly established. This is due in part to the fact that the opposing cusp is not worn by the amalgam, which is a consistent finding in artificial mouth studies. A linear relationship is also shown for the clinical study in Table 3 and Fig. 2.

A correlation coefficient of 0.938 in Table 4 between the clinical and artificial mouth studies shows a high degree of correlation out to 2 years of clinical wear. The greatest difference between the 2 studies occurs at 2 years as shown by Fig. 2. However, this may not be a true divergence as Fig. 2 shows the mean clinical datum point to be as far above the regression line as the artificial mouth point is below. Longer term studies would be required to decide what happens after 2 years of simulated wear in the artificial mouth.

The calculation of the coefficient of wear for amalgam shows it to be on the order of 10^{-5} (Table 5). This may be interpreted to mean that the friction junctions between the opposing enamel and the amalgam surface have to be made and broken 10^5 times before a wear particle is produced. This is an indication of the resistance of amalgam to wear. It is also suggestive that fatigue begins to play a part in the wear process.

The present study, in common with many others (6, 7, 8), shows that the wear particles are smeared on the opposing cusp. These adhesions are clearly shown on the scanning electron micrograph (Fig. 4). Energy dispersive analysis showed in every case that the adhesions were dental amalgam (8).

It is also suggested in the present study that the frictional forces responsible for the wear of amalgam are shear forces. This is indicated by the micrographs (Fig. 4) which in addition to amalgam adhesions show the underlying enamel with no evidence of abrasive surface change. If the frequently quoted values for the shear strength (16) and hardness pressure of amalgam

Table 5. Coefficient of wear for amalgam when opposed by a maxillary palatal cusp of a 3rd Molar in an artificial mouth

No. of masticatory cycles in thousands	Coefficient of wear K	Overall coefficient of wear
35	3.8×10^{-5}	
100	4.84×10^{-5}	
350 K	5.0×10^{-5}	
500 K	6.53×10^{-5}	$4.89\times10^{-5}\pm1.18\times10^{-5}$

Table 4

Time years	Clinical studies* (regression line) µm	Artificial mouth (raw data) µm	Correlation coefficient between artificial mouth and clinical studies
.12	26.8	20±11	
.4	39.3	39±3.9	
.8	57.2	57±1.7	
1.2	75.1	72±1.7	
2	110.8	94±2.5	0.938

* Lambrechts et al. (1, 2)

Fig. 4. Micrograph of enamel cusp after 500,000 masticatory cycles against amalgam. The edge of the contact area is shown with amalgam adhesions.

(17) are used to calculate the coefficient of friction, as indicated in the introduction, the following is arrived at:

$$\mu = \frac{S}{P} = \frac{188}{1200} = 0.156$$

This is quite close to the reported experimental values in the range of 0.1 to 0.18 (18, 19), and indicates that friction in the enamel/amalgam couple is due to slippage and shear within the amalgam.

In conclusion, it may be said that the present study confirms the adhesive wear of amalgam. The resistance of amalgam to wear is due to the moderately high fatigue strength under the clinical simulated conditions, which required about 5×10^5 flexions of an enamel/amalgam surface junction to produce a wear particle. Further, the wear particle was probably quite small due to the very shallow shear failure within the amalgam. Amalgam produced no measurable wear on the opposing enamel cusp.

The clinical mean wear data assessed by depth of loss shows a correlation of better than 90% with the mean wear data in the artificial mouth, at least as far as 2 years of wear. Although the mean wear data were very close in the 2 studies compared in this report, there was a substantial difference in the variance of the data. Typically, the artificial mouth shows a standard deviation of 10% of the mean. This is due to the control which is possible and means that fewer samples are required to produce significant results. Well-controlled clinical studies will produce standard deviations in the range of 50–70% of the mean. Whatever the source of this deviation, many more samples are required to produce significant results. Where the deviation is in the method of measurement, then efforts should be made to reduce it.

However, the source of deviation is also certainly in the biological parameters themselves. This is true not only from patient to patient, but also in a single patient. Many different kinds of occlusal contact are possible, including swallowing, masticatory and bruxing contacts, each giving a different degree of wear. Further, the masticatory surfaces of premolars show a degree of wear different from the molar surfaces. It is not common at present, in clinical studies, to define the clinical popula-

References

1. Lambrechts P, Vanherle G, Vuylsteke M, Davidson CL. Quantitative evaluation of the wear resistance of posterior dental restorations: a new three-dimensional measuring technique. *J Dent* 1984: *12:* 252–267.
2. Lambrechts P, Vuylsteke M, Vanherle G, Davidson CL. Quantitative *in vivo* wear of posterior dental restorations: four-year results. *J Dent Res* 1985: *62* (Spec Issue): Abst. No. 1759, 370.
3. Kusy RP, Leinfelder KF. Pattern of wear in posterior composite restorations. *J Dent Res* 1977: *56:*544.
4. Powell JM, Phillips RW, Norman RD. *In vitro* wear of composite resin, amalgam and enamel. *J Dent Res* 1975: *54:* 1183–1195.
5. Bailey WF, Rice SL. Comparative sliding-wear behavior of a dental amalgam and a composite restorative as a function of contact stress. *J Dent Res* 1981: *60:* 731–732.
6. Roberts JC, Powers JM, Craig RG. Wear of dental amalgams. *J Biomed Mat Res* 1977: *11:* 513–523.
7. Rice SL, Wayne SF, Bailey WF. Influence of variation in contact stress on the sliding-wear behavior of a dental amalgam. *Biomat* 1981: *2:* 46–48.
8. Mueller HJ, Mahendra SB, Knoeppel R. Human enamel-dental amalgam pin on disc wear. *Dent Mater* 1985; *1:* 31–35.
9. DeLong R, Douglas WH. Development of an artificial oral environment for the testing of dental restoratives: biaxial force and movement control. *J Dent Res* 1983: *62:* 32–36.
10. Coffey JP, Goodkind RJ, DeLong R, Douglas WH. *In vitro* study of the wear characteristics of natural and artificial teeth. *J Pros Dent* (in press).
11. Douglas WH, Sakaguchi RL, DeLong R. Frictional effects between natural teeth in an artificial mouth. *Dent Mater* 1985: *1:* 115–119.

tion in terms of all of these parameters.

In the present study, 250,000 defined masticatory cycles were used as the conversion factor for one year of clinical wear. This degree of occluso-masticatory effort was suggested by a comparison of the work of Coffey (10) with that of Ogle (20). Because the correlation coefficient was high, it appears that this conversion factor represents an averaging over all the kinds of contacts that might produce clinical wear. However, other kinds of contacts can be produced in the artificial mouth and they can be randomized with masticatory contacts. This is a topic for future development, if it is desirable for *in vitro* methods not only to produce the same mean clinical wear, but also the same variance as that produced by clinical studies.

Acknowledgements – This study was supported by National Institute of Dental Research No. 1R01 DE 06762-01, Bethesda, Maryland, 20205.

12. DeLong R, Pintado MR, Douglas WH. Measurement of change in surface contour by computer graphics. *Dent Mater* 1985: *1:* 27–30.
13. Burton RA. Friction and Wear. In: Szeri AR, ed. Tribology. New York: McGraw-Hill, 1980: 19–23.
14. Greenwood, JA, Williamson JB. Contact of nominally flat surfaces. *Proc Roy Soc (Lond)* 1966: *A295:* 300.
15. Archard JF. Contact and rubbing of flat surfaces. *J Appl Phys* 1953: *24:* 981–988.
16. Smith DC, Cooper WE. The determination of shear strength: a method using a micro-punch apparatus. *Br Dent J* 1971: *130:* 333–337.
17. Wing Phase identification in dental amalgam. *Austral Dent J* 1966: *11:* 105–113.
18. Tillitson EW, Craig RG, Peyton FA. Friction and wear of restorative dental materials. *J Dent Res* 1971: *50:* 149–154.
19. Douglas WH, DeLong R, Sakaguchi RL. Surface frictional changes in posterior materials during wear experiments in an artificial mouth. *J Dent Res* 1985: *64* (Spec Issue): Abst. No. 1764, 370.
20. Ogle RE, David LJ, Ortman HR. Clinical wear study of a new acrylic resin tooth material. *J Prosthet Dent* 1985: *53:* 807.

The wear of dental porcelain in an artificial mouth

R. DeLong, W. H. Douglas, R. L. Sakaguchi, M. R. Pintado
School of Dentistry, University of Minnesota, Minneapolis, USA.

DeLong R, Douglas WH, Sakaguchi RL, Pintado MR. The wear of dental porcelain in an artificial mouth. Dent Mater 1986; 2: 214–219.

Abstract – Simulated occlusal wear studies in an artificial mouth involving enamel occluding on porcelain demonstrated a high coefficient of wear for dental porcelain; in agreement with other workers, an abrasive wear process is postulated. Volume loss due to wear showed good linearity as a function of the number of masticatory cycles with slight flattening at higher masticatory levels. However, the depth of wear curve showed a pronounced deviation from linearity with flattening of the wear rate with time. A parabolic relation exists between volume and depth of wear and correspondingly between time and depth. Based on the coefficient of wear, the intrinsic wear of porcelain appears to be about one order of magnitude greater than that experienced by dental amalgam.

Key words: porcelain, wear, artificial mouth

Dr. William H. Douglas, Biomaterials Program, 16–212 Moos Tover, University of MN/School of Dentistry, 515 Delaware Street SE, Minneapolis, MN 55455, USA.

Received December 5, 1985; accepted March 24, 1986.

Early in the history of dental porcelain, the ceramic crown was indicated only for the anterior segment, typically canine to canine. The reasons for this constraint were the susceptibility of porcelain to brittle fracture and a high occlusal rate of wear. It is desirable that posterior enamel should be opposed by a material with a low potential for occlusal wear. Esthetic considerations and improvements in physical properties have encouraged the use of porcelain in stress-bearing areas. There remains nevertheless considerable clinical concern for the high rate of attrition when porcelain is opposed by enamel (1).

Because of the vitreous nature of ceramics, a great deal of research has been directed towards brittle fracture. Less attention perhaps has been given to the occlusal wear of these materials, although it is regarded as being very important. Mahalick (2) regarded the porcelain-porcelain combination as producing severe attrition under high occlusal force, but he indicates that the same combination would be acceptable under lower occlusal force as experienced in a removable prosthesis. Mahalick (2) also found high wear rates for enamel-enamel and the enamel-porcelain combinations. Monasky and Taylor (3) studied the wear of porcelain against enamel with special reference to the finishing of the porcelain surface. They found that the wear rate of porcelain was high initially but decreased with time, possibly due to the polishing effect of the wear process on the porcelain surface. They suggest that where the porcelain surface glaze is broken it should be repolished. Miller (4) studied the wear mechanism of porcelain under single pass sliding experiments, and found that track width was accounted for by elastic deformation of the porcelain. These authors regarded any adhesion between porcelain and its antagonist as unlikely. However, they noted small grooves within the tracks and attributed them to a ploughingout effect by the asperities on the diamond slider. Finally, these authors noted brittle failure of the porcelain surface, and considered the pressure at which the onset of brittle failure occurred as important.

It appears that most of the in-depth knowledge of the wear of dental porcelain has come from *in vitro* studies. The goal of the present study was to continue this process by reporting on the performance and mechanism of wear of dental porcelain when opposed by a natural tooth. A servohydraulic based artificial mouth was used, which was programmed to develop the masticatory cycle as defined by DeLong (5) and Sakaguchi (6).

Material and methods

The artificial mouth used in this experiment is a servohydraulic model capable of reproducing the main parameters of mastication, including a mode change from isotonic to isometric contraction (in engineering terms: stroke control to load control) on occlusal contact, as required by the physiology of the mouth. The apparatus has been extensively described in the literature (5–9) and is briefly referred to here.

The maxillary member was the palatal cusp of a maxillary third molar and the mandibular element was a porcelain* fused to metal disc†. The porcelain was built up in layers, baked and glazed, strictly according to clinical laboratory procedure. The samples were mounted in nylon rings and stored in deionized water at 37°C as described in detail in previous publications (5–9).

Before each masticatory test, the apparatus was configured to record occlusal anatomy of both the mandibular and maxillary elements as previously described in the literature (10). The occlusal surfaces were mapped and digitally recorded on 5¼" floppy disks, using a microcomputer. This procedure was followed at the beginning and end of each masticatory test, enabling the change in occlusal contour to be determined quantitatively and visually in terms of computer graphics.

The parameters of the defined masticatory cycle are shown in Table 1.

*Ceramco II, Ceramco, Inc., New York, N.Y.
†Talladium, Talladium, Inc., Los Angeles, Ca.

Four replications of each experiment were carried out and the total number of masticatory cycles for each enamel/porcelain couple was 500,000. Occlusal mapping of maxillary and mandibular elements took place at 0, 30,000, 100,000, 300,000 and finally 500,000 masticatory cycles. This comprised a total of 40 measurements of depth and volume of wear. Finally, S.E.M. photomicrographs were taken of the wear facet at the end of the experiment.

Table 1. Defined masticatory cycle

Maximum occlusal force	13.35 N (3 lbs)
Force profile	Half since wave
Lateral excursion	0.82 mm
Masticatory rate	4 Hertz
Environmental temperature	37°C
Fluid	Deionized water

Adhesive wear

$$\frac{V}{L} = \frac{K}{3}\frac{W}{H}$$

Abrasive wear

$$\frac{V}{L} = K\frac{W}{H} = \frac{\tan\theta}{\pi}\frac{W}{H}$$

Brittle abrasive wear

$$\frac{V}{L} = \frac{\eta}{\pi}\frac{W}{H}$$

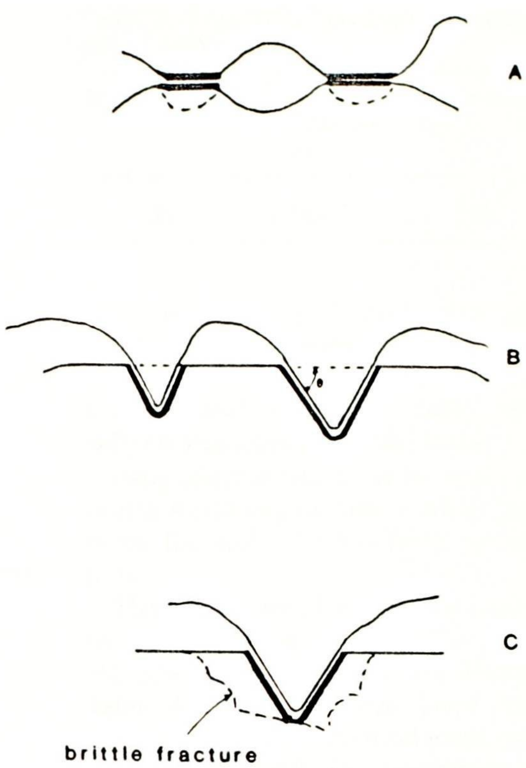

Fig. 1. Representation of different interfacial areas of contact with corresponding wear equations.

Mathematical concepts. The 3 equations of wear are shown in Fig. 1 with line drawings depicting the kind of interfacial junctions responsible for each kind of wear. They are developments of the basic wear equation:

$$\frac{V}{L} = K\frac{W}{H} \qquad 1$$

where K is the generalized coefficient of wear, V is the volume loss due to wear, L is the total sliding lateral excursion, W is the average occlusal force and H is the hardness of the surface in dimensions of pressure. Another useful form of this equation is:

$$\frac{V}{N} = K\frac{W}{H}E \qquad 2$$

where N is the number of masticatory cycles and E is the sliding lateral excursion of each masticatory cycle.

The adhesive wear formula has been applied to amalgam wear by DeLong (5). The remaining 2 equations are special cases of abrasive wear (11) as follows:

$$\frac{V}{L} = \frac{\tan\theta}{\pi}\frac{W}{H} \qquad 3$$

where θ is the angle which the asperity incline makes with the horizontal and is a measure of the roughness of the surface. Lawn (12) has developed an equation for abrasive wear in brittle glassy solids:

$$\frac{V}{L} = \frac{\eta}{\pi}\frac{W}{H} \qquad 4$$

where η is a linear factor relating the cross sectional area of the brittle wear particle to the radius of indentation.

The relationship between volume and depth of a wear facet. In a previous publication (6) it has been shown that there is a parabolic relationship between volume and greatest depth of the same wear facet.

$$V = \frac{\pi}{lm}\frac{Z^2}{2} \qquad 5$$

where V is the volume, Z is the greatest depth, and l and m are parameters which define the wear facet as follows:

$$Z = my^2 \text{ and } Z = lx^2 \qquad 6$$

at any depth Z:

$$X = \sqrt{\frac{Z}{l}} \text{ and } Y = \sqrt{\frac{Z}{m}} \qquad 7$$

It has also been shown in a previous publication (6) that there is a relationship between depth of wear and any of the 3 variables, total lateral excursion L, number of masticatory cycles N, or years of simulated clinical service T.

Table 2. Wear of dental porcelain opposed by a maxillary palatal cusp

Years of simulated clinical service*	No. of masticatory cycles	Volume loss of contour/mm³	Depth loss of contour/mm
0.12	30,000	.0185±.004	.0365±.009
0.4	100,000	.064 ±.015	.079 ±.016
0.8	200,000	.116 ±.028	.107 ±.018
1.2	300,000	.165 ±0.37	.127 ±.02
2	500,000	.238 ±.06	.157 ±.022

*based on 1 year of clinically simulated wear is equal to 250,000 masticatory cycles (5, 6).

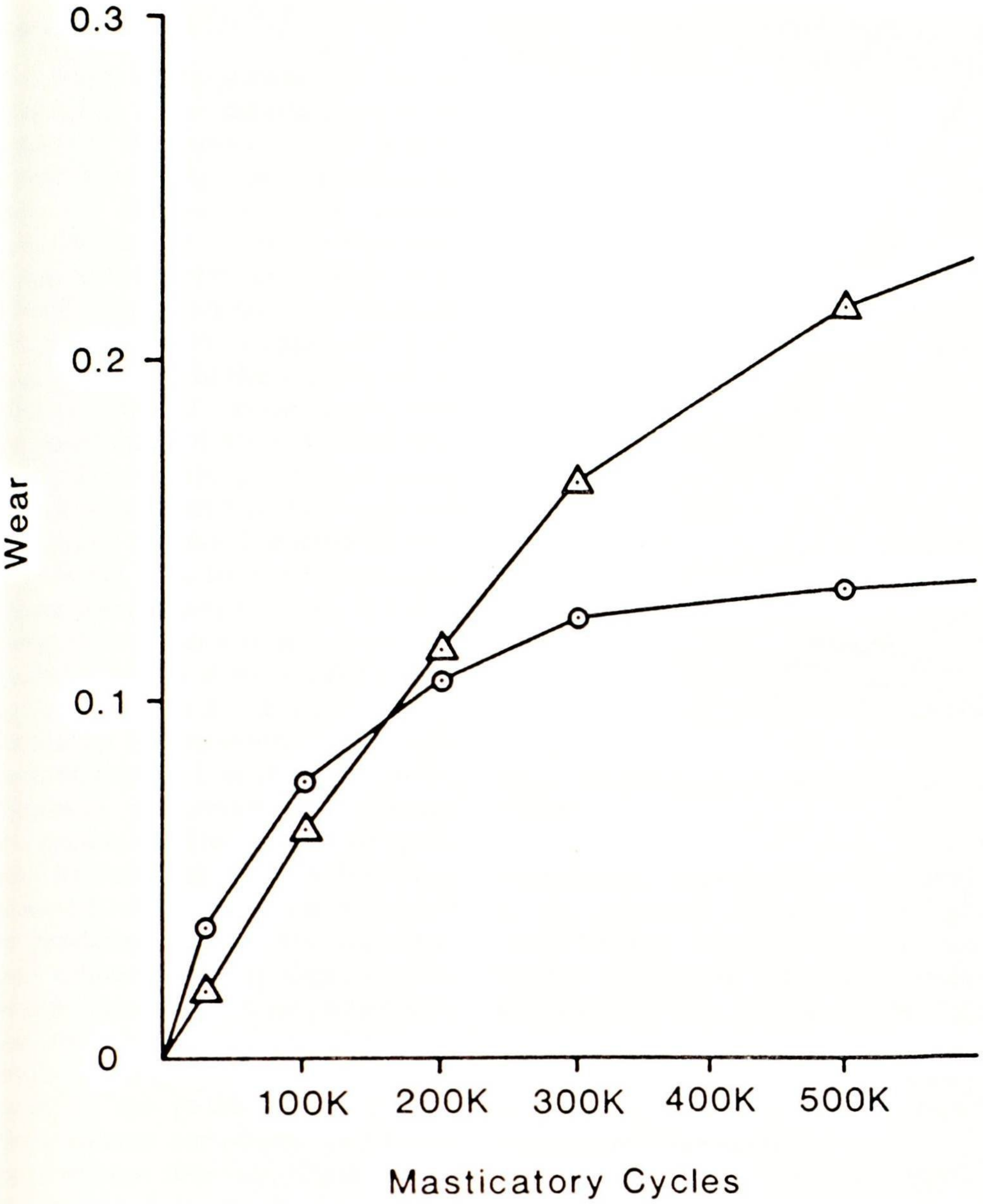

Fig. 2. Graph of loss of contour by volume and by depth and number of masticatory cycles (volume in mm^3 △; depth in mm ⊙).

Using subscripts 1 and 2 to apply to any 2 time periods, the following applies:

$$\frac{Z_1}{Z_2} = \sqrt{\frac{L_1}{L_2}} = \sqrt{\frac{N_1}{N_2}} = \sqrt{\frac{T_1}{T_2}} \qquad 8$$

Results

The means and standard deviations of the loss of contour by volume and depth due to wear in the mandibular porcelain are shown in Table 2. The results are shown in graphical form in Fig. 2. The volume curve is almost a straight line and the regression constants are shown in Table 3.

Occlusal maps of a porcelain wear facet are shown in Figs. 3 and 4. Fig. 3 is a computer graphics representation of the anatomy of the wear facet. Fig. 4 is a differences plot of the same facet. The differences plot is a graphics enhancement of Fig. 3, and refers to a graphics representation of the arithmetic difference between the baseline reading and the wear facet after 500,000 masticatory cycles. It has a reversing effect in which the wear depression is seen as a protrusion, which facilitates the task of identifying occlusal wear.

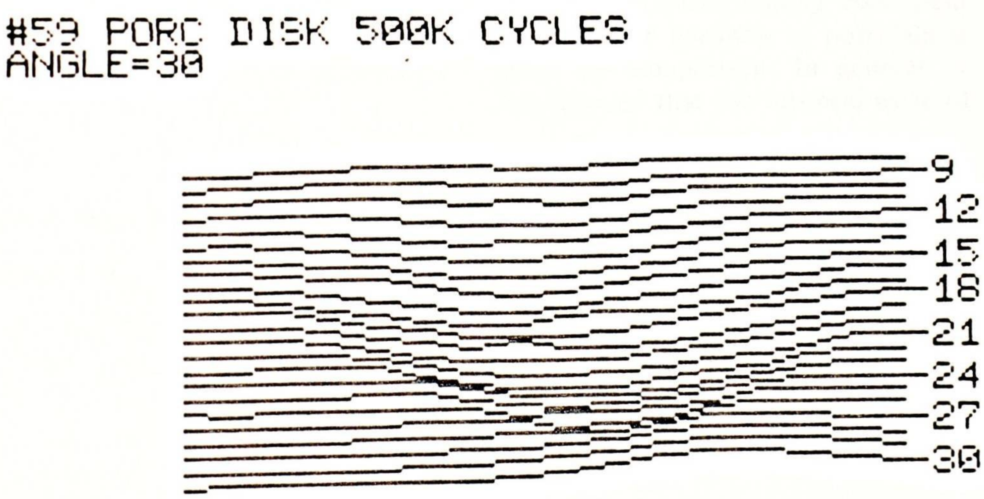

Fig. 3. Occlusal map of porcelain wear depression.

Table 3. Regression constants for volume loss of contour

Intercept mm^3	Slope mm^3/ masticatory cycle	Correlation coefficient
.01	4.79×10^{-7}	.99

The parameters l and m for each of the wear facets in porcelain after 500,000 masticatory cycles are shown in Table 4. These are calculated independently from the occlusal maps using equations 6 and 7. By substitution for the depth of wear and parameters l and m, the expected volume of the wear facet can be calculated. These calculated wear volumes are compared with the wear volumes measured directly from the occlusal maps, in Table 4 (see equation 5). There is no statistical difference between the means for the calculated and measured volumes in Table 4 at the 95% level of confidence.

The predicted ratios of depth of wear at 2 time intervals are shown in Table 5, and are compared with the raw data ratios in the same Table. The correlation coefficient for these 2 sets of ratios was very high at 0.98. Using the equation for general wear, 2 values for the coefficient of wear were developed. One is based on the hardness of procelain and the other is based on hardness of enamel. These are shown in Table 6.

Discussion

The results of the volume loss due to wear in Fig. 2 show good linearity as required by the equation. This is confirmed by the regression constants in Table 3. Nevertheless, the volume curve in Fig. 2 does show a little flattening at the higher masticatory level (500,000 K). Mulhearn and Samuels (13) suggest that the dropping off of the wear rate is due to the blunting of the abrasive particles, which agrees with the observation of Monasksy and Taylor (3), favoring the polishing of porcelain surfaces which have been adjusted for occlusal reasons. The depth of wear curve in Fig. 2 shows a pronounced deviation from linearity, which is a flattening of the wear rate with time. The results in Table 4 show that this rate of depth wear is a parabolic curve explained by the geometry of the wear facet. In Table 4, *l*, *m* and depth are independent measurements substituted into equation 5. The measure of agreement between calculated volume and measured volume indicates how good this prediction is. However, the calculated volume is usually slightly higher than the measured volume, which indicates that the estimates for the shape factors *l* and *m* are slightly low. The theory of the parabolic relation between volume and depth, and therefore, between time and depth is pursued in Table 5, the results of which are based on equation 8, and the raw data in Table 2. The ratio of depth of wear at 2 time intervals for 7 different cases is compared in the last 3 columns of Table 5. In addition to confirming the role played by the parabolic relationship in wear studies, equation 8 is very useful in the prediction of future wear. It would be most helpful at this point to be able to compare these predictions with clinical wear. Such studies are in progress in other centers, and are not available at present. Clinical comparison will, therefore, have to be reserved for a future publication.

Reviewing Fig. 1, it will be noted that the ratio of occlusal force over Hardness pressure (W/H) turns up in similar fashion in all 3 wear equations. While this is very convenient, Rabinowicz has pointed out that it is fortuitous (11). In the case of adhesive wear, W/H is an approximate measure of the true interfacial contact area. However, in abrasive wear theory, W/H is one of the parameters that controls the penetration of the harder element into the softer. It is this interpenetration of the 2 surfaces which produces the ploughing effect which is basic to the abrasive wear process.

When 2 different materials of 2 different hardness values are involved in the process of mastication, the problem arises of which hardness value should be substituted in the equation of wear. Intuitively, it may be thought that the wear process should be related to the hardness of the surface which is being worn away. However, the hardness penetration of 2 surfaces is controlled by the hardness of the softer of the 2 materials. Porcelain is somewhat harder than enamel (Table 6), and it seems likely that the extent of the interpenetration of enamel and porcelain surfaces, and therefore, the amount of abrasive ploughing would be controlled by the hardness of the enamel surface. Accordingly, in Table 6, the coefficient of wear of porcelain is calculated on the basis of the hardness of enamel, although the corresponding coefficient based on the hardness of porcelain is given for comparison. In general, it may be said that the intrinsic wear of

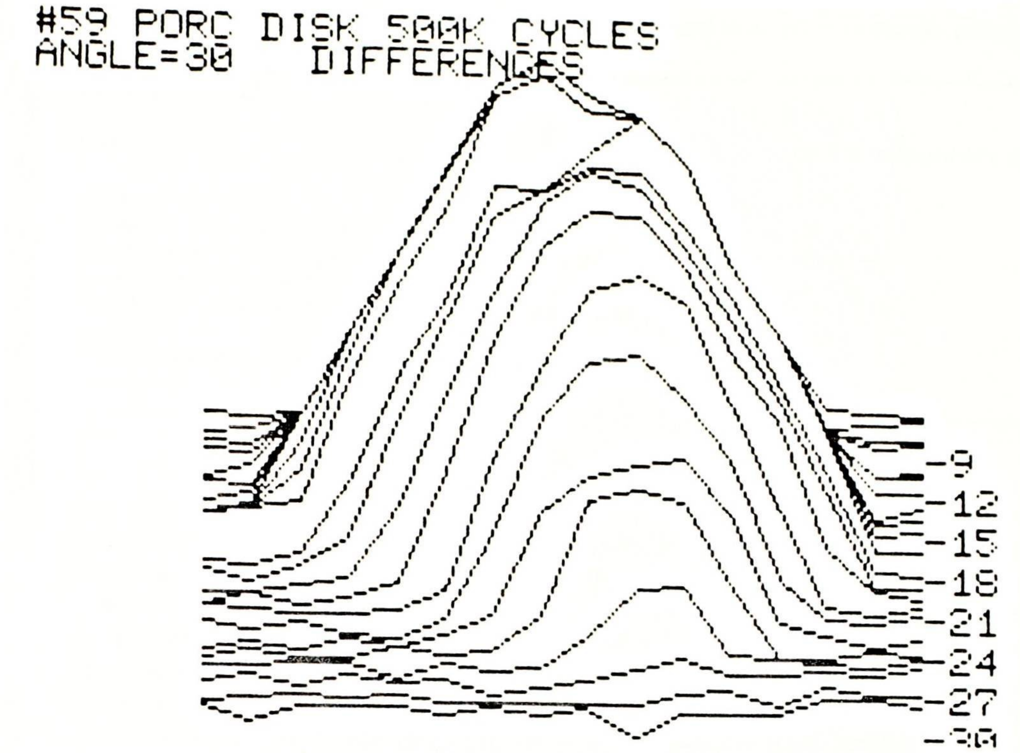

Fig. 4. Graphics enhancement of Fig. 3 in which the wear depression is shown as a protrusion.

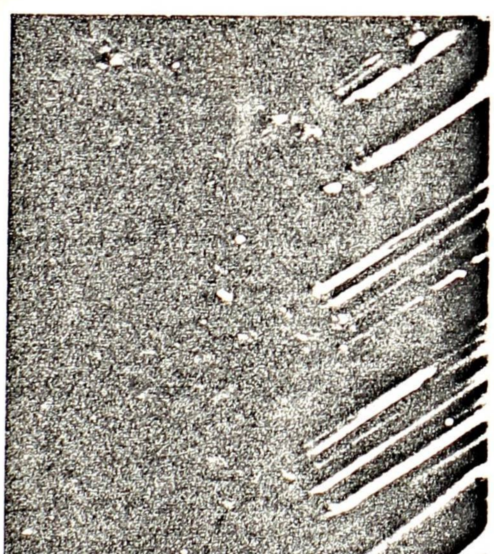

Fig. 5. Porcelain wear grooves at the edge of the wear facet.

Table 4. Shape factors of the porcelain wear facet after 500,000 masticatory cycles

Sample I.D.	*l*	*m*	Measured depth (raw data)	Calculated volume	Measured volume (raw data)
63	.098	.221	.179	.341	.287
64	.094	.205	.131	.194	.197
91	.089	.177	.139	.245	.163
59	.091	.197	.178	.372	.305
Mean	.093	.2	.157	.288	.238
Standard deviation	±.004	±.018	±.025	±.083	±.069

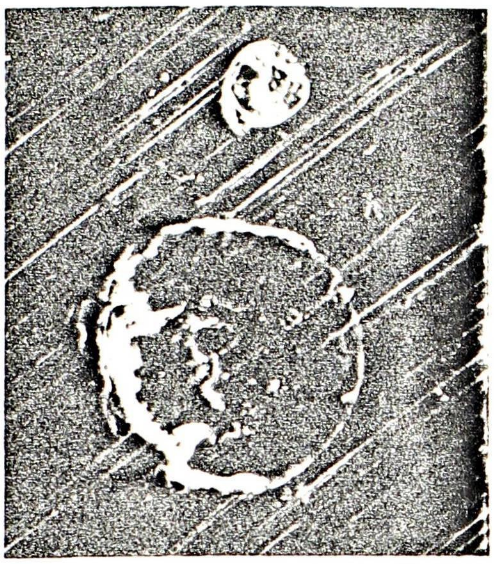

Fig. 6. Circular wear fracture developing in the middle of the porcelain wear facet.

Table 6. Coefficient of wear K for a porcelain fused to metal in an artificial mouth, calculated at two hardness values

Slope of volume wear curve $\frac{V}{N}$	4.79×10^{-16} m/masticatory cycle
Mean occlusal force	5.52 N
Hardness of enamel in dimensions of pressure	3.43×10^{9} N/m^2
Hardness of porcelain in dimensions of pressure	6.25×10^{9} N/m^2
Lateral excursion of each masticatory cycle	$.82 \times 10^{-3}$ m
Coefficient of wear porcelain based on hardness of porcelain	6.62×10^{-4}
Coefficient of wear of porcelain based on hardness of enamel	3.63×10^{-4}

porcelain is about one order of magnitude greater than that experienced by dental amalgam (5), based on the coefficient of wear.

However, the way in which these differences may manifest themselves in clinical practice is another matter. High volume wear rates exhibit less dramatic depth wear rates because of the parabolic relation referred to earlier. High wear rates also may be self-limiting because of the reduction in occlusal force as the restoration is worn away. Further, the occlusal and masticatory effects of occlusal wear is a subject which requires a great deal more study.

Substituting into equation 4 for brittle abrasive wear, gives a value for η of aproximately 10^{-3}. Lawn (12) quotes a value of $\eta = 1$ for soda lime glass which shows pronounced brittle chipping. It would appear that brittle chipping in the wear process of dental porcelain is not extensively involved under the conditions simulated in the artificial mouth. Scanning electron photomicrographs of the edge of the porcelain wear facet are shown in Fig. 5, exhibiting smooth wear grooves. Fig. 6 shows a photomicrograph of the center of a wear facet where a completely circular fracture is developing. This kind of defect was fairly frequent across the worn surface. It may have been due to porosity immediately below the surface.

Rabinowicz (11) has shown that it is not valid to assume that wear grooves necessarily mean an abrasive wear process. Nevertheless, on balance it does seem that the high coefficient of wear for dental porcelain indicates an abrasive rather than an adhesive wear process, at least under the conditions of the present study – a conclusion that has been reached by other workers (4). In the present study, the wear of the opposing cusp was also measured and was found to be of the same order of magnitude as the wear of porcelain. This data is being analyzed and will be submitted in a future publication.

Table 5. Ratio of wear at two time intervals based upon the parabolic relationship between depth of wear and time of service

Ratio of time intervals $\frac{T_1}{T_2}$(years)	Square root of no. of masticatory cycles $\sqrt{\frac{N_1}{N_2}}$	Predicted ratio of depth of wear, x $\frac{Z_1}{Z_2}$	Ratio of raw data, y (Table 2)	Correlation coefficient for 7 ratios
$\frac{.12}{1.2}$	$\sqrt{\frac{30{,}000}{300{,}000}}$	.316 (31.6%)	$\frac{.0365}{.127} = 29\%$	0.98
$\frac{0.4}{2}$	$\sqrt{\frac{100{,}000}{500{,}000}}$	.447 (44.7%)	$\frac{.079}{.157} = 50\%$	
$\frac{0.12}{0.8}$	$\sqrt{\frac{30{,}000}{200{,}000}}$	.387 (38.7%)	$\frac{.0365}{.107} = 34.1\%$	
$\frac{.12}{2}$	$\sqrt{\frac{30{,}000}{500{,}000}}$	.245 (24.5%)	$\frac{.0365}{.157} = 23.2\%$	
$\frac{1.2}{2}$	$\sqrt{\frac{300{,}000}{500{,}000}}$	.775 (77.5%)	$\frac{.127}{.157} = 80.9\%$	
$\frac{0.8}{1.2}$	$\sqrt{\frac{200{,}000}{300{,}000}}$	.816 (81.6%)	$\frac{.107}{.127} = 84.24$	
$\frac{0.4}{0.8}$	$\sqrt{\frac{100{,}000}{200{,}000}}$	.707 (70.7%)	$\frac{.079}{.107} = 73.8\%$	

Acknowledgement – This study was supported by National Institute of Dental Research grant No. 1RO1 DE 06762-02, Bethesda, Maryland 20205.

References

1. Shillingburg HT Jr, Hobo S, Whitsett LD. Fundamentals of fixed prosthodontics. Quintessence Books 1976: 317–329.
2. Mahalick JA, Knap FJ, Weiter EJ. Occlusal wear in prosthodontics. J Amer Dent Assoc 1971: *82*: 154–159.
3. Monasky GE, Taylor DF. Studies on the wear of porcelain, enamel and gold. J Pros Dent 1971: *25*: 299–306.
4. Miller GR, Powers JM, Ludema KC. Frictional behaviour and surface failure of dental feldspathic porcelain. Wear 1975: *31*: 307–316.
5. DeLong R, Sakaguchi RL, Douglas WH, Pintado MR. the wear of dental amalgam in an artificial mouth: a clinical correlation. Dent Mater 1985 (in press).
6. Sakaguchi RL, Douglas WH, DeLong R, Pintado MR. The wear of a posterior composite in an artificial mouth: a clinical correlation. Dent Mater 1985 (in press).
7. Coffey JP, Goodkind RJ, DeLong R, Douglas WH. In vitro study of the wear characteristics of natural and artificial teeth. J Pros Dent 1985: *54*:(2): 273–280.
8. DeLong R, Douglas WH. Development of an artificial oral environment for testing of dental restoratives: bi-axial force and movement control. J Dent Res 1983: *62*: 32–36.
9. Douglas WH, Sakaguchi RL, DeLong R. Frictional effects between natural teeth in an artificial mouth. Dent Mater 1985: *1*: 115–119.
10. DeLong R, Pintado MR, Douglas WH. Measurement of change in surface contour by computer graphics. Dent Mater 1985: *1*: 27–30.
11. Rabinowicz E. Abrasive and other types of wear. In: Rabinowitz E, Friction and wear of materials. New York: Wiley 1965: 167–197.
12. Lawn BR. A model for the wear of brittle solids under fixed abrasive conditions. Wear 1975: *33*: 269–372.
13. Mulhearn TO, Samuels LE. The abrasion of metals: a model of the process. Wear 1972: *5*: 478–498.

The wear of a posterior composite in an artificial mouth: a clinical correlation

R. L. Sakaguchi, W. H. Douglas, R. DeLong, M. R. Pintado
School of Dentistry, University of Minnesota, Minneapolis, U.S.A.

Sakaguchi RL, Douglas WH, Delong R, Pintado MR. The wear of a posterior composite in an artificial mouth: a clinical correlation. Dent Mater 1986: 2: 235–240

Abstract – The wear of a posterior composite against a maxillary palatal cusp was studied in an artificial mouth. The coefficient of wear for the composite was 2.58×10^{-5}. A retrospective clinical correlation with composite wear in the artificial mouth showed a correlation coefficient of 0.84 at 1 year of wear. The artificial mouth studies support a parabolic relationship between depth of composite wear and time. The ratio of 6 months depth of wear compared to 3 years was found to be 41% which supports the Leinfelder finding (5) of 49%. However, the correlation with the linear studies of Braem (2,3) was good as far as the mean depth of wear at 1 year was concerned. The disagreement between the linear and parabolic studies is small during the early wear process, but becomes serious during a longer term. It is important for future clinical wear studies to resolve the question of the nature of the wear rate curve in posterior composites, if accurate prediction of long term performance is to be achieved.

Key words: posterior composite, wear, artificial mouth, clinical correlation

Dr. William H. Douglas, Biomaterials Program, 16-212 Moos Tower, University of Minnesota, School of Dentistry, 515 Delaware Street SE, Minneapolis, Minnesota 55455, U.S.A.

Received November 12, 1985; accepted March 28, 1986

The occlusal wear of composites in the posterior segment is a process of great clinical significance and considerable theoretical interest. The clinical signs and symptoms of occlusal composite wear present as a generalized, horizontal loss of contour, which was quite unforeseen following the use of these materials in the anterior segment. These observations are strong indications that the biomechanics and the environment of the posterior aspects of the mouth are very different from those in the anterior aspects.

It is usual to report the clinical posterior occlusal wear of restorations on at least two places on the same occlusal surface. These are the occlusal contact area (OCA) and the contact-free area (CFA) (1), which are sometimes referred to as the areas of attrition and abrasion (2–4) respectively. A distinctive feature of posterior composites is that the ratio of the non-contact wear to the contact wear is high, typically in the range of 25% – 50% (2,3) which is responsible for the dished-out appearance of the wear facet. This is quite different for amalgam where the ratio is 10% (3).

The works of Braem (2), and Lutz (1) appear to indicate that the progress of wear in the occlusal contact area is linear with time, with little or no flattening of the wear rate. The clinical studies of Leinfelder (5) and Vrijhoef et al (6) indicate that the vertical loss of occlusal height shows a high wear rate initially, which reduces with time, giving a characteristic curved appearance to the wear curve. Vrijhoef et al (6), therefore, suggest that the basline evaluation should be made at 6 months when most of high initial wear has taken place. They attribute the high initial wear of posterior composites to the problems associated with the establishment of an ideal occlusion. These workers used a quantitative method of measurement which averaged the wear over the occlusal surface. Leinfelder (5) in many clinical studies has also noted the curved appearance of the wear rate curve. He has also used a quantitative measurement which gives a good indication of the generalized wear of the occlusal surface. The difference between the linear and curved wear rate curves may be a genuine controversy which is developing in the literature or it may be related to the method of clinical measurement.

The question of the nature of the wear rate curve is of great practical interest if accurate prediction of clinical performance is to be achieved. It is hoped that with a fewer number of observations, long-term results could be predicted, thus, reducing the cost of clinical evaluation and delivering the benefits of improved health-related technology to the public in a shorter time (7). From his observation, Leinfelder (5) noted that the wear at 6 months was 50% the wear at 3 years, which expresses quantitatively the curved nature of the wear rate he observed.

Substantial improvements have been made in the design of posterior composites (8) relative to the older conventional materials, such that they now form a separate generic group. Further, certain aspects of the wear process are quite well understood (9). An important step is the loss of resin followed by the exfoliation of particles from the composite. This results in a volumetric loss of contour and the development of a surface roughness which leads to a high friction which sustains the rate of wear and can be responsible for the accumulation of plaque and stain.

Although this wear model is well established. The quantitative relationships to which it leads have not been developed. The clinical wear rates already noted are empirical and have been developed with the prediction of clinical wear in mind. However, quantitative relationships built on a wear model may indicate where design improvements in these materials may be made and may assist in improving the correlation between *in vitro* and *in vivo* studies (10).

To address these problems, therefore, the present study reports on the wear in an artificial mouth of a posterior composite for which extensive clinical data is available. A well-defined masticatory cycle is used and the results are analyzed for information on the quantitative relation of the basic wear process in the occlusal contact area.

Material and methods

The artificial mouth used in this experiment is a servohydraulic model capable of reproducing the main parameters of mastication including a mode change from isotonic to isometric contraction (in engineering terms: stroke control to load control) on occlusal contact, as required by the physiology of the mouth. The apparatus has been extensively described in the literature (10–13), and is briefly referred to here.

The maxillary member was the palatal cusp of a maxillary third molar and the mandibular element was an autocured posterior composite* disk 12 mm in diameter by 3 mm in thickness. The material was mixed and finished† according to the manufacturer's instructions. The maxillary and mandibular elements were mounted in nylon rings and stored in deionized water at 4C as described in previous publications (10–13).

Before each masticatory test, the apparatus was configured to record occlusal anatomy of both the mandibular and maxillary elements as previously described in the literature (14). The occlusal surfaces were mapped and digitally recorded on 5¼" floppy disks, using a microcomputer. This procedure was followed at the beginning and end of each masticatory test, enabling the change in occlusal contour to be determined quantitatively and visually in terms of computer graphics.

During each masticatory cycle, the following parameters were maintained: the lateral excursion at 0.82 mm; occlusal force at 13.35 N (3 lbs.) with a force profile in the form of a half sine wave; time of cuspal contact 0.23 s; and a chewing rate of 4 cycles per s. Deionized water was circulated at 37 C during mastication. The fluid was conveyed through ducts onto the occluding surfaces.

Five replications were carried out for each experiment. The total number of mastications were carried out for each experiment. The total number of masticatory cycles for each enamel/composite couple was 300,000.

Occlusal mapping of both maxillary and mandibular elements took place at 0; 85,000 and 300,000 masticatory cycles. At each point, occlusal change was recorded in terms of depth and volume at the occlusal contact area (attrition, 1,2,3,4). Finally, SEM photomicrographs were taken of the wear facet at the beginning and end of each experiment. Previous experimentation on the wear of amalgam (10) had shown that with the masticatory cycle as defined in the present study, 250,000 cycles had produced one year's equivalent of clinical wear in the occlusal contact area.

The hardness of the composite was assessed using a Knoop diamond indenter under 1 kilogram load (9.8 N), after the masticatory experiment had been completed. The mean of 5 measurements was taken.

Mathematical concepts of occlusal wear. The general wear equation (15,16) has the following form:

$$\frac{V}{L} = K \frac{W}{H}$$

where V is volume loss of contour due to wear; L is the total Lateral sliding excursion; W is the average occlusal force and H is the hardness of the softer of the two materials involved in the wear process. H is expressed in the dimensions of pressure and is called the Hardness pressure. K is the coefficient of wear and like the coefficient of friction has no dimensions.

The wear equation can be developed further if it is known that adhesive or abrasive wear is predominant (16). However, where there is doubt it is advisable to leave the equation in its general form.

It is usual in clinical trials to report wear as a function of years of service and in the artificial mouth as a function of the number of masticatory cycles. Simple changes in the wear equation accomodate these differences.

$$\frac{V}{N} = K \frac{W}{H} E$$

$$\frac{V}{Y} = K \frac{W}{H} E\ 250{,}000$$

where N is the number of masticatory cycles; E is the length of the lateral excursion in each masticatory cycle; and Y is the time in years that the restoration was in service.

The slope of the wear curve from clinical studies or from studies in the artificial mouth allows the determination of the coefficient of wear K.

Relationship between the depth of wear and the volume of wear. Although the volume of wear is a more fundamental measurement, the depth of wear is more useful clinically since it determines the occlusal vertical dimension and, hence, the facial height with the teeth in contact.

The loss of material which gives rise to an elliptical wear facet can be described by the two parabolas in Fig. 1 with the origin at the deepest point Z of the occlusal contact area:

$$Z = my^2 \quad \text{and} \quad Z = lx^2$$

Thus, at any depth Z,

$$x = \sqrt{\frac{Z}{l}} \quad \text{and} \quad y = \sqrt{\frac{Z}{m}}$$

where l and m are the shape factors of the occlusal contact. The projected area of the wear facet in Fig. 1: area of ellipse = πxy

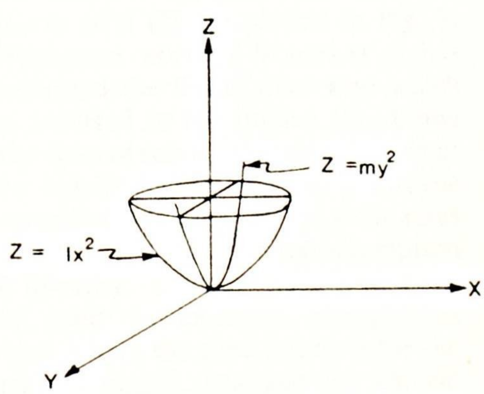

Fig. 1. The relationship between the depth of a wear facet and its volume.

* P10, 3M Company, St. Paul, MN
† Soflex disks, 3M Company, St. Paul, MN

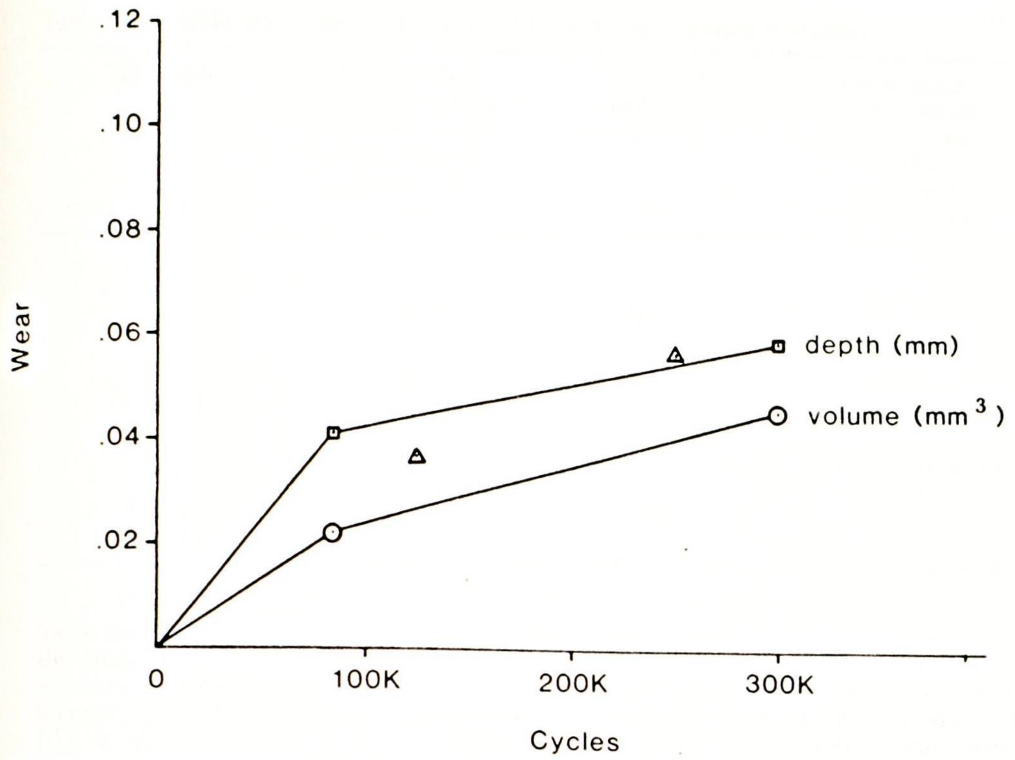

Fig. 2. Occlusal wear curves for artificial mouth depth □ and artificial mouth volume ⊙ and clinical depth △ Braem (2) calculated as one year equals 250,000 masticatory cycles.

Area at depth Z =

$$\pi\sqrt{\frac{Z}{l}}\sqrt{\frac{Z}{m}} = \pi\frac{Z}{\sqrt{lm}}$$

The volume of wear facet in Fig. 1:

Volume V at depth

$$Z = \frac{\pi}{\sqrt{lm}}\cdot\int_0^Z Z\ dZ$$

$$Z = \frac{\pi}{\sqrt{lm}}\cdot\frac{Z^2}{2}$$

This defines the relationship between the volume and the depth of a wear facet as a parabola. This will become very important in the prediction of future wear of composites as discussed later.

Theoretical relationship between the depths of wear in the occlusal contact area at two periods. It has been shown that the theoretical volume wear curve is expected to show a constant slope under defined parameters.

$$\frac{V}{N} = K\frac{W}{H}E = \text{a constant at all values of N.}$$

However, it has also been shown from the parabolic relation between depth and volume that:

$$\frac{V}{N} = \frac{\pi}{2\sqrt{lm}}\ \frac{Z^2}{N} \quad \text{for all values of N}$$

This must also be theoretically a constant.

Using subscripts for 0.5 years and 3 years.

$$\frac{\pi}{2\sqrt{lm}}\cdot\frac{Z_{0.5}^2}{N_{0.5}} = \frac{\pi}{2\sqrt{lm}}\cdot\frac{Z_3^2}{N_3} \quad \text{or}$$

$$\frac{Z_{0.5}^2}{N_{0.5}} = \frac{Z_3^2}{N_3}\ ;\ \frac{Z_{0.5}^2}{Z_3^2} = \frac{N_{0.5}}{N_3} \quad \text{or}$$

$$\frac{Z_{0.5}}{Z_3} = \sqrt{\frac{N_{0.5}}{N_3}}$$

Table 1 – Depth of volume of wear in the occlusal contact area of a posterior composite in an artificial mouth

	depth of wear mm		volume of wear mm³	
masticatory cycles sample I.D. no.	.85k	300k	85k	300k
57	.0313	.0463	.016	.037
65	.047	.068	.023	.049
80	.035	.052	.021	.047
61	.053	.072	.027	.057
71	.038	.057	.018	.040
mean (standard deviation)	.041 (± .008)	.059 (± .01)	.021 (± .004)	.046 (+ .007)

Table 2 – Regression constants for clinical and artificial mouth studies on the wear of a posterior composite in the occlusal contact area

	Intercept	Slope
artificial mouth volume of wear	3.58×10^{-3}	1.47×10^{-7} mm³/masticatory cycles
artificial mouth depth of wear	10 µm	1.746×10^{-4} µm
clinical study depth of wear (Braem 2,3)	4.7 µm	2.08×10^{-4} µm

Results

The wear results for loss of contour due to depth and volume in the artificial mouth are shown in Table 1. The mean of the twenty points for depth and volume are shown in graphical form for two periods in Fig. 2. For comparison, the results of the one year report of Braem et al (2) are plotted in Fig. 2. Subsequent work of Braem et al has confirmed the linear wear rate which he reported in his studies (4). Using zero time of service showing zero wear (i.e. baseline) as an essential point, the regression constants for the wear rates are shown in Table 2 on the assumption of linearity. The regression constants are used to calculate interpolated points where the time intervals for the artificial mouth data and the clinical data are different. The regression constants also provide the best estimate of

Table 3 – Correlation of clinical regression line to artificial mouth raw data

Time years masticatory cycles	Clinical data recalculated for artificial mouth time intervals Braem (2) μm	Artificial mouth data from Table 1 μm	Correlation coefficient of artificial mouth raw data to clinical regression line
0	0	0	
0.34 (85 k)	22.5	41±8	
1.2 (300 k)	67.4	59±10	0.84 (at the 95% level of confidence, coefficient lies in the interval 0.57, 0.94)
3 years (750 k)	161.4	142	

Table 4 – Parameters of the wear facets of a posterior composite in occlusal contact area in the artificial mouth

Sample I.D. #	*l*	m	masticatory cycles	measured depth mm (raw data)	calculated volume mm³	measured volume mm³ (raw data)
57	.056	.173	85 k 3000 k	.031 .046	.0152 .035	.0158 .037
65	.057	.36	85 k 300 k	.047 .068	.025 .050	.023 .049
61	.069	.21	85 k 300 k	.053 .072	.033 .071	.027 .057
71	.047	.27	85 k 300 k	.038 .057	.020 .045	.018 .040
80	.045	.173	85 k 300 k	.035 .052	.023 .047	.021 .047

Table 5. The ratio of depth of two time intervals based upon the parabolic relationship between volume and depth of the wear facet.

Ratio of time intervals $\frac{T_1}{T_2}$	Square root of ratio of no. of masticatory cycles in the artificial mouth $\sqrt{\frac{N_1}{N_2}}$	Ratio of depth of wear for the two time intervals $\frac{D_1}{D_2}$	Clinical study Leinfelder (5)	Clinical study Braem (6)
$\frac{0.5\ \text{years}}{3\ \text{years}}$	$\sqrt{\frac{125{,}000}{750{,}000}}$	0.41 (41%)	49%	23%*
$\frac{0.5\ \text{years}}{5\ \text{years}}$	$\sqrt{\frac{125{,}000}{1{,}250{,}000}}$	0.32 (32%)		
$\frac{0.5\ \text{years}}{7\ \text{years}}$	$\sqrt{\frac{125{,}000}{1{,}750{,}000}}$	0.27 (27%)		
$\frac{0.5\ \text{years}}{7\ \text{years}}$	$\sqrt{\frac{125{,}000}{1{,}750{,}000}}$	0.65 (65%)		

* The three year value is extrapolated on the basis of a linear relationship.

the slope of the wear curve which is required for the calculation of the coefficient of wear. In Table 3, the correlation of the clinical data at one year with the artificial mouth data is shown. The data is extrapolated to three years on the basis of linearity (2,4).

The details of each composite wear facet are presented in Table 4. These include the shape factors *l* and m and the calculated volume of the wear facet based on the parabolic relationship between depth and volume developed in the present report. The same relationship also allows the prediction of the ratios of depth of wear at two different times , and a number of these presented in Table 5. Finally, the calculation of the coefficient of wear for the parameters used in this study is presented in Table 6.

Discussion

The interest in the present study was to develop a statistical number of data points in the early wear process of a posterior composite. The regression constants for the data points, including the baseline zero, are shown in Table 2. The intercepts are very small as a result of including the baseline zero in the calculations.

On the basis of linearity, a correlation between the clinical data and the artificial mouth data is shown in Table 3 with a coefficient of 0.84. Using Fisher's method (17), the 95% confidence limits indicate that the correlation coefficient for artificial mouth raw data to the clinical regression line is between 0.57 and 0.94. This correlation coefficient applies only up to one year of wear. Beyond this, the artificial mouth data points are extrapolations as indicated by asterisks in Table 3. However, while this correlation is very encouraging from the point of view of predicting the mean depth of wear in the occlusal contact area at one year, the raw data from the artificial mouth indicates a parabolic relationship between depth of wear and time (or masticatory cycles). This is shown in Table 4 where the parameters *l* and *m* define the shape of the wear facet as defined in the section "materials and methods". A difference in value between *l* and *m* indicates an elliptical shape to the wear facet. The values of *l* and *m* change very little in Table 4 from sample to sample. This is an interesting observation, since the wear facets were devloped under the palatal cusps of different maxillary molars which were subject to the normal biological variation of occlusal anatomy. The measured depth in Table 4 was used to calculate the volume, and the very close agreement between measured volume and calculated volume in that Table indicates that the artificial mouth supports the premise that the depth of wear has a parabolic relationship with time (i.e.

Table 6 – Coefficient of wear K for posterior composite in the artificial mouth

Slope of the volume wear curve $\frac{V}{N}$	1.47×10^{-16} cubic meters per masticatory cycle
mean occlusal force	6.81 Newtons
hardness of composite in diminsions of pressure	9.8×10^{8} Newtons per meter
lateral excursions of each masticatory cycle	$.82 \times 10^{-3}$ meters
coefficient of wear	2.58×10^{-5}

a high initial wear rate, followed by a decline in the wear rate). The calculation can easily be carried out in the reverse direction, i.e., knowing the volume and calculating the depth. Depth of wear in the clinical area commands more interest because it determines the occlusal vertical dimension.

Since the theoretical and experimental studies in the artificial mouth support the parabolic nature of the wear facet in a posterior composite, the same relationship can be used to develop the ratio of wear at two different periods. This is a useful predictive tool and is shown in Table 5, where several ratios at different time intervals are shown, worked out on the basis that one year of clinical masticatory effort is equivalent to 250,000 defined masticatory cycles in the artificial mouth. The ratio of 6 months to three years is of particular importance.and may be compared to two clinical studies as shown in Table 5. It would appear that the artificial mouth studies support the Leinfelder study as far as the shape of the wear curve is concerned. However, it also supports the Braem clinical study as far as the mean wear values are concerned at 6 months and 1 year as shown in Table 3. The predictive power of *in vitro* and *in vivo* screening tests is an important goal for future research as indicated by Phillips (7). If this is to be realized, the shape of the wear rate curve, as well as the initial rate itself must be known. While the difference between the mean depth of wear for the linear rate and that for the parabolic rate may not be too serious at three years of clinical wear, the difference between these two wear curves, and hence their predicted values will be very different in long term performance. The percentage differences for two clinical studies are shown in Table 5.

It appears that if only the clinical evidence be considered, the shape of the wear rate curve for the posterior composite in question has not been finalized. If the evidence of the artificial mouth be considered along with the clinical data, then a parabolic rate curve is favored, with the rider that the mean depth of wear values produced by the linear clinical studies still show good correlation at one year of service.

Fig. 3. Scanning electron photomicrograph of wear facet of posterior composite after 300,000 masticatory cycles in an artificial mouth.

The coefficient of wear for the composite is shown in Table 6 and is the order of magnitude expected for high-wear materials (10). The coefficient of wear is dependent on a number of fundamental properties of the test materials, such as interocclusal friction, surface energy and also bulk properties such as interocclusal friction, surface energy and also bulk properties such as shear strength and yield point. However, the nature of the relationship is not understood and is a topic for future research if design is to play an important role in the development of posterior materials with good wear performance. However, the coefficient of wear has other useful functions. Once it has been determined for any wearing couple then the effect of changing the occlusal force and the lateral excursion can be predicted. This is very useful since the effects of clinically extreme conditions can be determined without rerunning the experiment. As indicated, the coefficient of wear depends on the volume of wear and can be determined from clinical studies (as well as artificial mouth studies) provided the relationship between clinical depth of wear and volume of wear is understood.

Fig. 3 shows the nature of the surface degradations after 300,000 masticatory cycles in the artificial mouth, which has been pointed out by other workers (7). Interparticulate resin, including the smaller particles are lost prematurely from the mass. The masticatory effort is borne by the larger particles until they are exfoliated because of excessive loss of resin. In the effort to improve these materials, it appears that the retention of the resin and the smaller particles within the composite mass is a major research goal.

Acknowledgement – This study was supported by National Institute of Dental Research grant No. 1RO1 DE 06752–02, Bethesda, Maryland, 20205.

References

1. Lutz F, Imfeld T, Phillips RW. P10-its potential as a posterior composite. *Dent Mater* 1985: *1*: 61–65.
2. Braem M, Haspeslagh L, Lambrechts P, anherle G. Four posterior composites: a one year report. *J Dent Res* 1985: *64* (4): 713 (Abstr. No. 88).
3. Lambrechts P, Braem M, Vanherle G. Accomplishments and expectation with posterior composite resins. In: Vanherle G, Smith DC. Posterior composite resin dental restorative materials. St. Paul, MN: 3M Company, 1985: 521–540.
4. Braem M, Vanherle G, Lambrechts P, Haspeslagh L. Two year quantitative wear results of four posterior composites. *J Dent Res* 1985: IADR-CED meeting, Paris, September 1985 (in press).
5. Linfelder KL. Evaluation of clinical wear of posterior composite resins. In: Vanherle G, Smith DC. Posterior composite resin dental restorative materials. St. Paul, MN: 3M Company, 1985: 501–510.
6. Vrijhoef MMA, Hendriks FHJ, Letzel H. Loss of substance of dental composite restorations. *Dent Mater* 1985: *1*: 101–105.
7. Phillips RW. Current status and future developments of posterior resin com-

pounds. In: Leinfelder KL, Taylor DF. Posterior composites. Chapel, North Carolina, 1982: 1–5.

8. Cross M, Douglas WH, Fields RP. The relationship between filler loading and particle size distribution in composite resin technology. *J Dent Res* 1983: *62*: 850–852.
9. Abeil AK, Leinfelder KL, Turner DT. Microscopic observations of the wear of a tooth restorative composite in vivo. *J Biomed Mat Res* 1983: *17*: 501–507.
10. DeLong R, Sakaguchi RL, Douglas WH, Pintado MR. The wear of dental amalgam in an artificial mouth, with a clinical correlation. *Dent Mater* 1985: *6*: 238–242.
11. DeLong R, Douglas WH. Development of an artificial oral environment for the testing of dental restoratives: biaxial force and movement control. *J Dent Res* 1983: *62*: 32–36.
12. Coffey JP, Goodkind RJ, DeLong R, Douglas WH. In vitro study of the wear characteristics of natural and artificial teeth. *J Prosthet Dent* 1985: *54* (2): 273–280.
13. Douglas WH, Sakaguchi RL, DeLong R. Frictional effects between natural teeth in an artificial mouth. *Dent Mater* 1985: *1*: 115–119.
14. DeLong R, Pintado MR, Douglas WH. Measurement of change in surface contour by computer graphics. *Dent Mater* 1985: *1*: 27–30.
15. Archard JF. Contact and rubbing of flat surfaces. *J Appl Phys* 1953: *24*: 981–988.
16. Rabinowicz E. Friction and wear of materials. New York: John Wiley, 1965: 167–179.
17. Steel RGD & Torrie JA: "Principles and procedures of statistics". Published by: McGraw-Hill, New York, 1960, p. 189.

Surface Frictional Changes in Posterior Materials During Wear Experiments in an Artificial Mouth.
W.H. Douglas, R. DeLong, R. Sakaguchi
School of Dentistry, University of Minnesota,
Minneapolis, Minnesota, 55455.

The coefficient of friction between porcelain, enamel and amalgam and an opposing natural cusp was masured before and after wear experiments were performed. The technology used was a servohydraulic based artificial mouth. The environmental fluid was a steady stream of water maintained at 37 deg C. A functional bruxing movement was used in which the opposing cusp travelled at 2 mm/sec.

Initially the coefficient of friction **on glazed porcelain was 0.12 +/- 0.02.** However very quickly with each masticatory cycle the friction between the porcelain and the opposing cusp increased dramatically to a stable **value of 0.54 +/- 0.025**. This can be rationalized by assuming that the glaze on the porcelain is quickly penetrated by attrition and the final friction is determined by the texture of the underlying structure. A similar performance was shown by enamel on enamel where the coefficient of friction rose from **0.46 to 0.77.** Enamel is extremely variable and the surface friction probably depends on the surface histology. **Amalgam showed a comparatively low coefficient of friction of .08.** If the process of wear is by abrasion it seems likely that these coefficients of friction would reflect the same ranking order in loss of contour.

At the end of the wear experiments in the present study the coefficient of friction of porcelain had increased to .62 and that of amalgam to .1. These increases may reflect an increasing rate of wear with time. Enamel however at the end of 30,000 masticatory cycles had shown a dramatic drop in the coefficient of friction. This may be due to the fact that the process of attrition had resulted in a smoother surface. It seems fair to conclude that this behavior with enamel would be very variable and again would depend on the surface histology at the point of contact between the cusp and the fossa.

JDR 1985: 64: 1764, p. 370.

Occlusal Wear of Posterior Materials in an Artificial Mouth - A Comparative Study.

R. DeLong, R. Sakaguchi, W. Douglas.
School of Dentistry, University of Minnesota

The artificial oral environment (DeLong and Douglas, JDR 62(1):32-36, 1983) was configured to test the wear resistance of posterior restorative materials when opposed by natural teeth. Discs of amalgam and glazed porcelain were mounted on the mandibular element of the artificial oral environment and were opposed by a freshly extracted maxillary premolar. Lower premolars were also placed in the lower element and opposed by maxillary premolars as a standard. One masticatory cycle consisted of a sine force pattern with a peak force of 3.0 lbs and a mean force of 1.5 lbs. All samples were tested in an artificial environment of continuously circulating 37' C distilled water. Volume loss and total loss of vertical height were determined at the end of 15 and 30 thousand cycles by means of computer digitization. The 30 thousand cycles in the oral environment corresponds to approximately two months of wear in the mouth. **In agreement with clinical findings it was found that amalgam wore the least and was the least destructive to the oral tisues.** The natural teeth showed the greatest amount of wear with a mean loss in vertical height of 110 u. The natural teeth also showed the greatest amount of variation. The corresponding values for amalgam and porcelain were 0.005 mm^3 and 0.019 mm^3 for volume loss and 44 u and 63 u for vertical loss, respectively. **When a comparison was made of the wear of the opposing natural dentition, it was found that porcelain was the most destructive causing no measurable wear on the opposing dentition.**

It should be noted that these results refer to a cusp on plate situation and are probably relevant to the early wearing in process. However, it is interesting that both in volume loss and vertical height amalgam lost less contour than all other materials.

JDR 1985: 64: 1765, p. 371.

Friction and Wear of Posterior Enamel in an Artificial Mouth.

R. Sakaguchi, R. DeLong, W. Douglas,
School of Dentistry, University of Minnesota.

A method for measuring frictional forces on enamel of natural teeth and restorative materials was developed using the Artificial Oral Environment (DeLong and Douglas, JDR 62(1):32-36, 1983). Enamel/enamel systems were tested using different oral fluids in a mini-environmental chamber capable of introducing biologic fluids between the occluding surfaces.

Matched, extracted opposing human premolars mounted in physiologic occlusion under an occlusal load of 3 pounds were bruxed at approximate masticatory velocities. A load cell measured the resulting horizontal forces and an X-Y record was attained. **31 independent measurements of friction in both buccal and lingual directions were performed** with the teeth dry, and with human saliva, Xerolube, and distilled water intervening.

It was found that typical values for **enamel/enamel coefficients of friction, u, were in the range of 0.1 to 0.42.** The coefficient of friction was indepenent of different fluids within any one enamel/enamel couple (coefficient of variation approx. 10%). However, the coefficient of friction of the enamel pair was highly dependent on surface texture. **Roughening virgin enamel led to a 3 fold increase in u.** Conversely, **surfactants present in mineral oil reduced the friction of roughened enamel by 3 fold.**

Where the wear process is by abrasion, it is likely that the reduction of the tangential forces due to friction could lead to reduced loss of contour. It is likely that finishing procedures in dentistry are important in this process. Finally the production of low friction restorative materials are clearly indicated as a future development.

JDR: 1985: 64: 1763, p. 370.

Occlusal Wear of Natural Enamel in an Artificial Mouth.

R.L. Sakaguchi, W.H. Douglas, R. DeLong, M. Pintado.
School of Dentistry, University of Minnesota, USA.

The artificial oral environment (DeLong and Douglas, JDR 62(1):32-36, 1983) was used to evaluate the wear experienced by natural human enamel when opposed by enamel, amalagam, porcelain, and a posterior composite. Discs of the restoratives were prepared and opposed by maxillary molar palatal cusps in the artificial oral environment. One masticatory cycle consisted of a sine force pattern with a peak force of 3.0 lbs and a mean force of 1.5 lbs. All samples were tested in a simulated oral environment of continously circulating 37 deg C distilled water. The occlusal surfaces were profiled and the surfaces computer digitized. Volume loss and total loss of vertical height were determined at the end of 85 and 300 thousand cycles for the composite. The enamel, porcelain, and amalgam samples were profiled at 30, 100, 250, 350, and 500 thousand cycles.

The results obtained were consistent with clinical findings. **The greatest wear of enamel occurred when it was opposed by porcelain. The least wear was experienced when it was opposed by amalgam.** At the end of 500,000 cycles the volume of wear experienced by the maxillary molar palatal cusp was **0.42 mm^3 when opposed by porcelain, 0 mm^3 (amalgam), and 0.09 mm^3 (natural enamel).** At 300,000 cycles for the composite, the volume of wear was **0.08 mm^3.**

Both porcelain and enamel produce a **relatively steady rate of volume of wear** on the opposing palatal cusp after the initial wear-in period of 30 thousand cycles. The slope of the porcelain/enamel volume of wear curve is approximately **8 times** that of the enamel/enamel wear curve. **No wear was experienced by the palatal cusp when opposed by amalgam.** SEM micrography revealed smearing of the amalgam on the palatal cusp.

JDR 1986: 65: 215, p. 749.

Remote-Site Clinical Measurement of Occlusal Wear.

R. DeLong, R.L. Sakaguchi, W.H. Douglas, M.R. Pintado.
School of Dentistry, University of Minnesota, USA.

The purpose of this study was to test the feasibility of a clinical research center being serviced by a remote-site clinical measurement center providing numerical and computer graphics measurement of clinical posterior wear.

The measurement technology was a variation of profilometry in which the stylus movement was part of a servohydraulic closed loop. An accurate x-y positioning stage was part of the system, and the three spatial coordinates of the stylus were fed into computer arrays. These arrays were assembled by computer graphics to provide a digital and visual record of the occlusal surface. The steps involved in remote-site clinical measurement: (1) receipt of high quality occlusal impressions, (2) pouring high quality epoxy models, (3) mounting models in space for profiling, (4) computer collection and fitting of sequential images, (5) analysis of occlusal change in depth, volume and anatomic site. **Factors contributing to feasibility of the process are:** (1) high performance of vinyl polysiloxanes **(.05% dimensional change)** and epoxy models, (2) physical mounting of successive models in values of **50 micrometers discrepancy.** This is remedied by two-dimensional fitting routines reducing the error to 15 +/- 4.3 microns at 6 months recall and 20 +/- 7.6 microns at one year recall (this is called the RMS fit). This is achieved by pattern recognition and does not involve marking the tooth. This measurement above all others indicates the feasibility of remote site clinical measurement, i.e. that the total errors in impression taking, transport, impression stability, models pouring and storage can be limited to 15-20 microns. The final stage is wear analysis. **Typical clinical systems show 50-100 um loss in the occlusal contact area which can easily be measured above the 15-20 microns RMS background fit.**

JDR 1986: 65: 216, p. 749.

Posterior Composite Wear in an Artificial Mouth: A Clinical Correlation.

W.H. Douglas, R.L. Sakaguchi, R. DeLong, M.R. Pintado.
School of Dentistry, University of Minnesota, USA.

Using a servohydraulic artificial mouth with a defined masticatory cycle, the wear performance of a posterior composite was assessed when opposed by a maxillary palatal cusp. Five replications were carried out for each experiment and occlusal mapping took place at 85,000 and 300,000 masticatory cycles. At each point, occlusal change was recorded in terms of depth and volume at the occlusal contact area. Previous experience with amalgam wear had shown that 250,000 defined masticatory cycles had produced one year of clinical wear. **The coefficient of wear for the composite was 2.58 x 10^{-5}. A retrospective clinical correlation (Braem et al, J Dent Res 1985: 64: 713) with the composite wear showed a correlation coefficient of 0.98 at one year of wear.** Artificial mouth studies support a parabolic relationship between depth of wear and time. **The ratio of 6 months depth of wear to 3 years was found to be 41% in the artificial mouth.** The disagreement between linear and parabolic studies is small during the early wear process, but become serious in the longer term. **It is important for future clinical wear studies to resolve the question of the nature of the wear rate curve, if accurate prediction of long term wear performance is to be achieved.**

Typically, clinical studies of occlusal wear show standard deviation in **excess of 50% of the mean.** Artificial mouth studies show standard deviations **less than 20% of the mean.** The desirability of the in vitro testing to produce the same variance as well as the same mean value of the clinical trial is a point for further discussion.

JDR 1986:65:647,p. 797.

Surface Friction and Porcelain Wear in an Artificial Mouth.

P.S. Olin, C.R. Lehner, R. DeLong, W. Douglas, R.L. Sakaguchi. University of Minnesota, Minneapolis, Minnesota.

The wear of dental porcelain when opposed by human enamel is important because of the wide spread use of porcelain as a restorative material. The palatal cusp of a maxillary molar was opposed by a glazed porcelain disk bonded to metal in an artificial mouth. The environmental fluid was a steady stream of water maintained at 37 deg C and directed onto the occluding surface.

A functional bruxing movement was programmed into the artificial mouth under a steady occlusal force of 13.35 N (3 lbs). The mandibular porcelain element moved laterally against the maxillary cusp at a speed of 2 mm/sec. The frictional force was measured as a function of the number of bruxing cycles.

The results indicated that the coefficient of friction between enamel and glazed porcelain was initially 0.09. This is very low and is comparable to dental amalgam. However at 5 bruxing cycles the coefficient of friction began to rise steeply and at 10 cycles it was 0.23. The equilibrium was reached at 50 cycles and coefficient was 0.69. **The slope at the curve during the wearing-in period was 0.16 units/bruxing cycle.** This can be interpreted as the penetration of the glaze by the enamel cusp. What is surprising is how quickly this occurs and the steep rise of the friction. This phenomenon is very likely responsible for the high wear potential of porcelain. **If the porcelain glaze could be preserved immediately under enamel contact it could lead to an improvement in the wear characteristics of this material.**

JDR 1987: 66: #219, p. 66.

Finite element analysis of the biomechanics of natural teeth.

E. Brust, R.L. Sakaguchi, W.H. Douglas, R. DeLong, M.R. Pintado. University of Minnesota, School of Dentistry, Minneapolis, Minnesota 55455.

An integrated experimental and computational method for the evaluation of the biomechanics of natural teeth was developed. The experimental component employed strain gages placed on natural premolar teeth occlusally loaded in a bruxing mode in an artificial mouth (DeLong and Douglas, J Dent Res 62(1):32-36, Jan 1983). Occlusal loads were varied as were the lateral excursions. Strain measurements were made on the buccal and lingual surfaces of the teeth at the gingival 1/2-1/3. A total of 21 measurements were made on each of 3 teeth. The strain measured at the buccal and lingual surfaces as the occlusal was loaded **increased linearly with the occlusal load** up to 10 lbs. The modelling component utilized the IFECS finite element computational system (Cross and Lewis, Appl Math Mod 2:165-167, 1978) operated on a Masscomp 68000 based minicomputer. A model was developed consisting of 199 nodes reproducing the morphology of the natural teeth. Strain values were calculated at each of 334 elements and a strain distribution and contour was produced. Occlusal loading was performed at similar locations and loads as the natural tooth. **Comparison of the experimental method to the computational demonstrated similar trends and strain values.**

Cuspal independence was observed in the bruxing mode as the occlusal loading element passed from the buccal incline through centric occlusion to the lingual incline.

JDR 1987: 66: #779, p. 204.